

A STUDY OF MICRO FIBER DISPERSION USING DIGITAL IMAGE
ANALYSIS

A Dissertation

by

JOONED HENDRARSAKTI

Submitted to the Office of Graduate Studies of
Texas A&M University
in partial fulfillment of the requirements for the degree of

DOCTOR OF PHILOSOPHY

August 2003

Major Subject: Mechanical Engineering

© 2003

JOONED HENDRARSAKTI

ALL RIGHTS RESERVED

A STUDY OF MICRO FIBER DISPERSION USING DIGITAL IMAGE ANALYSIS

A Dissertation

by

JOONED HENDRARSAKTI

Submitted to Texas A&M University
in partial fulfillment of the requirements
for the degree of

DOCTOR OF PHILOSOPHY

Approved as to style and content by:

Kenneth D. Kihm
(Co-Chair of Committee)

Jamal Seyed-Yagoobi
(Co-Chair of Committee)

Dennis Phares
(Member)

William H. Marlow
(Member)

John Weese
(Head of Department)

August 2003

Major Subject: Mechanical Engineering

ABSTRACT

A Study of Micro Fiber Dispersion Using Digital Image
Analysis. (August 2003)

Jooned Hendrarsakti, B.S., Texas A&M University;
M.S., Texas A&M University

Co-Chairs of Advisory Committee: Dr. Kenneth D. Kihm
Dr. Jamal Seyed-Yagoobi

The area of the digital image processing is getting more attention in the hope that it will increase the accuracy of any scientific measurements, such as in determining an object velocity, temperature, and size. While human vision is excellent to recognize and differentiate objects, it has been proven to be a poor tool when it comes to measure the object performance. One of many digital image processing applications is texture analysis whose purpose is to evaluate image patterns. The purpose of this dissertation is to investigate the use of texture analysis as a tool to micro fiber dispersion measurement. Micro fiber dispersion can be found in many applications such as in paper and industry powder engineering.

Three cases related to micro fiber dispersion were investigated in this study. The first case was the experimental study of the dispersion in open water channel. Sets of synthetic fibers were put into water channel to simulate a process that can be found in papermaking industry. The research investigated the effect of three operating parameters: fluid velocity, fiber consistency, and fiber aspect ratio to fiber dispersion. Using two-factorial experimental design technique, the main and interaction effects of these parameters were evaluated. The study found that increasing fluid velocity, fiber aspect ratio, and consistency decreased the dispersion level. The study also found that the effect of individual parameters is more pronounced than the role of the interactive terms on the fiber flocculation.

The second case considered was applying the fiber dispersion analysis to computer-synthesized images consisting of different arrangements of fibers. Four sets of sub-cases were presented. These sub-cases were divided based on the fiber-concentrated location and fiber distribution. The use of computer-synthesized images was found to be very useful to simulate real situation during fiber dispersion.

The third case investigated the fiber distribution on a dry paper. Images for different types of paper were taken and evaluated to see the dispersion level of each type of paper. It was found that the current texture analysis was applicable to determine the dispersion level for dry papers.

While three cases indicated that the texture analysis can be used to investigate the fiber dispersion, the texture analysis used here is not a perfect and universal method and may not be suitable to analyze other types of dispersions. The human vision will always be essential to determine if the texture analysis is applicable to any other problem.

To my Ibu & Bapak
To my wife and bestest friend: Nivo

ACKNOWLEDGEMENTS

I wish to express my sincerest thanks to my advisors, Drs. Kihm and Seyed-Yagoobi, who have given me the encouragement and independence in pursuing my research. I very much appreciate their wise advice and assistance for everything.

I would like to express my gratitude to Drs. Phares and Marlow for serving as members on my committee and giving of their valuable time.

Finally, but not the least, I would like to thank all my friends and colleagues in the Mechanical Engineering Department of Texas A&M University, especially the personnel of Drying Research Center and Micro-Fluidic research groups for their support and friendship.

TABLE OF CONTENTS

	Page
ABSTRACT.....	iii
DEDICATION.....	v
ACKNOWLEDGEMENTS.....	vi
TABLE OF CONTENTS.....	vii
LIST OF FIGURES.....	ix
LIST OF TABLES.....	xiii
CHAPTER	
I INTRODUCTION	1
1.1. Digital image processing.....	1
1.2. Application of digital image processing in fluid mechanics.....	1
1.3. Image properties.....	2
1.4. Texture analysis.....	4
1.5. Objective and overview.....	11
II TEXTURE ANALYSIS.....	13
III CRITICAL LITERATURE REVIEW TO FIBER DISPERSION.....	19
3.1. Introduction.....	19
3.2. Flocculation factors.....	19
3.2.1. Mason’s contributions.....	21
3.2.2. Mechanical factors.....	22
3.2.3. Chemical factors.....	33
3.2.4. Summary of mechanical and chemical factors.....	37
3.3. Theoretical models related to the fiber flocculation	39
3.4. Future developments and research... ..	42
3.6. Summary.....	48
IV WATER CHANNEL EXPERIMENT.....	50
4.1. Introduction.....	50
4.2. Water channel apparatus.....	50
4.3. Fiber properties.....	52
4.4. Image capture procedures	54
4.5. Two-factorial design.....	57
4.6. Operating parameters	58
4.7. Results and discussion.....	60
4.8. Summary.....	89

CHAPTER	Page
V COMPUTER-SYNTHEZIZED IMAGE ANALYSIS.....	92
5.1. Introduction.....	92
5.2. Image preparation.....	92
5.3. Case studies.....	94
5.4. Results and discussion.....	94
5.5. Summary.....	104
VI DRY PAPER EXPERIMENT.....	105
6.1. Introduction.....	105
6.2. Physics behind paper translucency.....	105
6.3. Description of paper samples.....	106
6.4. Experimental apparatus.....	107
6.5. Results and discussion.....	109
6.6. Summary.....	110
VII CONCLUSIONS.....	112
REFERENCES.....	116
APPENDIX A: NAIR'S TEST.....	121
APPENDIX B: F-RATIO TEST TABLE.....	122
APPENDIX C: COMPUTER CODE.....	123
APPENDIX D: TWO-FACTORIAL DESIGN.....	130
APPENDIX E: EXPERIMENTAL PARAMETERS AND CONDITION OF PREVIOUS STUDIES.....	131
APPENDIX F: FLUID DENSITY CALCULATION.....	132
APPENDIX G: SUMMARY OF ERROR ANALYSIS.....	133
VITA.....	135

LIST OF FIGURES

FIGURE	Page
1. Sample figures to describe texture primitives. Images are adapted from P. Brodatz [7].....	5
2. Comparison images with similar primitives from fine to coarse texture and their corresponding image after edge detection process.....	7
3. Description of neighborhood concepts as shown by arrows: (a)four neighborhood; (b)eight neighborhood.....	8
4. Relation between texture number and dispersion rating for difference samples of carbon black [11].....	10
5. Extraction 3x3 pixels window from image gray value.....	13
6. Illustration of requirement of texture appearance for each effect.....	15
7. Transformation of 3x3 pixels window to become pronum (local texture descriptor).....	17
8. Sample results of prospectrum (global descriptor of texture).....	18
9. Description of the fiber in paper sheet.....	19
10. Diagram of wet end of paper production.....	20
11. Crowding factor effect on the fiber flocculation at two different parameters: coarseness and beating rate.....	23
12. Illustration for the concept of fiber curl.....	25
13. Effect of the fiber curl on the fiber flocculation [27].....	25
14. Effect of shear rate on flocculation level [30].....	27
15. Effect of velocity on flocculation level [31].....	28
16. Effect of viscosity on flocculation [25].....	30
17. Effect of temperature on flocculation [26].....	30
18. Effect of pH on the flocculation level [26,27].....	34
19. Effect of electrolytes on the flocculation level. [27]	34
20. Addition of flocculent to the fiber flocculation [25].....	36

FIGURE	Page
21. Sample result of Hourani's thermodynamics model [33]: the electrostatic field effect on floc size distribution.....	40
22. Sample result of Hourani's thermodynamics model [33]: the comparison result between hardwood and softwood.....	40
23. Variation of dispersion over length of fiber [47].....	41
24. Concept of dynamic and static equilibriums.....	43
25. Example to illustrate the flocculation level under [50] concept.....	44
26. Description of three different cases with similar flocculation level calculated by [50] method.....	45
27. Illustration of the concept of image as a moving object	47
28. Water channel configuration.....	51
29. Water channel utilized for this study.....	52
30. Fiber diameter measurement description.....	53
31. Imaging apparatus and configuration.....	54
32. Apparatus configuration using PIV concept	56
33. Sample images using PIV concept: (a)C=0.05%, (b)0.2%, (c)0.25%.....	57
34. Arrangement of experimental settings.....	59
35. Sample image at different operating conditions.....	61
36. Mean and standard deviation of experimental results.....	64
37. Three-dimensional description of two-factorial design prediction.....	67
38. Comparison of consistency and aspect ratio of current results with literatures.....	69
39. Comparison of fluid velocity effect of current study results with published results in literatures at two different conditions: constant velocity (b and c).....	73
40. Four set configurations for further velocity study.....	74
41. Sample images taken with different velocities at C=0.1% and L/D=400.....	77

FIGURE	Page
42. Sample images taken with different velocities at $C=0.4\%$ and $L/D=400$	78
43. Sample images taken with different velocities at $C=0.1\%$ and $L/D=200$	79
44. Sample images taken with different velocities at $C=0.4\%$ and $L/D=200$	80
45. Experimental data of fluid velocity as a function of texture number.....	81
46. Variation of apparent viscosity with shear rate for $L/D=400$	83
47. Variation of apparent viscosity with shear rate for $L/D=200$	83
48. Assumed velocity profile.....	84
49. Texture number variation based on Reynolds numbers.....	85
50. Experimental data from Beghello [26] with constant fluid velocity and consistency.....	86
51. Dimensionless variable to describe degree of effect of each parameter....	89
52. Single fiber dimension.....	93
53. Sample images with different densities used in Case 1: (a)288, (b)5760, (c)10080 (d)20160, and (e)30240 fibers.....	95
54. Variation of texture number with fiber density.....	96
55. Sample image used in Case 2 with constant higher density blocks at 315 fibers/small block and varied lower density blocks: (a) 0, (b)23, (c)80, (d)158,(e) 269, and (f) 315 fibers/small blocks.....	97
56. Variation of texture number with fiber density of smaller density blocks.....	98
57. First proposed mechanism of dynamic equilibrium.....	99
58. Second proposed mechanism of dynamic equilibrium.....	99
59. Sample images used for Case 3 with 6 different blocks: (a) 2x2; (b) 4x4; (c)8x8; (d) 16x16; (e) 32x32; (f) 64x64.....	100
60. Texture variation with number of blocks for Case 3.....	101

FIGURE		Page
61.	Image used to test the border length differences and the corresponding texture number.....	102
62.	Sample images used in Case 4 with varied ratio between lower and higher density blocks. (a)0:10080; (b) 1440:8640; (c)2880:7200; (d)4320:5760 and (e) 5040:5040 fibers.....	103
63.	Texture number variation as function of the ratio of fiber densities of lower to higher blocks.....	104
64.	Apparatus schematic of the dry paper analysis.....	107
65.	Sample images of different dry papers.....	108

LIST OF TABLES

TABLE		Page
1.	Mechanical factors that influence the fiber flocculation from the fiber characteristics.....	37
2.	Mechanical factors that influence the fiber flocculation from the fluid characteristics.....	38
3.	Chemical factors that influence the fiber flocculation.....	38
4.	Mean and standard deviation of low and high values of each parameter used for experiments.....	59
5.	Results analysis using BeghELLO's procedures.....	63
6.	Two-factorial design analysis results.....	65
7.	Corresponding crowding factor for different consistency and aspect ratio.....	68
8.	Results of additional study of velocity effect.....	76
9.	Calculated dynamic viscosity (μ) at experimental fluid velocity.....	84
10.	Summary for each case for computer-synthesized image texture analysis.....	94
11.	Dry paper types and their corresponding texture numbers.....	110

CHAPTER I

INTRODUCTION

1.1. Digital image processing

Digital image processing is becoming a widespread technique to analyze scientific data in many disciplines. While human vision is still essential to recognize and distinguish images, it is unable to measure quantitatively the image properties. Similar limitation in fact can be found in any other disciplines, for instance in fluid science, human will easily be able to distinguish two different fluid flows, but clearly it is not capable quantitatively measure the fluid flow velocity and direction. One important tool in recent years to cover this human weakness is digital image processing as some people call computer vision. Digital image processing, using variety of techniques and procedures, is able to identify and measure many properties of an image, such as quality, edges and lines, and size and shape. These digital image processing techniques become more popular due to the fact that they are not only easy to operate and cost-friendly, but their results are relatively accurate and dependable as well. Cheaper and more powerful computers also play important role to increase the digital image processing use in variety of research areas.

1.2. Application of digital image processing in fluid mechanics

In fluid mechanics area, digital image processing techniques have been developed mainly in particle-in-fluid tracking and object size and shape determination. Various algorithms have been developed to track the particle motion in fluid flow using multiple image sequences. The flow is made visible by injecting small particles inside flow and integrating with laser based equipment to provide lighting for images. The tracking results are used to determine the fluid velocity and direction.

This dissertation follows the style and format of *Journal of Pulp and Paper Science*.

In object size and shape determination, the shape irregularity and micro size become the main interest. In this technique, producing high quality imaging becomes essential to recognize the exact shape and size of the object. Blur and any other distortions will eliminate the accuracy of the technique regardless how good the technique and procedures are.

1.3. Image properties

A two dimensional picture is a flat object whose brightness or color may vary from point to point. This variation can be represented mathematically by a function of two spatial variables represented by a single real valued function $f(x,y)$. A digital image of $f(x,y)$ has been discretized both in spatial coordinates and in brightness. An image then can be considered as a matrix or an integer array whose row and column indices identify a point in the image and the corresponding matrix element values identify the color value at that point. The smallest entity exists in the image are called picture element or abbreviated as pixels or pels. How exact the matrix representation to the real image will depend on the resolution number. The resolution number represents the amount of pixels used to represent a certain real image region. The higher resolution number, the better the image representation is; on the other hand, smaller resolution can mislead representation of real image.

Another factor to image quality is bit color of image. Color bit represents the numbers of colors are shown on the picture. The least number of color can be used is two and usually the image is called binary image. For current study the color used will be only in gray values that have 256 color divisions between black and white colors.

Techniques in digital image processing may be divided into four principal categories as summarized by Gonzalez and Wintz [1]: image digitization, image enhancement and restoration, image encoding, and image segmentation, representation, and description. Digitization problem is one of converting continuous brightness and spatial coordinates into discrete components. Problems here include digitization process and its effect on image quality. This category includes the theoretical treatment and mathematical tools of sampling of digitization process. Image scanning process is

developed based on the need on improvement of digitization process. Enhancement and restoration techniques deal with the improvement of a given image for human or/and machine perception. Image enhancement and restoration procedures have been used to improve degraded image depicting uncoverable objects or experimental results that are too expensive to duplicate. These enhancement and restoration mostly are intended for human interpretation. Various softwares that help to easily improve and enhance the outlook of images can be found everywhere in the market. As image enhancement for computer vision, the difference from human interpretation problem is that in machine vision the various informations are extracted from an image based on the property of the image. This information can be in form of statistical analysis, Fourier transform, and distance measures.

Image encoding procedures are used to reduce the number of bits in a digital image. The encoding process is used mainly to minimize storage and data transmission. Clearly, small file containing a lot of data and information will be easier and faster to transport and favorable compared to the big files. In this area, researchers have found different formats of images that help to reduce the image file size without any significant loss on image quality. The improvement in encoding process becomes important issue during these days where Internet has been a common tool to communicate people. Easy and fast digital data transmission has become daily need of many people. Segmentation is the process that subdivides an image into its constituent regions or objects. Segmentation algorithms generally are based on one of two basic properties of gray-level values: discontinuity and similarity as discussed by Jahne [2]. Discontinuity is based on abrupt changes in gray level, and principal areas include point, line and edge detection in an image. The principal approaches in the second category are based on thresholding, region growing, and region splitting and merging. Segmentation becomes an integral part in image representation and description because at this step the object are extracted from an image for subsequent processing.

1.4. Texture analysis

An important approach to image representation and description is to quantify the texture content. Texture can be viewed as a descriptor measure of properties such as smoothness, coarseness, and regularity [3]. Texture could be defined as a structure composed of a large number of more or less ordered, similar elements or patterns. Textures normally range from micro to macro. A micro texture appears only in a small area of the image with a very high gray level variation, i.e. significant tonal variation within a small image region. Micro textures can be studied effectively using local properties. The quantified local property of a micro texture is called the local descriptor. In this method, the macro texture can be represented by compiling the micro texture appearance [4-6].

As in [1], three principal approaches used in image processing to describe the texture of image region are statistical, structural and spectral analysis. In statistical approaches, image texture can qualitatively be evaluated as having one or more of the properties of fineness, coarseness, smoothness, granulation, randomness, lineation, or being mottled, irregular, or hummocky. Each of these adjectives translates into some property of the tonal primitives (a small structure with which the entire image can be generated, examples are shown in Fig. 1) and the spatial interaction between the tonal primitives. Texture is one of the most important characteristics for analyzing the images that have repetition and fundamental image elements. The texture analysis has been used in many areas to interpret and classify images. However, quantitatively, it is difficult to measure the texture level of an image, since there is a lot of possibility of primitive appearances.

Structural techniques deal with the arrangement of image primitives, such as the description of texture based on regularly spaced parallel lines. Haralick et al. [6] believed that image texture is considered to be non-figurative and cellular. It can be considered as organized area phenomena. The organization of texture in structural approaches can be viewed into two dimensions. The first dimension is for describing the primitives out of which the image texture is composed, and the second dimension is for the description of the spatial dependence or interaction between the primitives of an

image texture. The first dimension concerned with tonal primitives or local properties and the second dimension concerned with the spatial organization of the tonal primitives.

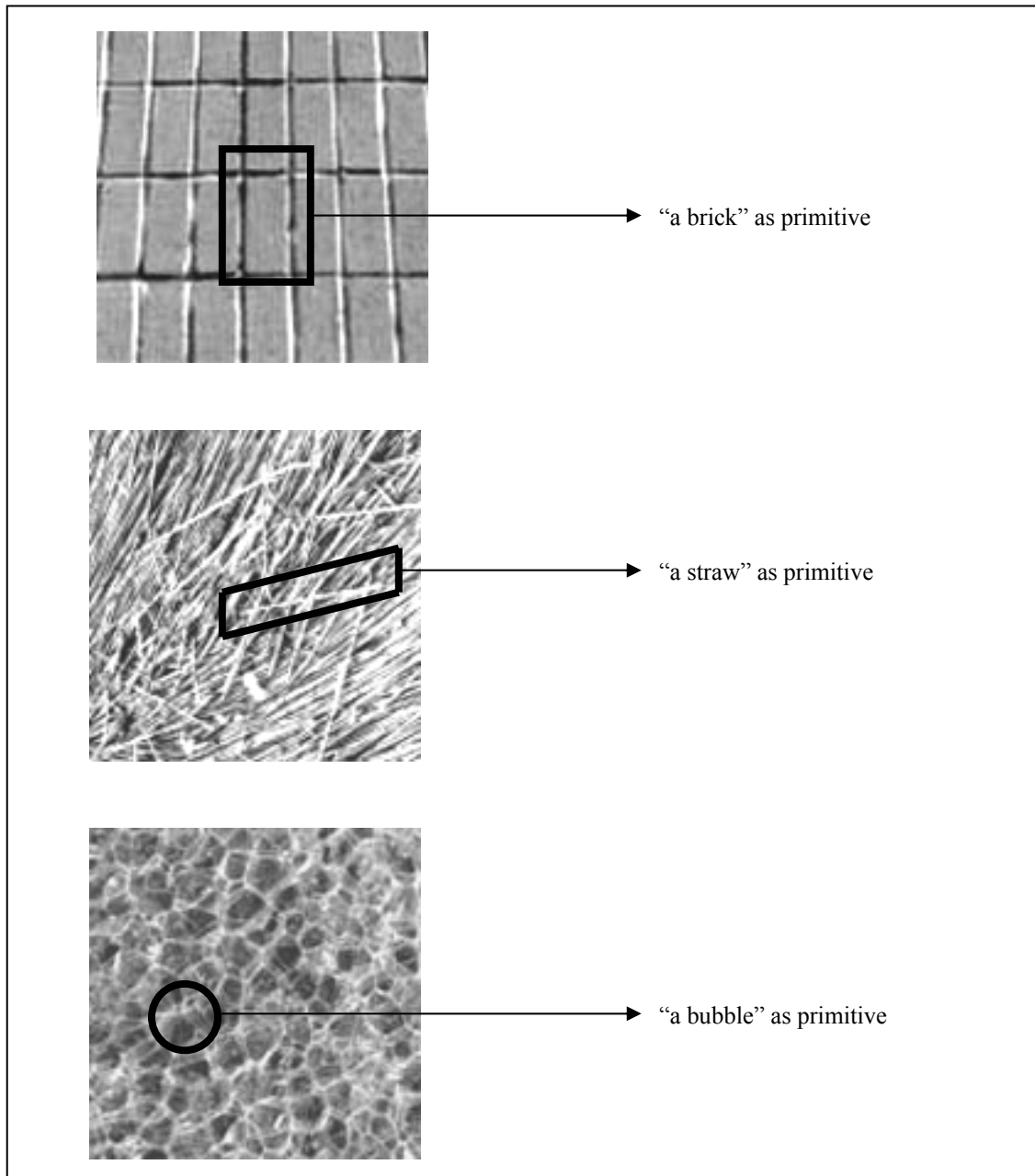


Fig. 1. Sample figures to describe texture primitives. Images are adapted from P. Brodatz [7].

Spectral techniques are based on properties of Fourier spectrum and are used primarily to describe the directionality of periodic or almost periodic two-dimensional patterns in an image. Three features of Fourier spectrum that are useful in texture description: (1) prominent peaks in the spectrum give the principal direction of the texture patterns; (2) the location of the peaks in the frequency plane give the fundamental spatial period of the patterns; (3) when any periodic components are eliminated through filtering, non periodic image element can be described by statistical techniques.

There have been at least eight statistical approaches to the measurement and characterization of image texture as reviewed by Haralick et al. [5]. One common approach is by measuring spatial frequency image directly or indirectly. Spatial frequency is related to texture because fine textures are dominated by high spatial frequencies while coarse textures are dominated by low spatial frequency. Another way to view texture as spatial frequency distribution is to view the texture as amount of edge per unit area exist on the image. Coarse textures have a small number of edges per unit area and vice versa for fine textures. The comparison of images with different coarseness based on the frequency of edge detected is illustrated in Fig. 2.

These coarse textures can be further defined as the ones for which the gray level distribution change slightly with distance, and fine textures are one for which distribution changes rapidly with distance [5]. One common method to find the edge is by comparing the gray level of the center pixel of an image window with the gray levels of its four or eight-neighbors connectivity (see Fig. 3 for description of neighborhood pixels). It is very important to set an appropriate window size. This window will ultimately determine how many pixel neighbors are used in calculation. If the size is too small, it might not be able to detect the edge, and if too large, it makes computation inefficient. Finally, it is important to appropriately set the threshold value that will ultimately determine whether the edge exist at the window. Often human observation is still needed to determine the correct image window and threshold color values.

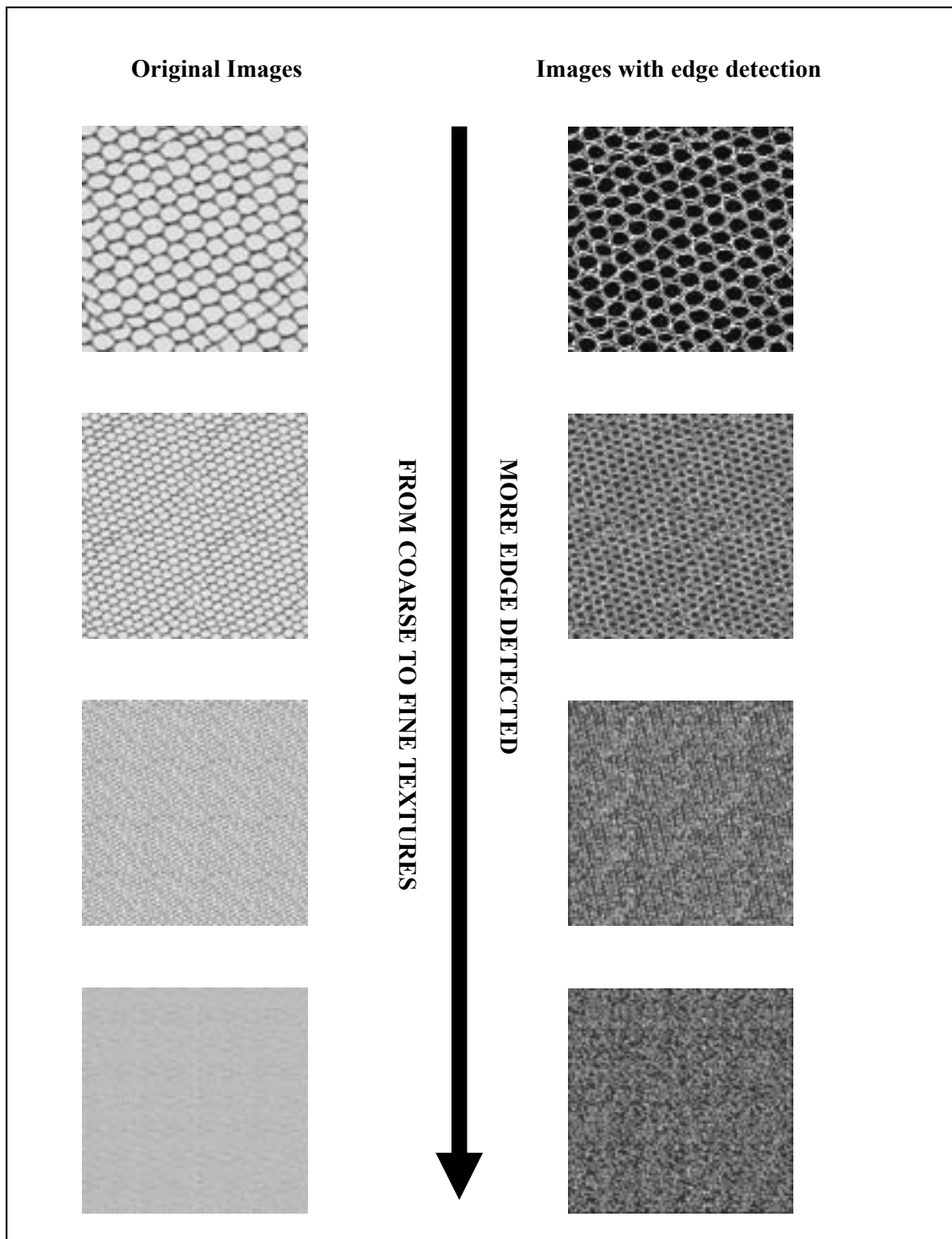


Fig. 2. Comparison images with similar primitives from fine to coarse texture and their corresponding image after edge detection process.

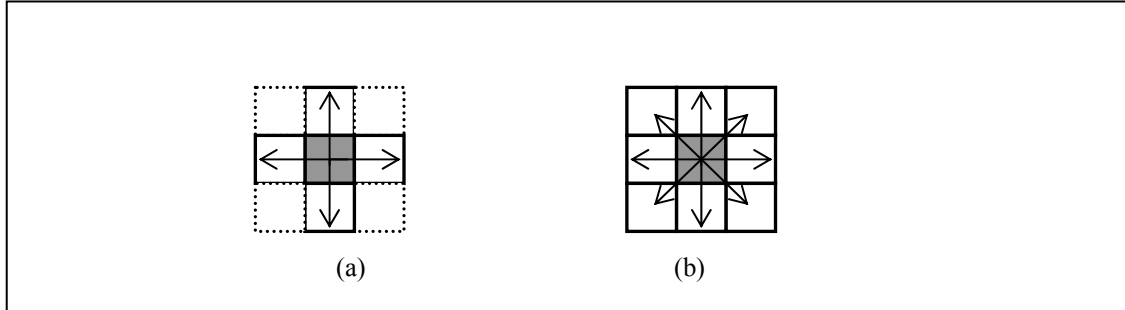


Fig. 3. Description of neighborhood concepts as shown by arrows: (a). four neighborhood; (b). eight neighborhood.

Recently, Bhattacharyya and his colleagues [3, 8-13] introduced a new statistical design of experiment-based method for texture representation. In this method, the texture representation is based on the appearance of the frequency appearance of the edge of the texture object. Bhattacharyya and Ganesan [3] analyzed various types of images using the technique on the basis of a complete set of orthogonal polynomials to obtain the interaction factors similar to two-factorial design analysis. In this method, initially $n \times n$ pixel size window is set. In this particular window, the interaction analysis is using the gray values in x and y direction as the parameters. This analysis will yield some constants that show relationship between pixels: main effect and interaction effects constants. Main effect is obtained when one pixel coordinate is set to be constant and the other coordinate is varying, on the other hand the interrelation effect related when both coordinates are varying. These constants are then compared with published statistical table that provides the threshold value to detect existing edge. If these constants pass the tabulated statistical values, the edge is said to be detected or exist in the image. Then based on the appearance of the edge, the detected texture is represented locally by encoding the measure of significance called pronum as an integer number ranging from 0-255. Higher pronum number appears when more constants pass the statistical test. Higher pronum number then indicates that the image region has more edge, and finally finer the texture appearance. The method has the power to describe the texture in terms of the number and the type of the primitive and their spatial organization. To obtain global descriptor, the analysis is repeated to the whole image

region by applying similar window to whole image area. Finally after calculating the pronum of all local textures of the image, the texture level of the image is represented using the frequency of occurrences of pronums called prospectrum as global descriptor of the texture image.

This method was implemented to several cases successfully [10-13]. This method may bring an effective measure to the dispersion analysis in particle when their method successfully measured the dispersion of carbon black in rubber and related the level of dispersion of the texture number. Carbon black is a mixture that is produced by partial combustion of hydrocarbon materials such natural gas, bones, or other plant or animal tissues. Carbon black is usually used in pigments for inks and paints and also as reinforcing agents in the manufacture of rubber products. The properties of these rubber products depend highly on uniform dispersion of reinforcing fillers of carbon black. Poor dispersion will lead to poor appearance, poor processing, and most importantly, poor performance. In their study, Ganesan and Bhattacharyya [11] generated some image samples of the carbon black dispersion in reinforcing rubber, and they analyzed those images using the texture measurement techniques mentioned above. They found that as the dispersion rating of carbon black inside rubber increases, the texture number also increases as shown in Fig. 4.

Using their conclusions, the current research study implemented the texture analysis to investigate several dispersion cases related to pulp and paper problems. Very similar to the problem found in carbon black in rubber, the dispersion of pulp fiber is critical factor to determine the final quality of paper. Poor fiber dispersion similarly will lead to poor appearance and performance of paper. Degree of fiber dispersion is controlled by various mechanical and chemical factors from fluid and fiber properties. Some of these factors have been already receiving important consideration during papermaking, while the others are still questionable on how they affect the fiber dispersion. However, the exact level of how individual factor will affect the fiber dispersion is relatively unknown. One problem is that no method/procedure is widely accepted as a tool to measure fiber dispersion. Many researchers came with different tools and methods. While finding the standard method will be a challenging task, the

motion of fibers that is non-repeatable inside turbulence flow is another task that is almost impossible to solve. Each individual fiber will act and move differently relative to other fibers or group of fibers inside the flow. No fibers will move uniformly according the fluid flow. This phenomena will make the each researcher will have different degree of fiber dispersion depending on their apparatuses and experimental condition, although in general they may have similar conclusion regarding the role of some dispersion factors.

While the current study might not give the whole solution to those problems, the study gives different outlook to the use of digital image processing in dispersion problem in pulp and paper. The results of this study are not only useful in papermaking industry but also in other industries, such as powder and textile industries.

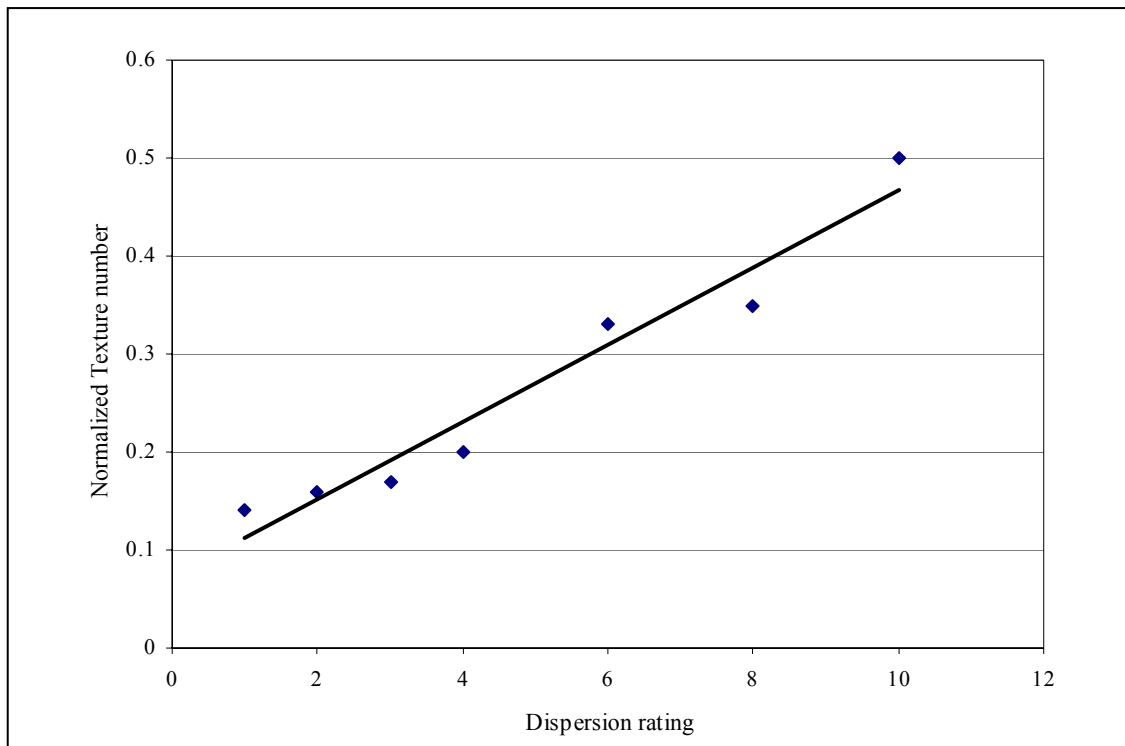


Fig. 4. Relation between texture number and dispersion rating for difference samples of carbon black [11].

1.5. Objectives and overview

The complete description of the texture technique used in this research will be shown in Chapter II. The main purpose of this study is to introduce new view and approach to fiber dispersion research. Using the relationship between texture level and dispersion level introduced by Bhattacharyya and Ganesan [8], three cases in pulp and paper-related area have been studied. The objectives these studies are:

1. to investigate the cylindrical-shape particles or fibers dispersion inside water flow. This problem is as mentioned above inspired by development and application in pulp and paper research. In this study two-factorial design was used to determine the interaction effect between the operating conditions of the experiment: fluid velocity or Reynolds number, fluid consistency, and fiber aspect ratio. The intensive reviews on the factors affecting the fiber dispersion were reviewed in Chapter III. Some critical result from various distinguished researchers will be discussed. This review will also mention some other important tasks in fiber dispersion study. The complete detail of the fiber dispersion study inside water flow can be found in Chapter IV. The comparison of current results with previous literature will also be discussed.
2. to simulate the dispersion analysis of fibers inside computer-generated images. Unlike the first problem, in this problem, the exact number of fibers and their distribution in image can be controlled. However similar to the first problem, the exact location and direction of the fibers are set to be random. Four different cases were introduced in this problem with variation of number of fiber and distribution. These four cases represent ideal cases that are impossible to achieve in fiber dispersion study in Chapter IV. The complete results for this problem can be found in Chapter V.

3. to investigate fiber dispersion inside dry paper. In this problem, several different types of papers are investigated. This study signifies the fiber dispersion inside different paper final product. The comparison with the results found using fiber inside water flow study (Chapter IV) and using computer-generated image (Chapter V) will be discussed. The complete results for this problem can be found in Chapter VI.

Conclusions containing final summary and discussion of the research will be presented in Chapter VII.

CHAPTER II

TEXTURE ANALYSIS

The current study used the texture analysis by Ganesan and Bhattacharyya [4-6] as a method to investigate particle dispersion problems. The following is their method to determine the level of texture:

1. Preparing the input of a grayscale matrix of an image. This task can be done using any of image processing software available in the market. In this particular study, MatlabTM was used.
2. Start by extracting an $n \times n$ pixels image window region where its matrix can be represented as a function of x and y [f_{xy}]. The smallest window is 3×3 pixels, which will be used in this research as described in Fig. 5. Steps 3-9 are described using this small window region.

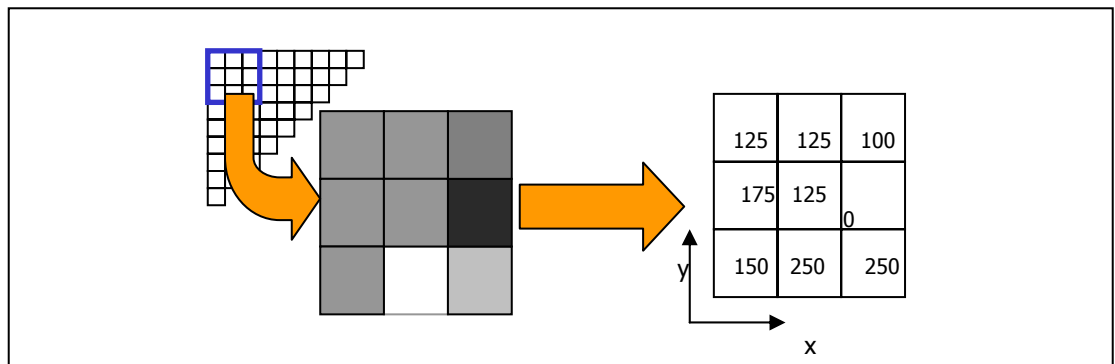


Fig. 5. Extraction 3x3 pixels window from image gray value.

3. For computing orthogonal effects due to spatial variation. The function [f_{xy}] can

$$[f_{xy}] = \sum_{i=0}^{n-1} \sum_{j=0}^{n-1} Z_{ij} \hat{P}_i \hat{P}_j^T \quad (1)$$

be approximated by a set of orthogonal vectors P_i and P_j and spatial variation coefficient Z_{ij} :

4. Define a matrix M consisting of orthogonal vectors P_1 and P_j , and for 3x3 pixel image region, M can be [14]:

$$[M] = [P_1 \quad P_2 \quad P_3] = \begin{bmatrix} 1 & -1 & 1 \\ 1 & 0 & -2 \\ 1 & 1 & 1 \end{bmatrix}$$

where the numbers used for P_i and P_j can be arbitrary numbers, as long as they are orthogonal each other. Hence

$$[f_{xy}] = [M] [Z] [M]^T \quad (2)$$

The orthogonal effect can be computed as

$$[Z] = ([M]^t[M])^{-1} ([M]^t[f][M]) ([M]^t[M])^{-1}$$

5. Using similar matrix manipulation, mean square of spatial variance can be obtained:

$$[Z^2] = ([M]^t[M])^{-1} ([M]^t[f][M])^2 ([M]^t[M])^{-1} \quad (3)$$

$$[Z^2] = \begin{bmatrix} Z_{00} & Z_{01} & Z_{02} \\ Z_{10} & Z_{11} & Z_{12} \\ Z_{20} & Z_{21} & Z_{22} \end{bmatrix}$$

6. $A = [Z^2_{01}, Z^2_{02}, Z^2_{10}, Z^2_{20}]$ were variances due to the main effect and $B = [Z^2_{11}, Z^2_{12}, Z^2_{21}, Z^2_{22}]$ were variances due to the interaction effect. The main effect appears when the one factor is set to be uniform and the other factor set to be varied. The interaction effect appears when both factors were varied. For the image, the factors will be the gray scale variation in x and y coordinates.

The existence of significant tonal variation over a small image region indicates the presence of micro textures. Since the two factors (spatial coordinates) x and y do not operate independently and the effects of one is dependent on the level of the other, texture characterization is done based on the fact that texture causes interaction effect more significantly than the main effects. In order to cover this, Bhattacharyya and Ganesan [4-6] proposed the following conjectures as illustrated in Fig. 6:

- a. For a texture region, each interaction mean square (set A) does not estimate the same variance (need to be more divergent)
- b. For a texture region, each main mean square (set B) may estimate the same variance (need to be more convergent).

These conjectures are applied to test whether the image region has texture or not.

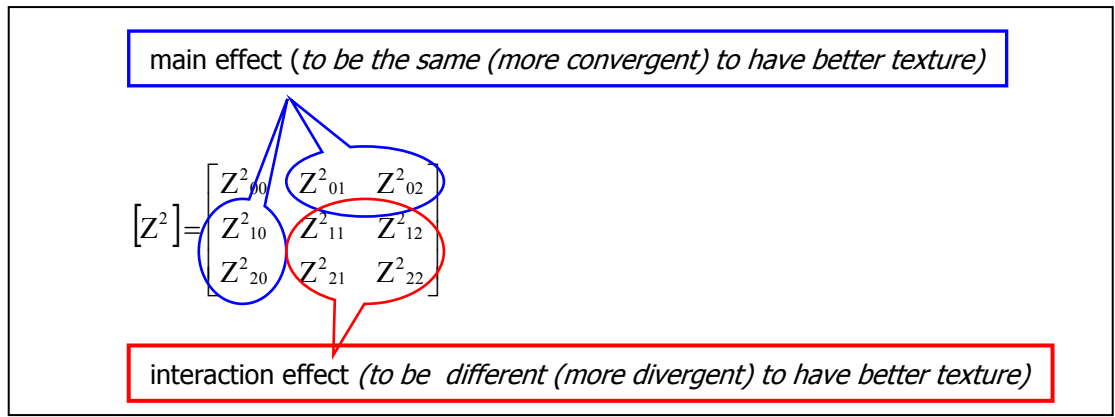


Fig. 6. Illustration of requirement of texture appearance for each effect.

7. Perform a statistical test to check the homogeneity of variances using Nair's test for sets A and B to see if the texture exists. The Nair's test is presented in detail at Appendix A [15].

Following each conjecture above, if all the four variances at each set do not validate Nair's criteria then eliminate one variance at a time and perform the test again. At least there must be two variances present. If no variances present, it is concluded that no texture region exists.

8. Calculate mean square error variance (msv) of main effect variance (B) that passes Nair's test:

$$\text{msv} = \frac{\sum Z^2_{i,j} \in U}{\|U\|} \quad (4)$$

where U is homogenous variances (variances from main effect that pass Nair's test) with $||U||$ is number of the variances from set A that pass Nair's test.

9. Besides the main effects used at step 8, the significance of the other main effects (the mean squares of which are not estimates of the same variance) and all the interaction effects towards their contribution to the experiment are evaluated by conducting another statistical test called the F-ratio test of the mean squares corresponding to the main and interaction effects against the mean square error variance.

$$F_{\text{calc}} = \frac{\text{Each spatial variance of A \& B}}{\text{msv}} \quad (5)$$

If F_{calc} value for one variance falls below the tabulated values at F-ratio test table as presented at Appendix B [16] at certain confidence level and degree of freedom, the corresponding position at image pixel region p_i is set to be 1, otherwise 0.

At the end we will have a matrix consisting of values of 0 and 1 and shown as s_0 to s_8 :

$$s = \begin{bmatrix} s_0 & s_1 & s_2 \\ s_3 & s_4 & s_5 \\ s_6 & s_7 & s_8 \end{bmatrix}$$

The summary of transformation of window region is shown in Fig. 7.

10. Based on matrix established at step 9, compute the pronum (x_i) for the image region as $\text{pronum} = \sum s_i (2^{i-1})$, the range will be between 0-255. Pronum is the local descriptor for micro textures for the quantified local properties of a micro texture at the center pixel of the [f]. Higher number of pronum represents more edges have been detected, and finer texture as described in Fig. 2.
11. Repeat the procedure by sliding the matrix 3x3 pixels to the adjacent pixel so that the whole image is mapped into an array of pronums.
12. Appearance of different pronums and their recurrence reflect the variation of possible combinations of orthogonal effects. Different textured images will have

difference occurrence of these pronums. These variations can be shown using the graph of the frequency of occurrences of pronum or prospectrum ($F(x_i)$) as the representation of the whole texture image (x_i is the pronum value ranged 0-255). Sample result is shown in the Fig. 8.

13. Compute the weighted mean values of the prospectrum graph.

$$M = \frac{\sum_0^{255} x_i F(x_i)}{RC} \quad (6)$$

RC is the total number of pixels in the image (total row times total column).

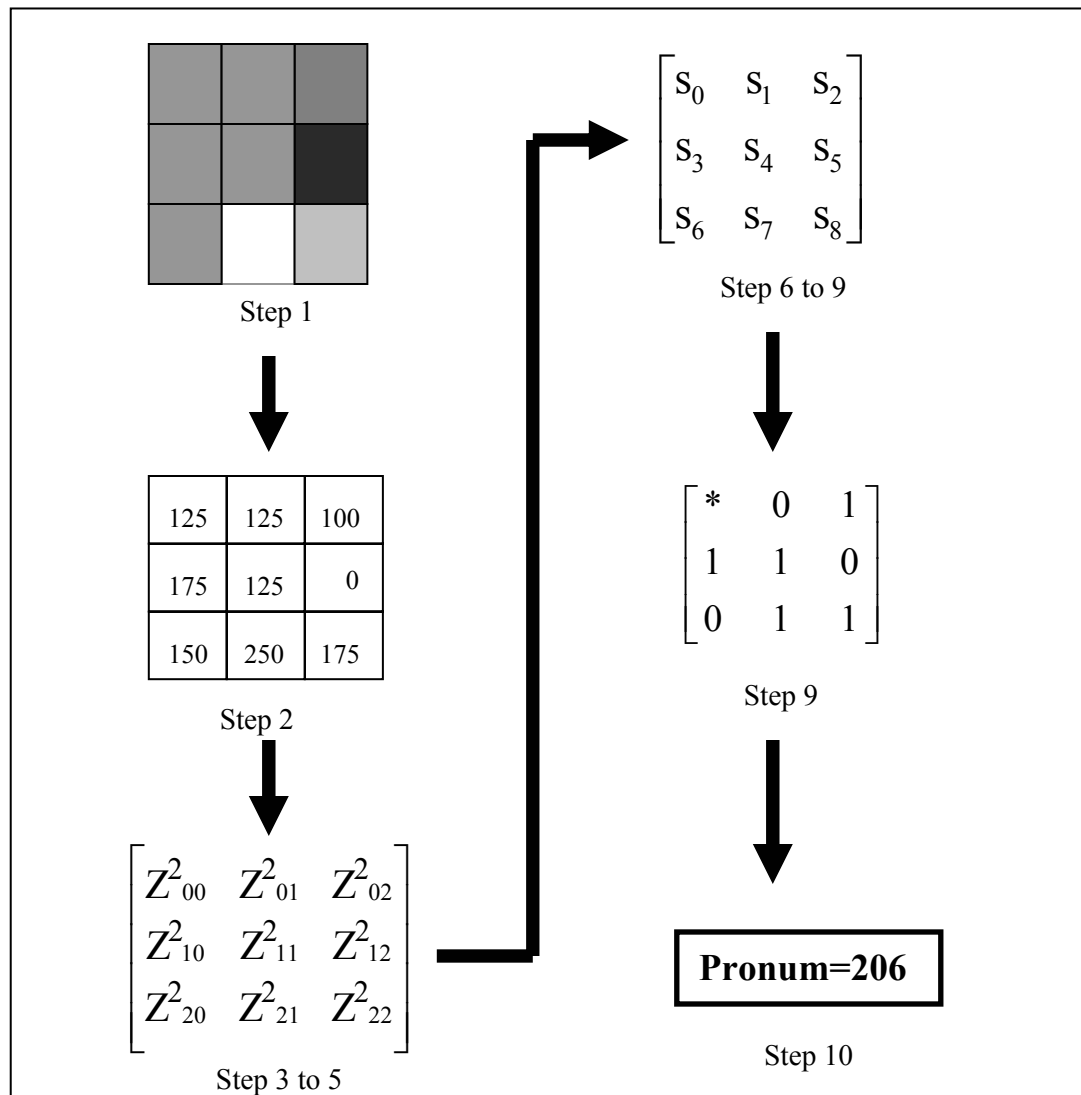


Fig. 7. Transformation of 3x3 pixels window to become pronum (local texture descriptor).

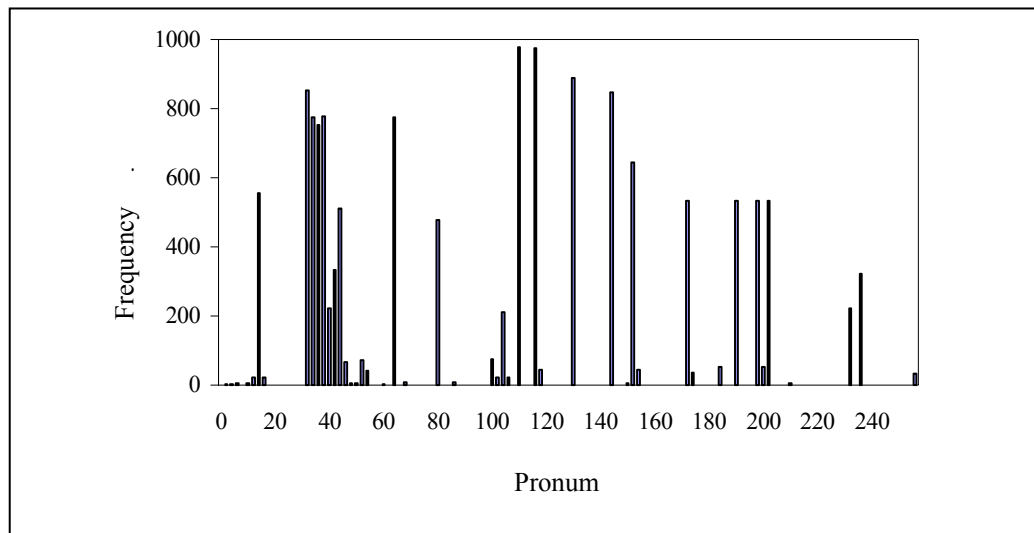


Fig. 8. Sample results of prospectrum (global descriptor of texture).

CHAPTER III

CRITICAL LITERATURE REVIEW TO FIBER DISPERSION

3.1. Introduction

The Chinese is believed to invent the technique of papermaking about twenty centuries ago. Around the year of 750 AD the battle fought between the Muslims and Chinese at Samarkand in Turkestan spurred the development of paper outside China's region [17]. While basic principal of papermaking has no significant change since then, the research development to achieve better quality paper and more efficiency production seem never ends. One aspect of paper quality is how well the fibers are dispersed or distributed inside the sheet. A flocculation of the paper fibers described as localized fibers compound is the opposite of the dispersion and clearly is not favorable during the papermaking. Figure 9a shows how one can observe the fibers in their final form in a sheet of paper. When a sheet of paper that is hung over a source of light, one can see the some part of the light transmitted by microstructure of the sheet that is formed by fibers. Figures 9b and c describe these fiber structures while they are still in pulp condition, each at different magnifications.

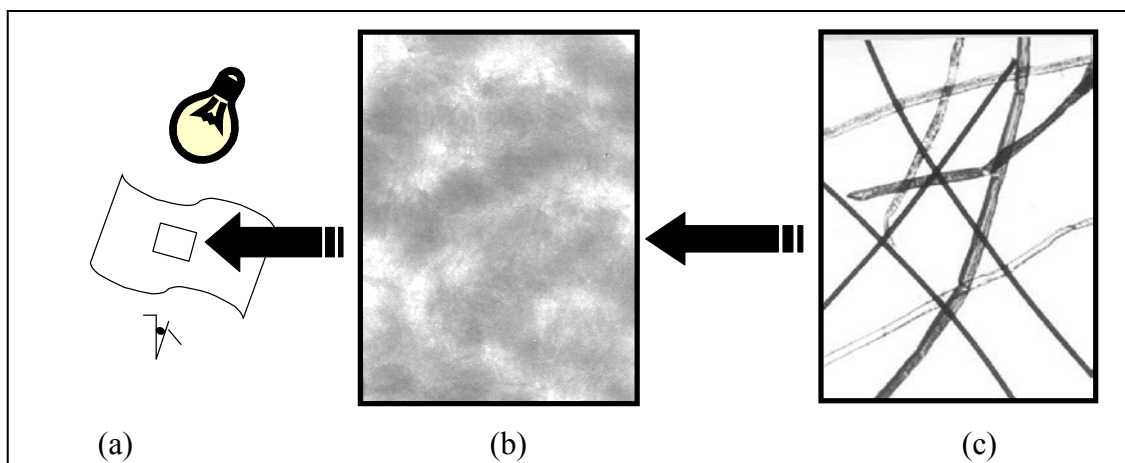


Fig. 9. Description of the fiber in paper sheet.

To improve the dispersion of fibers it is important to understand the fiber pulp suspension stage inside equipment called the headbox during the paper production as described in Fig. 10. A headbox is designed to regulate the turbulent flow of pulp suspension and force the flow out as a thin flat turbulent jet to the wire mesh of fourdrinier for water drain process. Headbox becomes a critical place to determine whether the fibers are well distributed or not. The paper pressing processes beyond the headbox and fourdrinier devices are not of interest in this literature review since the processes become insignificant in fiber formation. Extensive studies have been carried out to achieve a good paper formation. Mason [18] concluded two major factors affecting fiber flocculation: mechanical and chemical factors. Since then many theories and postulates have been developed to explain the fiber flocculation mechanisms for both factors. Mechanical factors describe the geometry property of the fiber while the chemical factors describe the surface properties of the fiber.

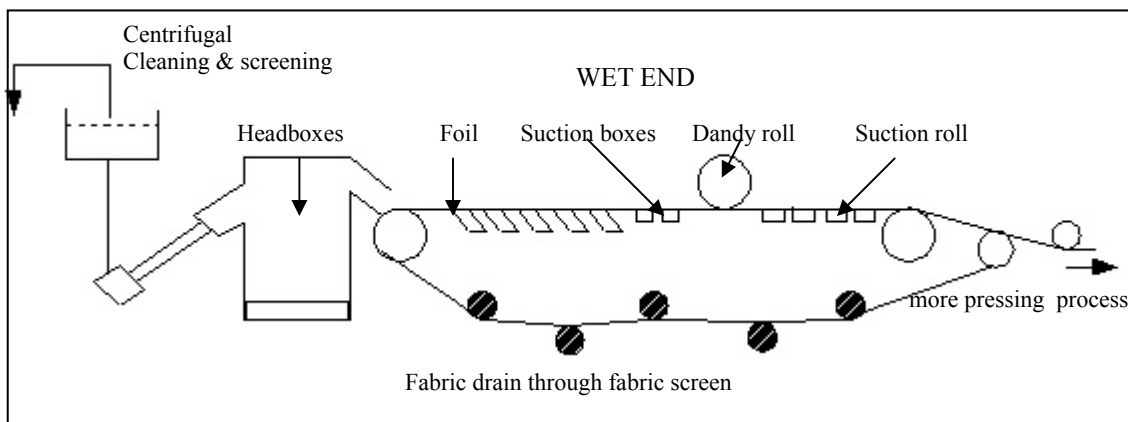


Fig. 10. Diagram of wet end of paper production

Since the early research by Mason and his colleagues [18-20], many scientists have been actively involved in conducting the experiments focused on mechanical factor of fiber flocculation as presented here. Some of chemical factors studied are also discussed. Since there exist number of studies for mechanical and chemical factors, a comprehensive literature summary of experimental, theoretical, and numerical studies will be useful to have introductory idea of fiber flocculation and also to further extend

the existing research scope. While the theoretical results are rare compared to the experimental results, three theoretical solution related to fiber flocculation are presented. In spite of an intensive development in fiber flocculation research, many unanswered questions are still left behind. Critiques and future developments presented also in this literature review meant to be guidance and tool to answer those questions.

3.2 Flocculation factors

3.2.1. Mason's contributions

Mason and colleagues [18-20] studied the suspended fiber flocculation under a shear flow. Their investigations resulted in three major issues that are still relevant and critical to fiber flocculation study these days. Firstly, Mason [18] introduced a concept called dynamic equilibrium of the floc size. Accordingly, the level of shear rate will be critical in determining the “steady state” size of the flocs formed. Moreover, during the forming process, the flocs will continuously break down and build up under the given shear rate. This concept will be discussed more thoroughly in section 3.5.a. Secondly, it is believed that there exists a concentration level that becomes a buffer of two different types of fiber collision mechanism: forced and chance collisions [18]. This concentration is called critical concentration (C_c) [18] that is defined in Eq. (7). The critical concentration is defined as the ratio of the actual volume of the fiber to the volume of an imaginary sphere with the diameter equals to the length of the fiber (L). Above a critical concentration, the fiber will not be able to rotate freely because of insufficient spacing between the fibers. In this upper concentration, the fiber collision is called forced collision while below the critical concentration is called chance collision.

$$C_c = \frac{3}{2} \left(\frac{D}{L} \right)^2 \quad (7)$$

where L and D are length and diameter of the fiber respectively.

The third important contribution is that flocculation factors can be categorized into mechanical and chemical conditions [19]. The mechanical part involves the geometrical shape of the fibers while the chemical part involves the surface condition of the fibers. It is found that the mechanical factors are not only easier to test it but also to

explain its mechanism compared to the chemical factors. It was concluded that the mechanical factors tend to be a dominant force to determine the fiber flocculation [20].

3.2.2. Mechanical factors

The mechanical factors can be sub-divided mainly into the effect of the fiber and fluid characteristics. The fiber characteristics include the length (L), diameter (D), aspect ratio (L/D), coarseness, curliness, stiffness, the present of hook, splits, surface roughness, and others. The fluid characteristics include the fluid shear rate, viscosity, velocity, turbulent, and other aspects like density and time exposure to the shear rate. Effect of each factor on fiber flocculation is followed.

a. Aspect ratio

The aspect ratio of fibers is considered to integrate the individual effects of the fiber length (L) and diameter (D). Kerekes and his colleagues [21-24] introduced the concept of crowding factor (n_{crowd}) as shown in Eq. (8) that has resemblance in some manners to the aspect ratio. The crowding factor describes the number of fibers that are packed inside a sphere that has a diameter equivalent to the fiber length. The crowding factor, that is derived by extending the Mason's critical concentration concept in Eq. (3.1) relates the fiber length (L), diameter (D), aspect ratio (L/D), and suspension volume concentration (C_{vol}) into one formula.

$$n_{\text{crowd}} = \left(\frac{2}{3}\right) \left(\frac{L}{D}\right)^2 C_{\text{vol}} \quad (8)$$

Kerekes and Schell [22-23] continued the study used this concept to relate the effect of fiber length to flocculation. They used various nylon and pulp fibers subjected to cyclic flows of turbulence. They determined the degree of flocculation by taking photos, which were quantified through an image analysis. This image analysis would give two parameters: contrast intensity (I) that measures the image brightness variance and specific perimeter (S) that measure the “grain” of the texture of the image.

They found that, contrast intensity increased with the fiber length while the specific parameter (S) decreased with increasing fiber length. The study showed that the flocculation increased with fiber length, aspect ratio and crowding factor increased. They concluded that the increase in aspect ratio leads to the increase in the degree of possible contacts between fibers, and in turn can lead to larger floc sizes.

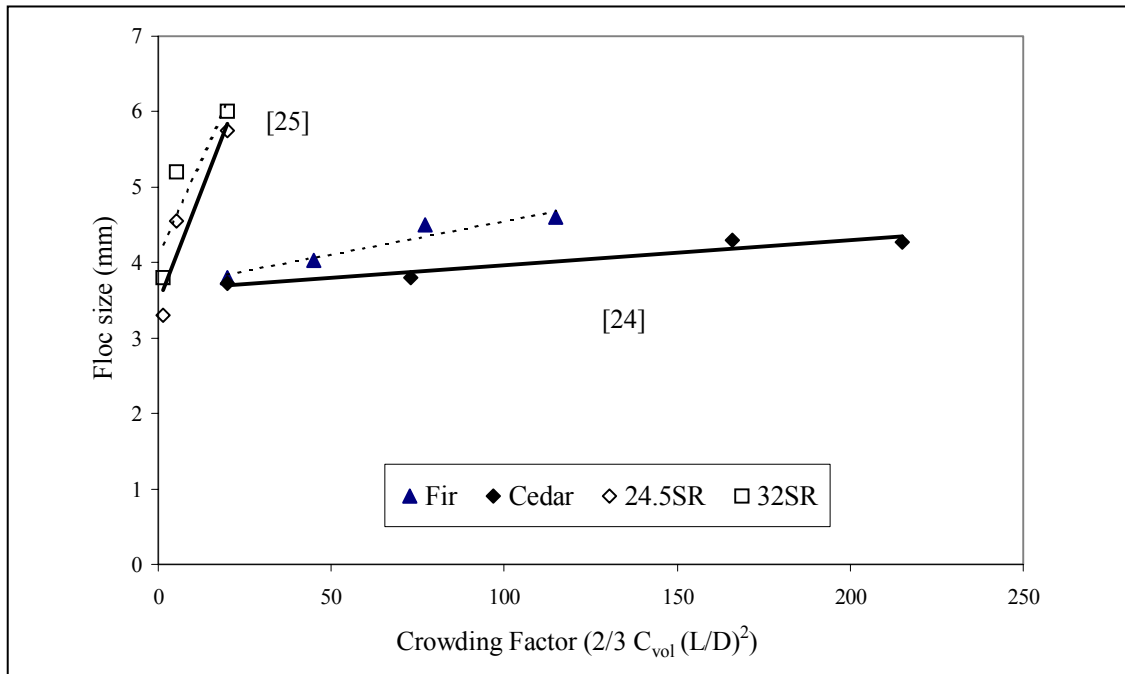


Fig. 11. Crowding factor effect on the fiber flocculation at two different parameters: coarseness and beating rate.

BeghELLO and his colleagues [25-28] further examined several fiber flocculation factors including aspect ratio affect to the flocculation using spectral analysis of photographs taken during the experiment [28]. The fiber material used was commercially bleached sulphate softwood pulp. Their conclusion agreed well with results shown by Kerekes and Schell [22,23]. BeghELLO and Eklund [24] noted that fiber length encourages the fiber to have more flexibility and the flexibility exerts a large influence on the flocculation process by building more entangled networking. Figure 11 shows an example work by BeghELLO and Eklund [25] and Kerekes and Schell [24] describing the effect of the aspect ratio to the flocculation. BeghELLO and Eklund [25]

analyzed the crowding factor effect at two different beating rates while Kerekes and Schell [24] studied at two different coarseness level of the pulps. Beating rate and coarseness will be discussed later on the review. Figure 11 shows that as the crowding factor increases, the floc size also increases.

Other studies on fiber length effect also have been done by the: Hubley et al. [20] and Jokinen and Ebeling [29]. Both results persistently showed that fiber flocculation would increase with the increase of fiber length.

b. Fiber coarseness

The fiber coarseness is defined as the ratio of the fiber mass over the fiber length. When a constant fiber diameter is assumed, the fiber coarseness can be treated similar to the density of the fiber since the density can be represented by coarseness per unit area. Kerekes and Schell [24] studied the effect of the coarseness on fiber flocculation using cedar (coarseness= 12.3 mg/100 mm) and Douglas-fir pulps (coarseness= 25.1 mg/100 mm). They found that under constant fiber length, consistency, and crowding factor, the increasing coarseness could increase the flocculation as described in Fig. 11, by affecting the mobility of the fibers through three factors: number of fibers, degree of fiber bending, fiber stiffness. As the number of fibers inside the spherical volume with diameter L increase, sphere becomes more crowded and the fibers have a lower mobility. Similar to the fiber length effect, the coarseness increases the bending and leads to more entanglement while the stiffness makes each individual fiber harder to break and leads to more contacts between the fibers. These bending and stiffness parameters also certainly make the fibers moving less mobile.

The coarseness effect can possibly explain the reason, why the hardwood pulp (higher coarseness) tends to flocculate more aggressively compared with the softwood pulp (less coarseness) as shown by Tichy and Karnis [30] and Takeuchi et al. [31].

c. Fiber curl

Beghella and Eklund [25] also studied the effect of the fiber curliness. They measured the fiber curliness by using a parameter called Curl Index (CI) whose formula

is shown in Eq. (9) and description is shown in Fig. 12. They found that there was no significant effect of the curliness to flocculation level of the fibers as described in Fig. 13.

$$CI = (L/L_p) - 1 \quad (9)$$

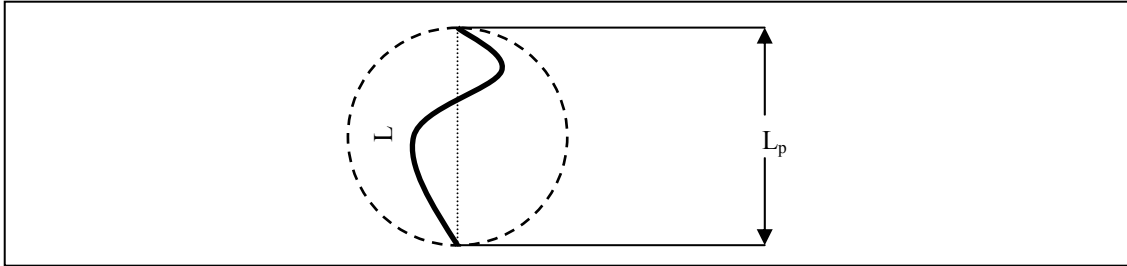


Fig. 12. Illustration for the concept of fiber curl.

Their results were unexpected since the higher curliness tends to increase the fiber flexibility and therefore the entanglement of the fibers was more likely occur. It is expected too that a higher Curl Index will increase the length of the fibers therefore as discussed early it will increase the level of fiber flocculation. Beghello and Eklund (1997) [25] unfortunately were not able to verify these theories.

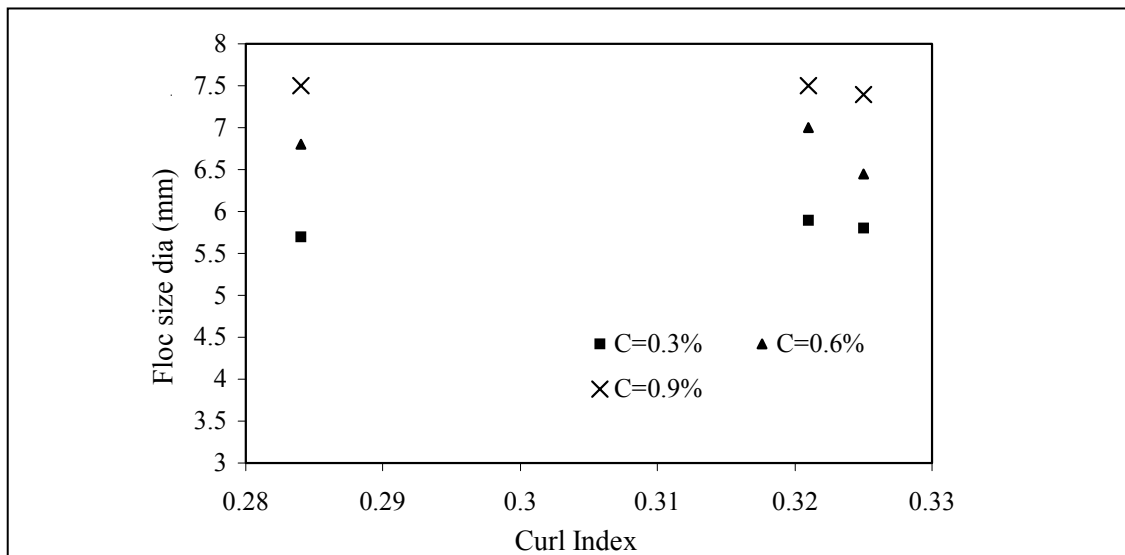


Fig. 13. Effect of the fiber curl on the fiber flocculation [27].

d. Fiber stiffness

Although it is mentioned above, the fiber stiffness still can be stand as different entity since there exist a situation at which the fiber has the same coarseness but different stiffness. Dotson [32] noted that longer, stiffer fibers tend to make larger, stronger flocs than shorter, more flexible fiber at the same mass density. Stiffness will have less slippage and more contact points between the fibers. Thus, it can be concluded that stiffer and more curvy of the fibers lead to more fiber flocculation.

e. Other mechanical factors from fiber characteristics

While our literature survey was not able to locate any published studies on the other factors such as hooks, splits, surface roughness of the fibers, these factors are expected to increase the flocculation as they increase the possibility of entanglement between fibers.

f. Consistency

Important feature of the crowding factor is the suspension consistency that describes the volume concentration level of the fibers inside a suspension. Kerekes and Schell [23,24], as previously mentioned, studied the effect of the crowding factor on the flocculation process. The higher consistency increases the flocculation by increasing the collision frequency of fibers inside the suspension as shown in Fig. 11.

Beghello and Eklund [26] reached the same conclusion as Kerekes and Schell [23,24], They used image visualization and analysis for the fiber rayons of 2,3, and 4 mm in length and 10,12, and 20 μm in diameter at different beating rate. Their work can be represented also as a function of crowding factor as shown in Fig. 11.

g. Shear rate

To examine the shear rate effect on flocculation Hubley et al. [20] generated a simple shear field in two concentric glass cylinders with the outer cylinder rotating. The fiber suspension was filled in between and a photocell attached to the outer cylinder captured transmission of the light-emitting beam from the inner side. The amount of

light transmitted through the suspension was assumed to increase with more flocculation since the well-distributed fibers will give more obstruction for the light to get transmitted. Their result as presented in Fig. 14 shows that the shear rate tends to decrease the flocculation rate. The shear rate tends to break up of the flocs easier, and as the shear rate increases, the size of flocs formed will decrease.

h. Velocity

Takeuchi et al. [31] studied the flow velocity effect on the fiber flocculation. As presented in Fig. 15, the result shows that the fluid velocity will decrease the degree of fiber flocculation. The high flow velocity can more effectively break the floc structures and reduce the flocculation.

Jokinen and Ebeling [29] also studied the velocity effect using pine and birch kraft. They used a laser light transmission method to measure flocculation under the suspension velocity of 0.15, 0.3 and 0.6 m/s. They found that for a 100% increase in flow velocities, the flocculation would decrease about 14%. This result again matches to the conclusion drawn by Takeuchi et al. [31] above. Another experiment by Tichi and Karnis [3.14] also drew the same conclusion.

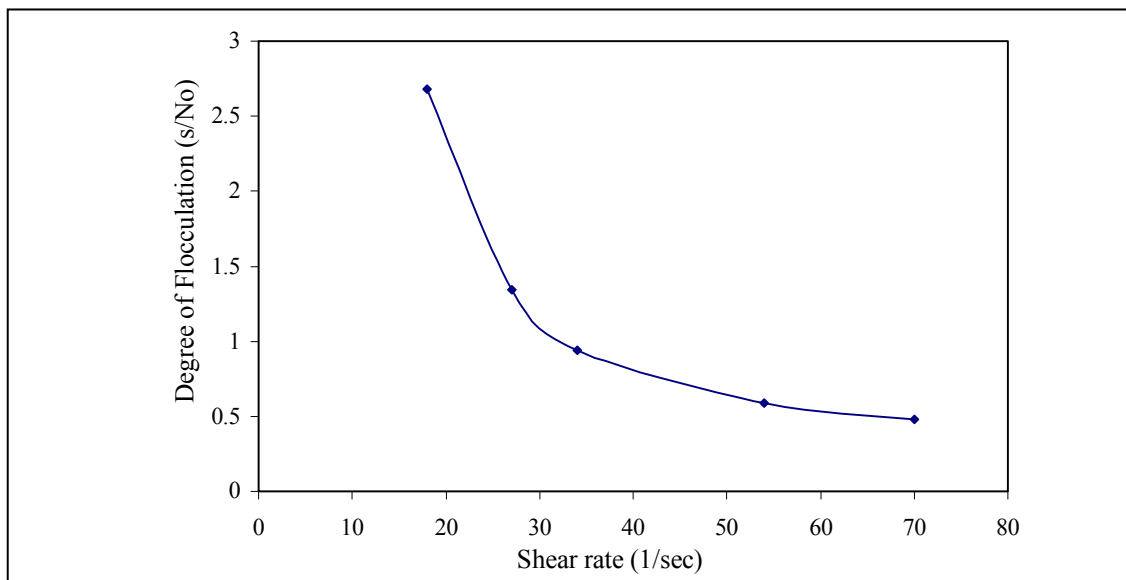


Fig. 14. Effect of shear rate on flocculation level [20].

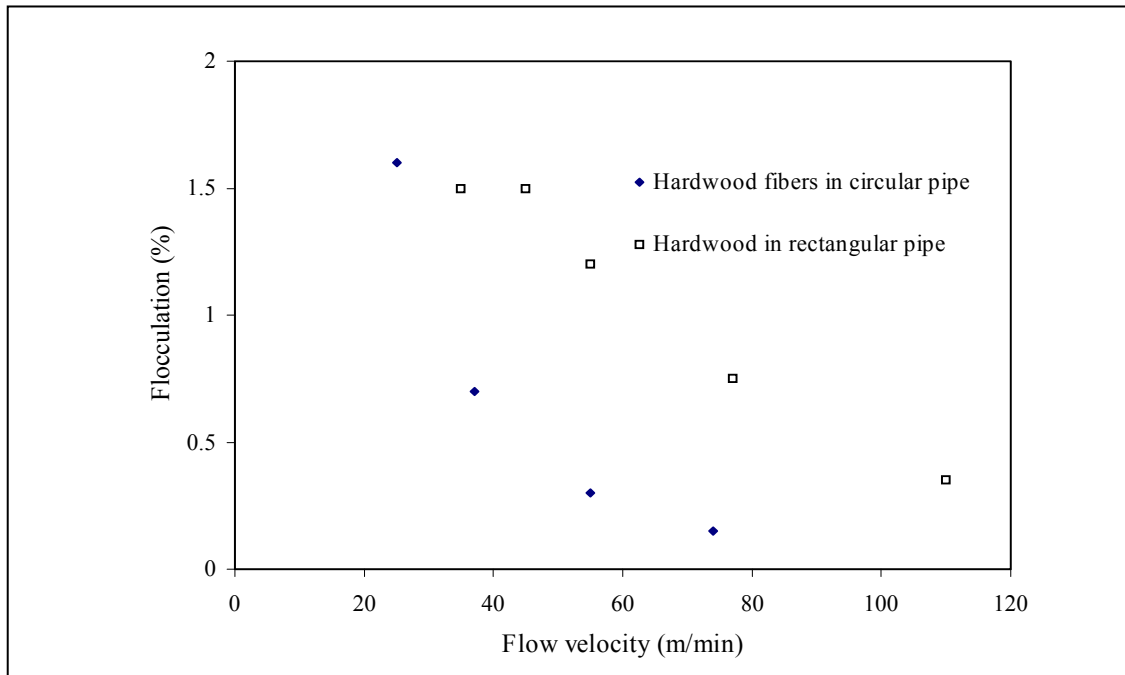


Fig. 15. Effect of velocity on flocculation level [31].

Hourani [33,34] indicated conflicting results on the velocity effect depending upon the fluid consistency and fiber length. At a certain range of consistency, the higher flow velocity helps flocculation while at different consistency level, the velocity factor reduces the flocculation. The presence of vortices favoring flocculation and the shears breaking the flocs are dependent on the consistency and fiber structure. All these factors might have a closer relation of one another than expected. Hourani [34] also noted that during the papermaking, generally it is accepted that higher flow tends to decrease flocculation at a proper range of consistency. The flow velocity, however, is limited by the paper mill conditions. The suspension becomes unstable when exceeding a certain flow velocity limit.

i. Viscosity

Zhao and Kerekes [35] studied the effect of the suspension viscosity on the flocculation by adding the sucrose into the solution. They found that the viscosity tends to decrease the degree of flocculation. While it is understood that the viscosity reduces the friction on the fiber surfaces, Zhao and Kerekes [35] postulated that the presence of

relative fluid motion is the one that determine if the flocs will occur and not the surface friction within the fibers. High viscosity fluids will impose low Reynolds number, therefore, giving high viscous shear on fibers. Thus, the relative motion in the system will decrease and the fibers will follow the relative motion more easily. This will tend to diminish flocculation, since when the flocs are formed, the higher viscous forces on fibers will tend to break the flocs. This postulation was offered after they found that there was no significant change in mechanical strength of fibrous network with increasing viscosity of suspending liquid. The insignificant change of the mechanical strength of the flocs network implies no significant surface friction changes due to the change of the fluid viscosity. Instead, viscosity helps dispersion through changing the dynamic of the fiber motion. Kerekes [36] furthermore introduced the fiber Reynolds number in Eq. (10) to relate the viscosity to how ease the fiber will follow the fluid flow. As described in Eq. (10), the collision within the fibers has higher possibility at high Reynolds number or at low viscous force.

$$\text{Re}_f = \frac{\rho D G_e L}{\mu} \quad (10)$$

where L and D are fiber length and diameter, G_e is the elongational strain rate, μ and ρ are the fluid viscosity and density.

Beghello and Eklund [25] conducted another experiment on the viscosity effect. They added CMC (carbomexymethanol) and sugar into the solution. As described in Fig. 16, their result also shows that the viscosity will reduce the degree of flocculation of the fiber.

j. Temperature

The suspension viscosity decreases with increasing temperature. To obtain good paper formation, high fluid viscosity is desired and so is the low suspension temperature.

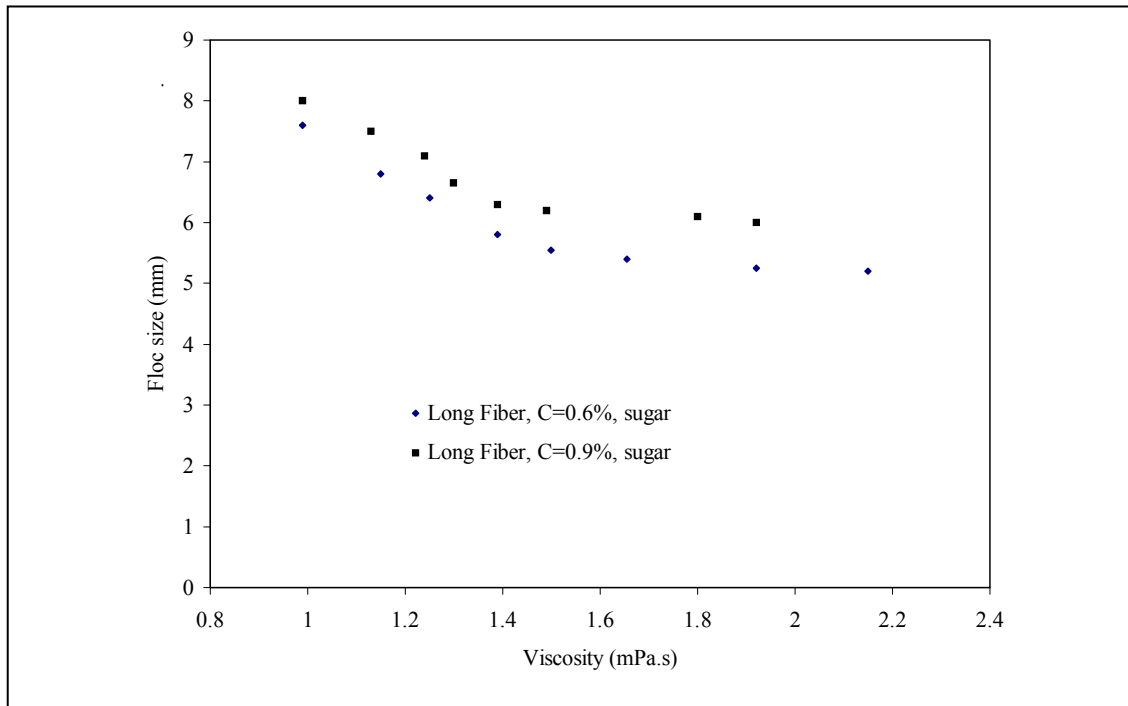


Fig. 16. Effect of viscosity on flocculation [25].

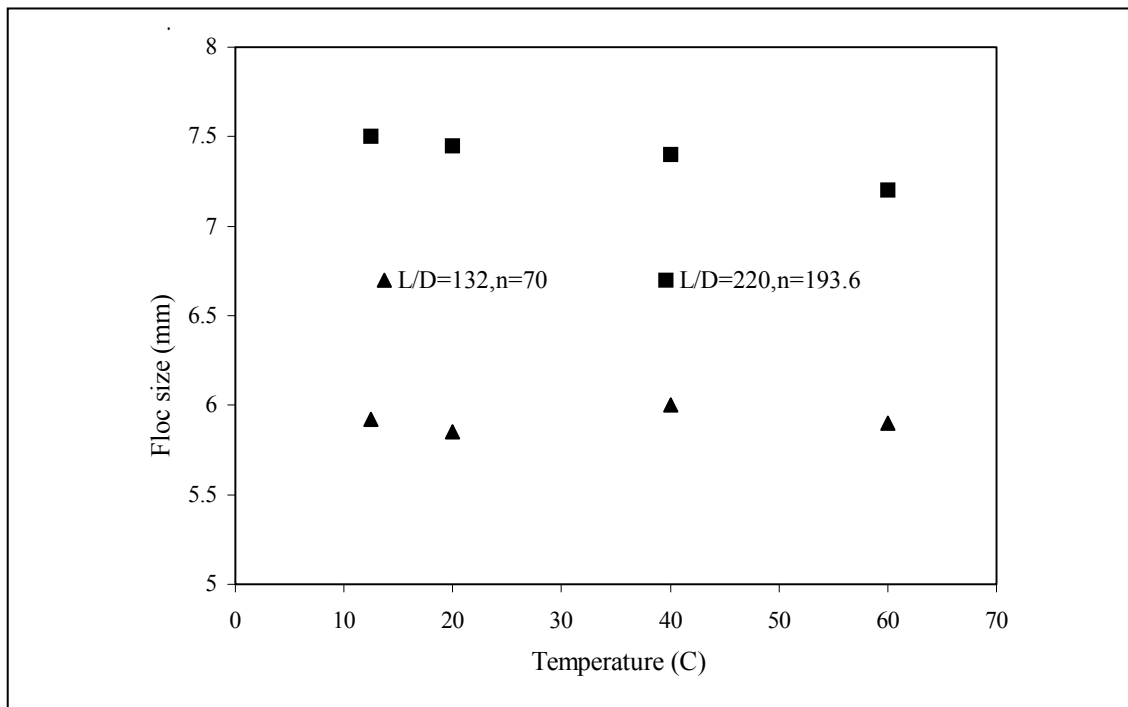


Fig. 17. Effect of temperature on flocculation [26].

Ersparmer [37] conducted an experiment to examine the temperature effect on flocculation. While he found that the temperature helps the flocculation, he questioned whether the temperature-viscosity relation would be the sole factor that could affect the flocculation. He proposed that the other factors such as the appearance of hydration film around the fibers that affects the colloid stability, that might be removed with the increasing temperature.

Hourani [33,34] concluded that lower temperature would reduce the flocculation. However, he noted that the use of low temperature to form better formation might conflict with the common papermaking practice of heating the stock to improve the drainage process.

A study by Beghella and Eklund [26] indicated that there is no significant change of flocs size for the temperature range of 10-60⁰C. They used nylon fibers to conduct their experiment. The result is shown in Fig. 17. Jokinen and Ebeling [29] conducted another study on the temperature effect. They found that there was no significant effect on the flocculation of pine and birch kraft suspensions at temperature range of 18-35⁰ C.

k. Turbulence

Robertson and Mason [18] found that increasing turbulent intensity and decreasing of eddies scale could reduce the size of pulp flocs. As the turbulent intensity gets higher, the fluid flow is more capable to break up the flocs. Smaller eddies will make it easier for fluid to penetrate to the inner region within fibers of the flocs and, therefore, the rupture process becomes easier to occur.

l. Beating rate

The beating is one of the important steps in to complete papermaking. The beating process itself tends to shorten the fibers and make them more flexible. 'Beating' is the term used to describe a process where pulp is mechanically agitated while in solution. The wet pulp is passed between rotors with bars or knives which compress the individual cells. Generally, chemical pulps respond to beating more easily with cells

becoming more flexible and compressing, while pulps with higher lignin content require significantly more treatment. Paper made from unbeaten pulp is bulky, porous and has less tensile strength than from beaten pulps. This is because unbeaten pulp fibers tend to be stiff and springy, and do not collapse as well when the paper mat is pressed

As presented before, the shorter and more flexible fibers tend to make less flocculation. Jokinen and Ebeling [29] conducted a study of the effect of beating rate to fiber flocculation. They used 100% bleached pine kraft beaten in both Valley Hollander and a Sutherland disc refiner. Their experimental results indicated that the change in beating rate did not change significantly the flocculation level as expected.

Beghello and Eklund [25] conducted a study on the effect of the beating rate of commercial bleached sulphate softwood pulp on fiber flocculation at the rate of 24.5 and 32 °SR. The result shown in Fig. 11 concluded that the beating rate had no significant role in changing the flocculation level.

m. Other mechanical factors from fluid properties

Other factors such as density of fluid have not been investigated thoroughly. For the time exposure to shear rate, Jagannadh [38] studied the strength of the flocs at different time exposure. Their results did not indicate comparison in term of flocs formation. Kerekes [36] as mentioned earlier introduced the concept of fiber Reynolds number representing how easily the fibers can follow the fluid flow. This fiber Reynolds number stated in Eq. (10) is proportional to the liquid density. If a fluid has low density, then the fibers will have a low Reynolds number where the viscous force is dominant. Therefore, the fibers will tend to follow the fluid flow more easily. During the flocculation, the temperature not only affects the viscosity but the density as well. No published literature has been found on the study of the suspension density effect on fiber flocculation. Similarly, the significance of Reynolds number for fiber flocculation has not been thoroughly studied to date.

3.2.3. Chemical factors

The significance of the chemical factors in flocculation have always been an intriguing issue, not only because of the nature of complexity, but also because of the fact that in many cases the mechanical and chemical factors exist simultaneously. Many scientists have been trying to dig into the mystery by postulating different theories. One important property of the fiber flocculation is cellulose surface charge of zeta (ζ) potential or electrokinetic forces [39]. Retention of fines and fibers can be increased through zeta potential control. In order to have flocculation, the zeta potential must be close to zero causing fibers attracted to each other. Researchers have been trying to modify the zeta potential by various methods but it seems that very small success have been achieved in understanding the real mechanism.

a. pH level

pH level determines if a substance, when dissolved in water, produces H_3O^+ (H^+) or OH^- . A substance that produces H_3O^+ (H^+) when it is dissolved in water is called an Acid and will be at low pH. It is a proton donor and an electron pair. On the other hand, a Base is a substance that produces OH^- when dissolved in water, and becomes a proton acceptor or an electron donor. Clearly, a Base will be at a high pH. During the flocculation process, pH factor could affect the zeta potential and produce an attraction force that is applied not only within the fibers but within the flocs as well [39].

Erspamer [37] conducted a study on the effect of pH on fiber flocculation. His study showed that for the pH range 4.0-7.2, the fiber flocculation remained relatively the same. It is not clear based on his result, if the attraction forces really do not exist or they do exist but not strong enough to appear.

Beghello et al. [27] conducted an experiment on the effects of chemical environment, pH, and electrolyte content. He added HCl or NaOH to control the pH of the suspension. Using rayon fibers of length 3 mm and a diameter of 12 μm , he showed that at the pH range of 5 to 9, there was no significant impact of pH on the floc sizes as shown in Fig. 18. Despite of the insignificant results, he believes that the pH variations

still exert a certain influence on the electrical double layer of the fibers, but not directly influencing the floc size, or at least not significant enough.

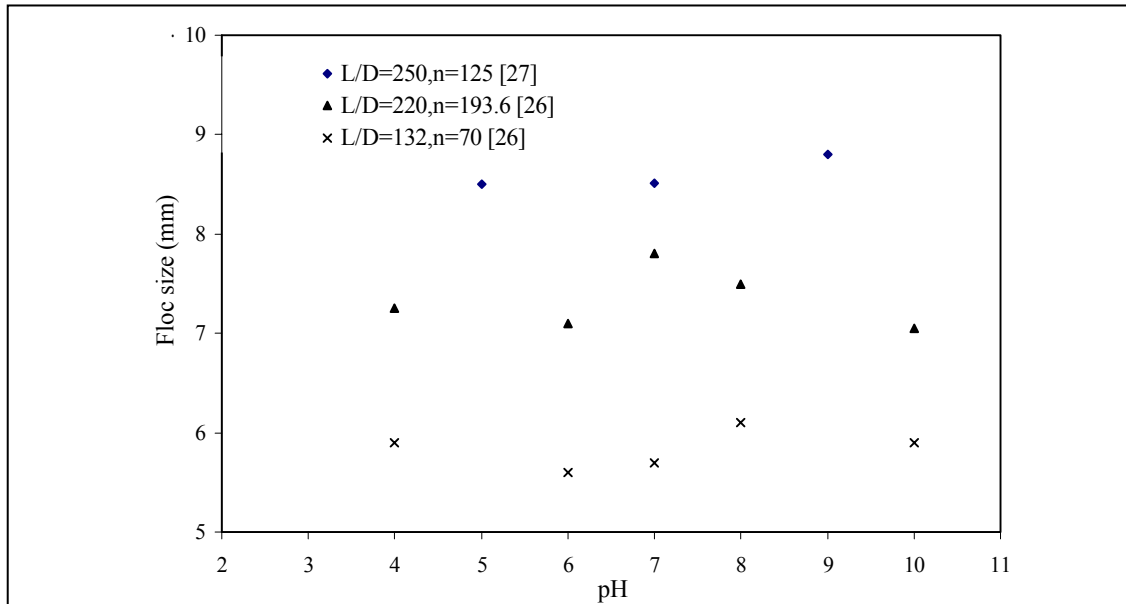


Fig. 18. Effect of pH on the flocculation level [26,27].

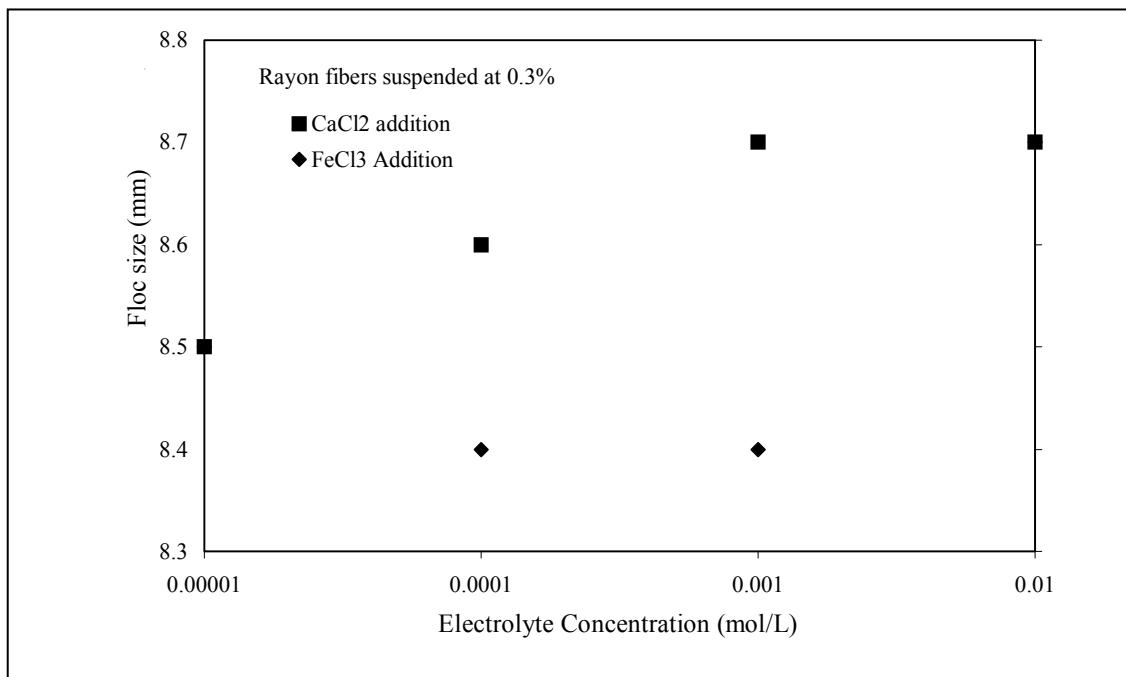


Fig. 19. Effect of electrolytes on the flocculation level [27].

Beghello [27] used NaCl, CaCl₂ and FeCl₃ to study the effect of electrolytes to fiber flocculation. The electrolytes used above do not appear to influence the flocculation process significantly as shown in Fig. 19. This is consistent with the conclusion derived by Strazdins [39].

Early investigation by Mason [18] also indicated that no significant effect of multivalent cations and their concentration on the degree of flocculation of sulfite pulp dispersed in water. After comparing his results with his other studies in mechanical factor of flocculation, Mason concluded that the adhesive forces due to the chemical nature between fibers play no important role in fiber flocculation process. Hubley and Mason [20] attempted to explain the flocculation phenomenon in terms of negative zeta potential but did not succeed.

b. Formation aid

People have been trying to invent formation aids (deflocculants) for not only for papermaking but also for other applications. However, depending on the application, the formation aids could be used on the other way around to encourage the flocculation (Flocculents). Zhao and Kerekes [35] divided the types of flocculants aids into three category: gums and mucilages, synthetic and natural polymers, and high viscosity liquid. The first class, gums and mucilages class, improves the uniformity by being adsorbed onto fiber surfaces and then lower the friction coefficient between fibers. It makes the slippage between fibers easier; therefore the fibers are easier to disperse.

Wasser [40] postulated that the second class, synthetic and natural polymers help the paper uniformity by inducing a change in the rheological properties of the suspending medium and results in formation improvement. Effective polymeric additives also produce unusual flow behavior leading to better dispersion. Lindstrom [3.25] also believed that long-chain polymeric additives, which in some cases works as drag-reducing agent, achieve their effect by increasing the elongation viscosity of suspending, water. Lindstrom [41] also noted that in small amount, polymer would not be sufficient to lower the surface friction of the overall fibers.

Soszynski and Kerekes [42,43] investigated the third class of the formation aid by adding sucrose to water at high concentration. They found that the sucrose prevent the flocculation of nylon fibers under flow condition at which flocs would form when no sucrose exists. The sucrose tends not only to make the fibers follow the flow more closely so that the collision frequency between fibers decreases but also to reduce the relative velocity within fibers.

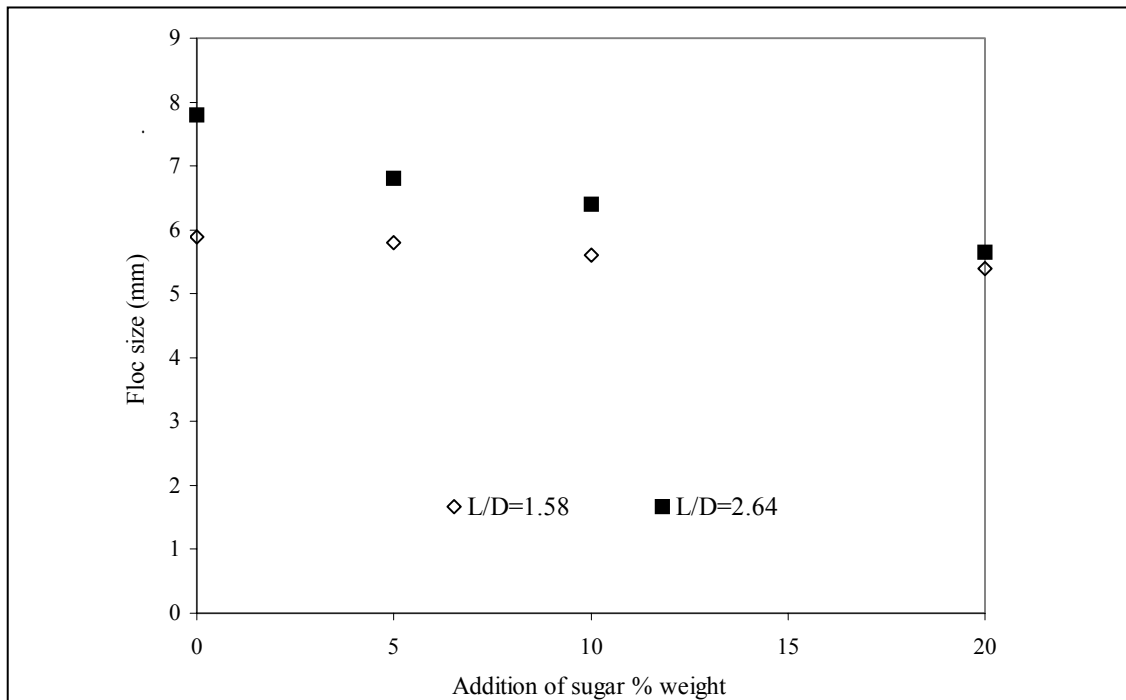


Fig. 20. Addition of flocculent to the fiber flocculation [25].

Beghello [25] conducted also the research on the effect of the fluid viscosity to fiber flocculation by adding the carbo mexymethanol (CMC) into the solution. He found a similar conclusion to the results presented by Soszynski and Kerekes [42,43], that the viscosity tends to decrease the fiber flocculation as presented in Fig. 20. Although for the last class of the formation aids, the explanation has no direct implication on the chemistry of the fibers, it will be interesting to examine whether the chemistry on the fiber gets affected at different values of viscosity.

Further studies should be done to determine the more rigorous reasons for the chemical factor affecting the fiber flocculation. An extensive study investigating on how dominant the chemical factors would be compared with the mechanical factors also needs to be conducted. The General conclusion of previous studies is that the chemical factor is not significant to fiber flocculation compared to the mechanical factor. However, how insignificant the chemical factor compared to the mechanical factor is still need to investigated

3.2.4. Summary of mechanical and chemical factors

Tables 1 to 3 summarize the discussion of the mechanical and chemical factors to the fiber flocculation. The bracket shown in the “RESEARCHERS AND RESULTS” column represent whether the study found increase (+), decrease (-), or no change or unknown [?] of the fiber flocculation due to each factor.

Table 1. Mechanical factors that influence the fiber flocculation from the fiber characteristics.

No.	FIBER CHARACTERISTICS	RESEARCHERS AND RESULTS
1	Length of fiber	Mason[18] (+), Beghello[25] (+), Kerekes & Schell [23] (+), Beghello[27] (+), Jokinen & Ebeling[29] (+)
2	Diameter of fiber	Beghello[27] (-)
3	Aspect ratio (L/D)	Beghello[27] (+),
4	Coarseness (m/L)	Tichi and Karnis[30] (+), Takeuchi et.al.[31] (+), Kerekes & Schell [24] (+)
5	Stiffness	Dodson[32] (+)
6	Fiber curl	Beghello[25] (+),
7	Others: hooks, splits, surface roughness	

Table 2. Mechanical factors that influence the fiber flocculation from the fluid characteristics.

No.	FLUID CHARACTERISTICS	RESEARCHERS AND RESULTS
1	Consistency	Wollwage [44] (+), Robertson et al.[19] (+), Beghello [25] (?), Beghello [27] (+),
2	Shear rate	Mason [18] (-)
3	Fluid viscosity	Beghello [25] (-), Zhao and Kerekes [35] (-)
4	Temperature	Wollwage[44] (+), Beghello [25] (?), Jokinen & Ebeling [29] (?)
5	Rate of beating	Wollwage [44] (?), Beghello [25] (-),
6	Fluid velocity	Tichi and Karnis [30] (-), Takeuchi et.al.[31] (+), Kerekes [36] (-), Jokinen & Ebeling [29] (-)
7	Turbulent intensity and eddies' size	Duffy and Norman [45] (-)
8	Other: time exposure, liquid density	

Table 3. Chemical factors that influence the fiber flocculation.

No.	CHARACTERISTICS	RESEARCHERS AND RESULTS
1	PH	Beghello [26] (?), Beghello [26] (?), Jokinen & Ebeling [29] (?)
2	Electrolytes	Erspamer[37] (-), Wasser [40] (-), Beghello [25] (?), Beghello [26] (?)

3.3. Theoretical models related to the fiber flocculation

Many scientists have proposed various mathematical models for fiber flocculation, although a complete quantitative model to predict the state of fiber flocculation is still under development. This section will discuss different perspectives: thermodynamics modeling, and analytical modeling.

a. Hourani's thermodynamics model

Hourani [33,34] tried to provide more understanding of the chemical factor by presenting a mathematical model to quantitatively describe the flocculation process. The model is based on the mass action law and on the energy spectrum of turbulent flows. The mass action law allows to evaluate the thermodynamics relations, properties, and the population density of each possible floc in the pulp. The free energy of fiber formation then can be calculated to obtain the relation between the number of flocs and flocs size as:

$$X_N = \exp \{N[(-\Delta G_N^0/RT) + \ln X_{fd}]\} \quad (11)$$

where X_N is the weight fraction at flocs with N fibers, N is the number of fibers in flocs, R is the gas constant (8.314 kJ/kmol K), T is the temperature, X_{fd} is the weight fraction of dispersed fibers, and ΔG_N^0 is the total free energy of excluded volume, surface, compression, electrostatic, and adsorption free energies. The model was developed based on the previously developed theory on surfactant aggregate formation [46]. The model gives a new perspective from thermodynamics point of view about fiber flocculation. Figures 21 and 22 show examples of his works. Figure 21 describes how electrostatic field affects the distribution of floc size. Figure 22 describes the floc size distribution for both theoretical and experimental results of two different types of pulps. The theoretical results match well for softwood pulps while the theoretical results slightly underpredict the experimental data for hardwood. Notice also that the results agree with the conclusion that coarser pulp (hardwood) yields higher floc size as concluded previously.

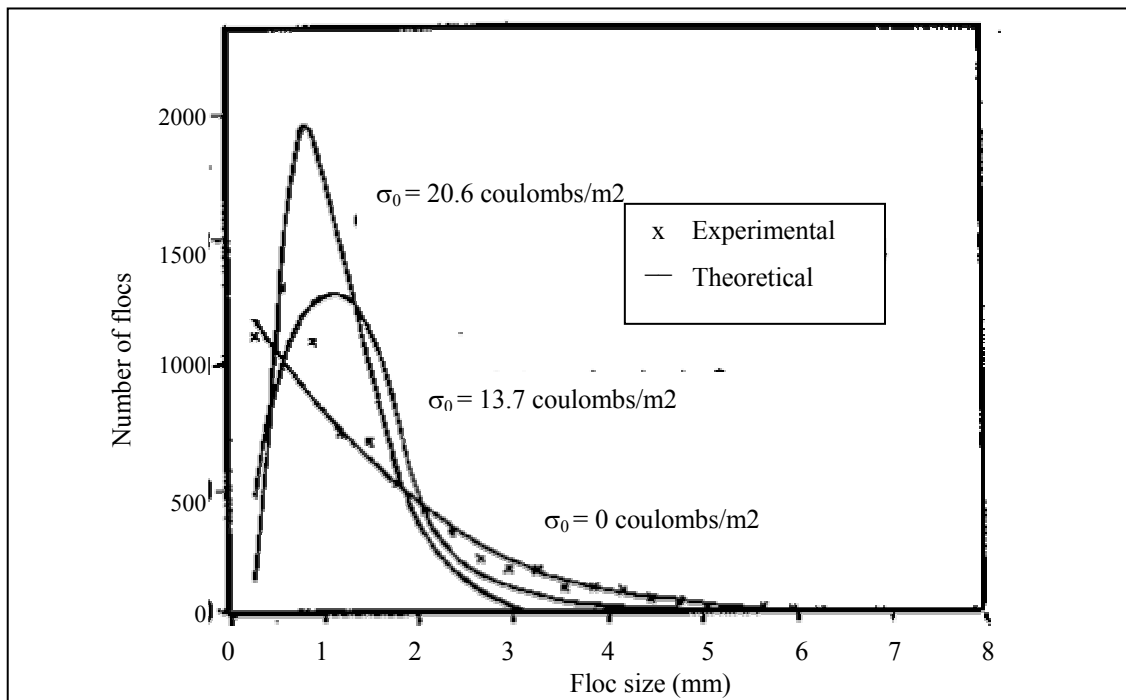


Fig 21. Sample result of Hourani's thermodynamics model [33]: the electrostatic field effect on floc size distribution.

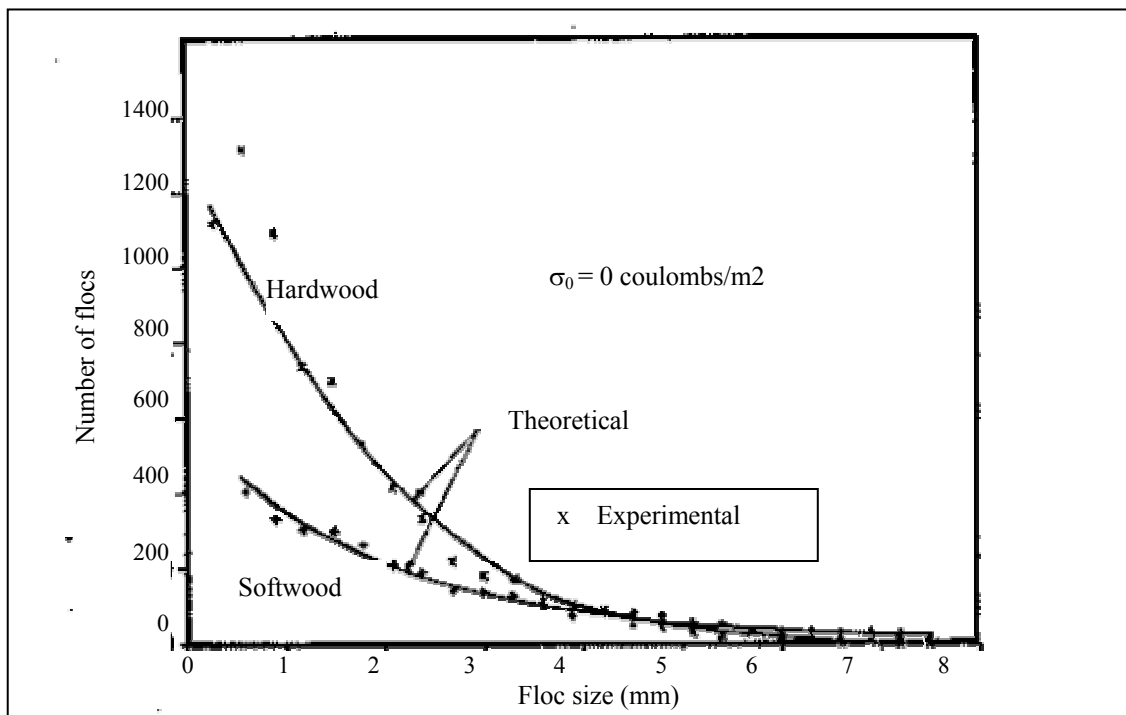


Fig. 22. Sample result of Hourani's thermodynamics model [33]: the comparison result between hardwood and softwood.

b. Olson and Kerekes dispersion coefficient calculation

Olson and Kerekes [47] proposed equations of mean and fluctuating velocities in rotation and translation of rigid thin inertialess fibers moving in a turbulent fluid. The rotational and translational dispersion coefficients were also derived. Their results show that as the ratio of the fiber length to the integral length scale of turbulent fluctuation increases, the dispersion coefficient decreases. It agrees fairly well with the experimental data shown previously in that the increasing length of the fiber enhances the flocculation. Figure 23 shows an example of his works. Figure 23 describes that the translational movement of the fibers apparently has higher effect of dispersion than the rotational movement. It is agreeable when knowing that the entanglement of fibers would occur more easily when the fibers' orientation is not uniform due to the fiber rotation.

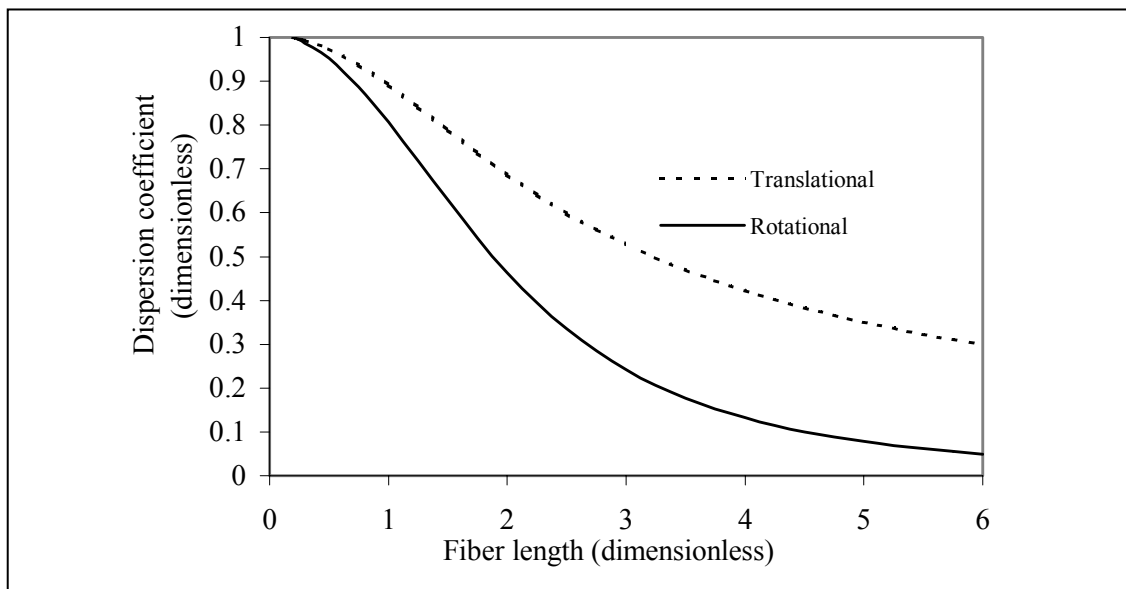


Fig. 23. Variation of dispersion over length of fiber [47].

The mechanical and chemical factors are the main parts of fiber flocculation. The study of these factors on fiber flocculation should be continuously studied. Although

some factors, such as fiber aspect ratio and fluid viscosity have been extensively studied and perhaps additional study using a new equipment or theory will be highly demanded. Other factors, especially chemical factors, may need more attention in future studies. It must be mentioned here that the flocculation factors indicated above might not include all the essential factors. More importantly is that some unknown factors may exist, but not yet discovered or studied. Theoretical models on fiber flocculation in a turbulent flow have been proposed in several studies, but there are still plenty unexamined areas that have not been observed yet or maybe even unobservable.

3.4. Future developments and research

The research and study on the subject of fiber flocculation have been done extensively. However, there is still a lot of the promising studies need to be conducted. A discussion of some aspect of fiber flocculation that will be interesting to study is presented below. Parts a and b are subject that many researchers have spent a lot time on. Unfortunately there are unanswered question regarding these subjects. Parts c to e represents some subjects that still need to be investigated and not many resources are found in these subjects.

a. Concept of dynamic equilibrium vs. static equilibrium

Mason [18] proposed a dynamic equilibrium concept in flocculation process for dilute suspensions in turbulent regime. This concept indicates that during the flocculation process, an individual floc is continuously formed and dispersed under cyclic process while the amount of fibers inside the floc remains the same. Kerekes and his colleagues [22,36] were questioning if the “true” concept of dynamic equilibrium does exist. They postulated that the floc itself might undergo a static equilibrium at which the flocs remain as stable intact entities or maybe even a transient equilibrium as shown in Fig. 24. On the static equilibrium state, once a floc reaches its steady state size at which there are no fibers will be added ($FA=0$) into nor released ($FR=0$) from the floc. On the opposite side, the dynamic equilibrium describes a state at which a floc undergoes a state that the fibers added ($FA=N$) into or released ($FR=N$) from the floc has

the same amount of the numbers of fibers that form the floc (N fibers). Between these two states, there is a transient equilibrium at which the fiber added or release will be between the amount 0 and N fibers. Kerekes [23] pointed out that the flow condition for dynamic equilibrium is not known and also the location and fiber properties for each equilibrium still need to be studied. Some models and theories based on the dynamic equilibrium assumption, for example, Hourani's thermodynamical model, then would need to be modified and extended when all three type equilibrium are considered.

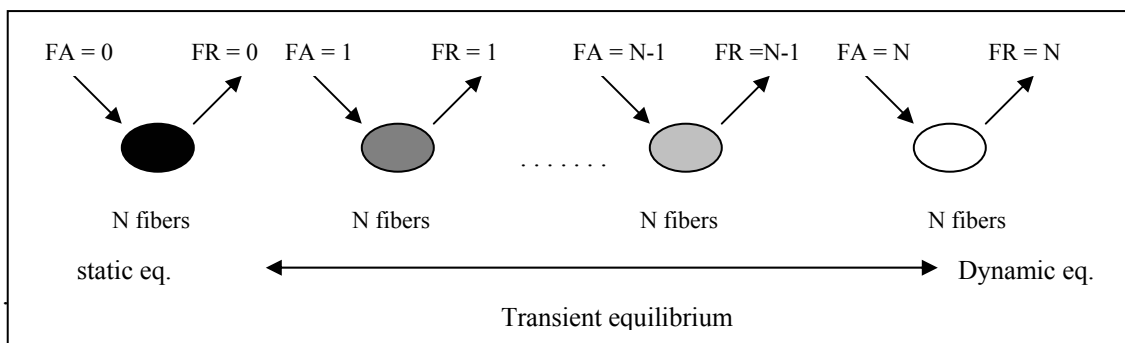


Fig. 24. Concept of dynamic and static equilibriums.

b. Concepts of the flocculation level

While people have been trying to understand the fiber flocculation mechanism in order to produce a good quality paper, apparently there exists no clear definition of “good quality” in term of fiber flocculation. Clearly, flocculation is unfavorable to exist in the paper pulp, but at the same time, pulp can not be so disperse and dilute that the paper becomes not possible to be produced. In this section several different approaches to fiber flocculation measurement were discussed.

Jacqueline [48] introduced the concept of “coherent flocs” defined as the flocs that had sufficient strength to withstand rupture in the flow in which they were formed. The parameter and condition of the coherent factor to the fiber flocculation was not clearly defined. Uniformity of coherent flocs may be necessary since each floc will have different strength depending upon the physical structure of the flocs and the friction factor within the fibers. Note that two different flocs of an equal strength do not

necessarily represent the same mass or number of fibers. Ramin et al. [49] introduced three possible model structures for a stable network of unfolded fibers. How the floc structures may affect the strength of the flocs or how the strength of flocs can determine the level of dispersion will be another area of where further study is needed.

Norman and Wahren [50] proposed Eq. (12) to calculate the flocculation level (F) based on mean (σ) and standard deviation (μ) of grayscale value of image. Originally the formula is built to analyze the mass distribution of the fibers, however, in this case, the formula is used to analyze the intensity distribution.

$$F = \sigma/\mu \quad (12)$$

From Eq. (12), one can see that at a high value of standard deviation (μ) will represent wider spread of black-white color that leads to more contrast of the gray intensity. This will result in the high flocculation level. On the other hand, a low value of standard deviation, the spread is small that leads to the good distribution of fibers or low flocculation level.

A simple example will be represented here. Figure 25 shows two different gray intensity pictures of 2x2 pixels with their corresponding value of the gray intensity. Figure 25a yields mean of 0.5 and standard deviation of 0.577, therefore the $F = 1.1547$. Figure 25b yields mean of 0.625 and standard deviation of 0.433, so $F = 0.692$. From eyes-observation itself, it is clear that Fig. 25b has a better distribution or lower flocculation level than Fig. 25a.

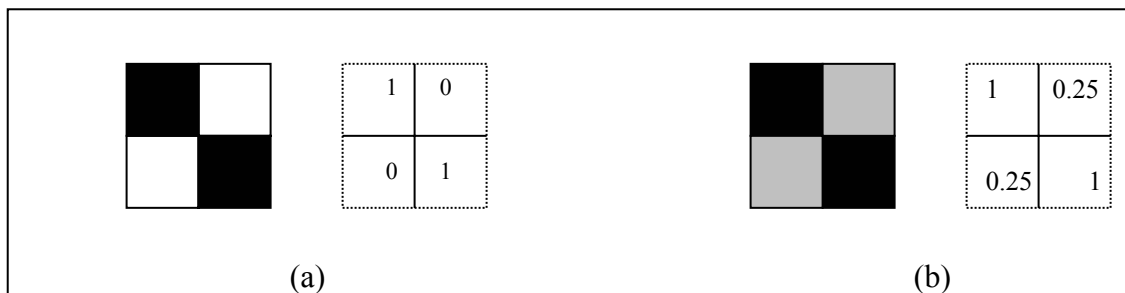


Fig 25. Example to illustrate the flocculation level under [50] concept.

A problem with this method of measurement is that it only measures the whole area of the image without any consideration to local distribution as described in Fig. 26. In this Figure, three different cases were presented. Using Eq. (12) above, the flocculation levels of these three cases were similar, although it is obvious from observation that Fig. 26a part a has a better grayscale distribution level, followed by parts b and c. An obvious improvement of this method can be made by dividing the image into smaller windows, and for each window, the flocculation level is calculated. At the end, the flocculation levels of all windows are combined and averaged.

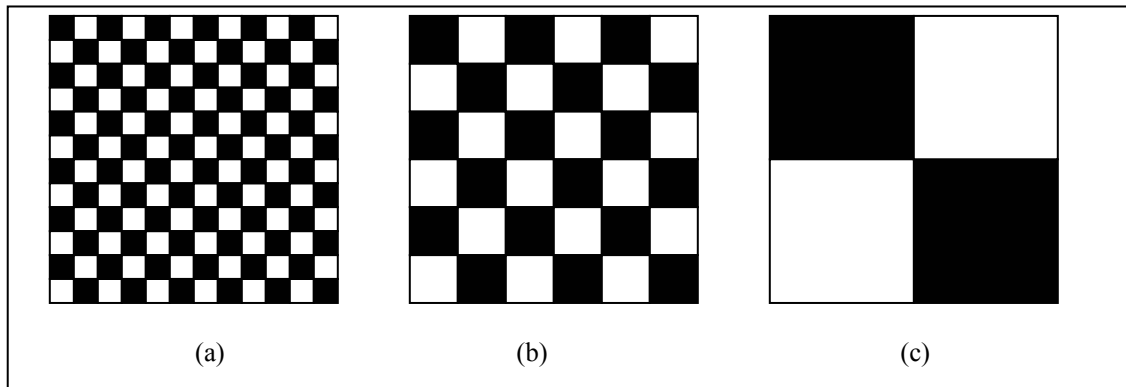


Fig. 26 Description of three different cases with similar flocculation level calculated by [50] method.

Kerekes and Sozynski [42,43] relied on the concept of crowding factor that is defined as the number of fibers inside the spherical volume with the diameter of the fiber length. They conclude that the crowding factor would determine the flocculation level based on the aspect ratio (L/D) property. However, there is no explanation on how they relate this flocculation or dispersion level with the quality of paper.

Kerekes and Schell [15,16] used the term of mass uniformity to fiber flocculation. The mass uniformity may imply the number of fiber uniformity assuming that all fiber has the same dimension and weight. They defined that the uniformity concept can be divided into two parameters: intensity and scale. Intensity refers to the

local mass variation in basis weight while the scale refers to the size of the zone in weight basis. What degree of the mass uniformity using these two parameters, i.e. how intents or how small the flocs should be, to achieve a good quality paper, still remains as an open question.

Beghello et al. [20] introduced another analysis based on Fourier transform property. The analysis is mainly based on the fact that an image of a moving object can be treated to have not only space information but also time information. Figure 27 illustrates the example of the process. As the object moves, the intensity probe will record the change in the intensity level of the object over the time. If the probe is assumed to be able to read at exactly one column of pixels, continuous signal intensity for that particular column of pixels can be produced. In the image processing proposed [20], instead having a continuous signal from the probe, the image will produce a digitized signal that has division of the number of pixels per column. After all columns and row signals are obtained, the intensity matrix can be generated.

The data matrix is then normalized by setting the mean (μ)=0 and amplitude (A)=1. By recording the variation of the physical quantity along the straight line with constant scanning velocity, the signal is obtained with the small components produce high-frequency variations, while larger components yield variation of lower frequencies. By performing a frequency analysis on the signal, the intensity of components of different size can be estimated. The Fast Fourier Transform (FFT) analysis [51] is used to achieve this purpose. Power spectrum resulting from FFT process is then calculated for both rows and columns of the image intensity matrix by averaging each individual column and row spectra respectively. Power spectrum itself represents a spectral distribution of the variance, that is, the square of the intensity distribution. The wavelength can be used instead of the frequency of the periodic components, so that the signal is represented as wavelength spectrum. The results will then be independent of the speed at which the physical quantity is recorded, and is dependent only on the geometric dimensions in the investigated area. The conversion formula from frequency into wavelength spectrum is proposed by Norman and Wahren [50]:

$$E(u/f) = E(\lambda) = f/u P(f) = u/\lambda^2 P(u/\lambda) \quad (13)$$

where $E(u/f)$ is the wavelength range power spectrum at the specific flow velocity u , and frequency f . $P(n)$ is the power per unit frequency and l is the wavelength. Due to the fact that scanning process will yield the large range wavelength variation, the location of the characteristic wavelength is obtained at the average value of the power spectral located. It can be done by calculating the area under the power spectrum curve and taking the location of the half of the total area as the characteristic wavelength. The characterized flocs size (FS) itself is considered to be half of characteristic wavelength since the characteristic wavelength is the whole length of both flocs and non flocs region.

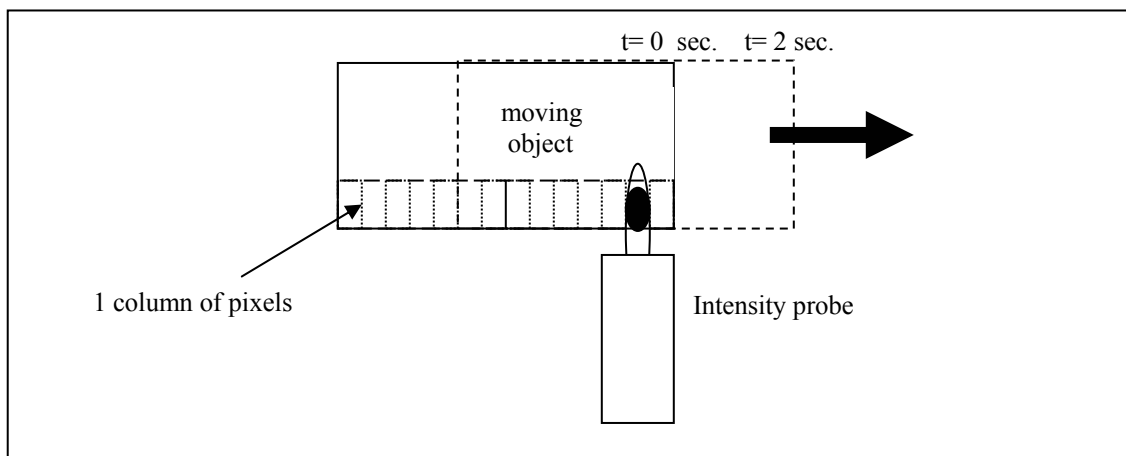


Fig. 27. Illustration of the concept of image as a moving object.

c. Preferential orientation of fibers in suspension

The mechanism of how to direct fibers or flocs to a certain orientation must be known. Shear rates and turbulence intensity will be the two most important mechanisms to be studied to understand the preferential orientation of fibers. Previous studies of turbulence and shear rate had focused more on the effect of turbulent and shear rate on the fiber flocculation level but not specifically on the direction of fibers or flocs. The fiber-fiber, fiber-floc and floc-floc interactions are other factors that make the problem more complicated to be studied

d. Preferential flocculation of fibers by turbulence

Eaton and Fessler [52] conducted a study about the preferential concentration of particles suspended in turbulence. Preferential concentration describes the accumulation of dense particles within specific regions of the instantaneous turbulence field. It can be necessary to expand their research into the flocculation process due to the fact that the turbulence also exists in the headbox. This concept may highly relate to the mass uniformity concept parameters introduced by Kerekes and Schell [23,24]: intensity and scale since the flocs might have higher/lower intensity and scale values. The turbulence intensity and length scale, shear rate, velocity, and headbox geometry might play important roles. The boundary layer analysis will also need to be considered. No extensive research on the preferential flocculation has been found in literature surveys to date.

e. Combined flocculation factors

Hourani [33,34] studied on how combined factors among velocity, length, temperature, and consistency affecting the flocculation. Although he came up with fairly reasonable conclusions, further study needs to be done not only on the Hourani's combined factors also other combinations of fiber flocculation factors. Another possible study of the combined factors will be the fibers aspect ratio against its length and diameter. As previously mentioned, one excellent example is a work by Kerekes and Schell [23,24] representing the relation of these three factors in term of crowding factor.

3.6 Summary

Determination of the mechanism of fiber dispersion is necessary to ensure the quality of paper. Mason [18] has categorized two major factors in fiber flocculation: mechanical and chemical. The mechanical factors tend to be a dominant force in determining fiber flocculation while the chemical factors have secondary effects. Different researchers using different methods and procedures have tried restlessly to determine how each factor affect the fiber dispersion. While most of factors have been

explained on how they affect the dispersion, some factors are still unclear in that regard. More systematic and extensive study on dispersion is necessary to explore best possible method to explain how the dispersion/flocculation factors affect the dispersion behavior. Some unsolved questions related to fiber dispersion were also presented here. These topics are very important to bring understanding the mechanism behind fiber flocculation process.

CHAPTER IV

WATER CHANNEL EXPERIMENT

4.1. Introduction

In this chapter a digital image analysis using optical texture study is presented to analyze non-cellulose fiber dispersion. The existing technique had been successfully applied to analyze the dispersion of carbon black in Rubber by Ganesan and Bhattacharyya [11-13] as discussed in Chapters I and II. The texture analysis was extended to experimental study of fiber dispersion inside water flow in open channel configuration. Two-factorial design was implemented to determine the effects of selected parameters on fiber dispersion. These selected parameters are critical in fiber dispersion process. The results were then compared with previous studies.

4.2. Water channel apparatus

An open water channel with the size 3 m in length and 0.35 m in width had been built to accommodate the experiments. The configuration of the water channel is shown in Fig. 28 and the actual photo is provided in Fig. 29. Conducting this particular experiment on the open channel became a challenging task. An obvious drawback from using the open channel for this investigation is that its incapability to achieve relatively high flow velocity. On the other hand, some industrial applications of fiber dispersion, such as in papermaking, do deal with the open channel situation and unfortunately most of the previous researches of fiber dispersion have been conducted using the closed channel. With this lack of information of fiber dispersion on open channels, further theoretical and experimental studies using an open channel on fiber dispersion were needed. The images were taken at about 2.5 m downstream to ensure the assumption that one-dimensional uniform flow velocity occurs inside the channel. One-dimensional flow velocity distribution assumption is normally used in fluid mechanics field [53,54] as three-dimensional velocity distribution analysis inside an open channel is too complicated.

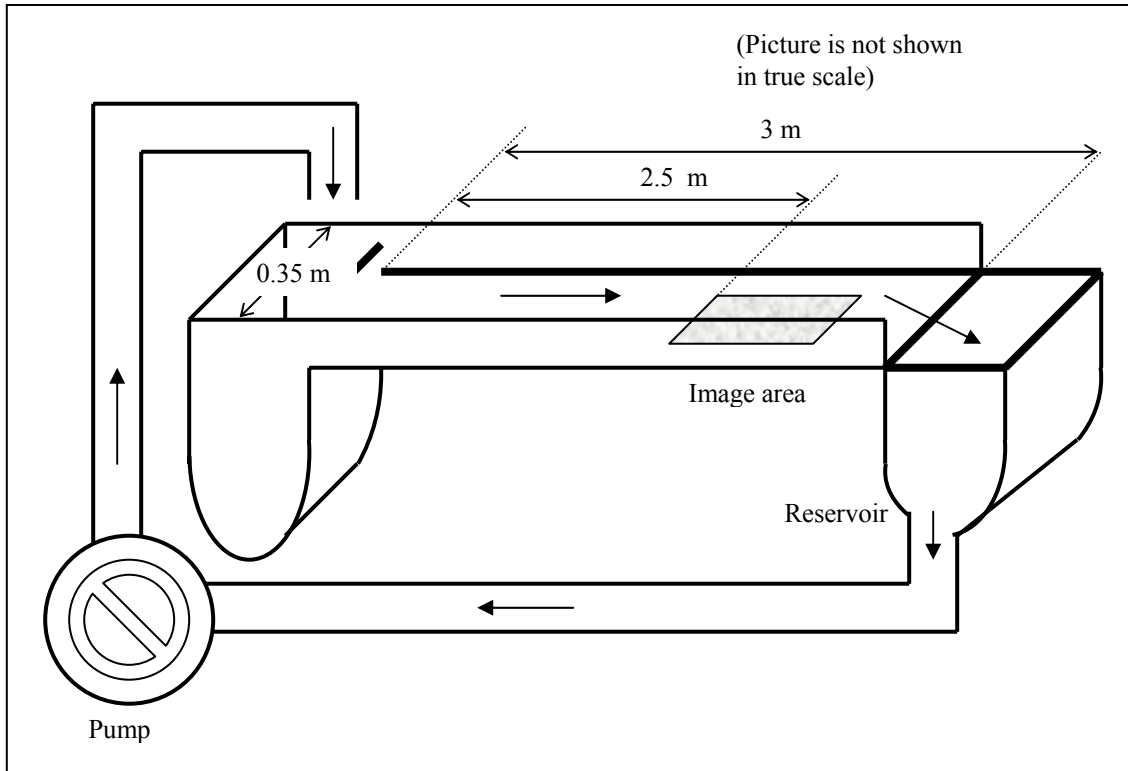


Fig. 28. Water channel configuration.



Fig. 29. Water channel utilized for this study.

To produce the water flow, a regular centrifugal water pump from Ingersoll-Rand was used. This pump is equipped with open impeller that enables the pump to handle slurries and particles. This capacity is necessary for the study where fibers were suspended in water flow. The flow velocity was determined by measuring the flow rate produced by the pump and the cross section of the water flow. The reservoir was used to ensure that the pump has enough water to circulate.

Since water depth dimension is far smaller than the length and width of the channel, it can be assumed that the changes in cross section area from upstream to downstream are very gradual and minimal [53]. The water channel contraction at upstream also was assumed to have no effect to properties of fibers and water flow at downstream where the images were taken.

4.3. Fiber properties

The synthetic Nomex fibers were used in this study. While the fibers came with specified sizes from fiber manufacturer a large numbers of fiber samples were re-measured using microscope and its appropriate reticle to find the smallest dimension

entity of the fibers, in this case is the diameter. The description of measurement under the microscope is shown in Fig. 30.

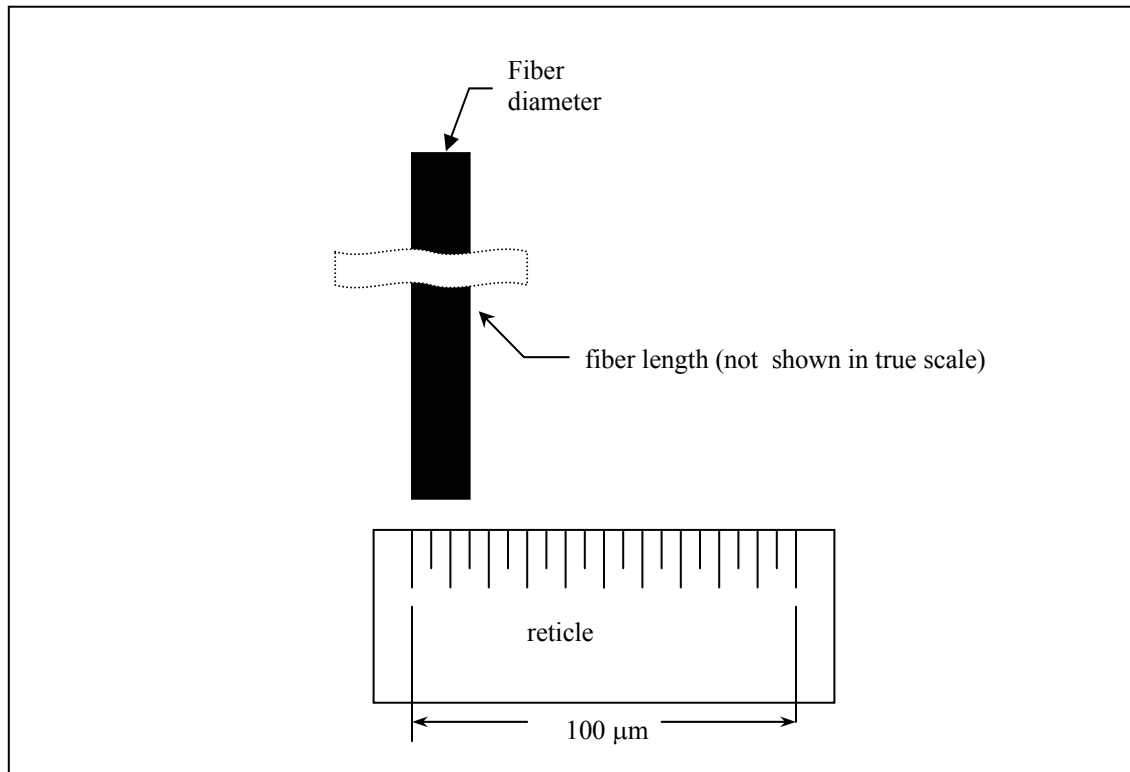


Fig. 30. Fiber diameter measurement description.

The fiber mean diameter was found to be $15 \mu\text{m}$ with negligible variation of $\pm 0.5 \mu\text{m}$. Fiber lengths on the other hand were measured using a Vernier Caliper. During the study, the fiber concentration was measured using standard TAPPI method (T 240 om-93). In this method is cups are used to withdraw sample of solution that then was put inside a beaker. The net weight (g_b) of solution sample is determined by subtracting the total weight (beaker and sample solution) to the initial tared weight of beaker. This sample is then filtered through a filter paper with a weight of f_p in Buchner funnel. This filter paper and its filtered sample are heated in drier until steam appears. The total weight of filter and solution sample (w_{fs}) is then measured. Successive weight readings after additional drying are done until a constant weight is obtained. The dry solution

sample weight is then measured by subtracting the total weight of filter and solution samples to the tared weight of paper filter.

The percent consistency of solution is then:

$$\text{Consistency (\%)} = [(w_{fs}-f_p)/g_b] \times 100 \quad (14)$$

Other conditions such as density, temperature, and viscosity effect of fibers were assumed to constant during experimental operation. While they may contribute to level of fiber dispersion, their effects are expected to be negligible.

4.4. Image Capture Procedures

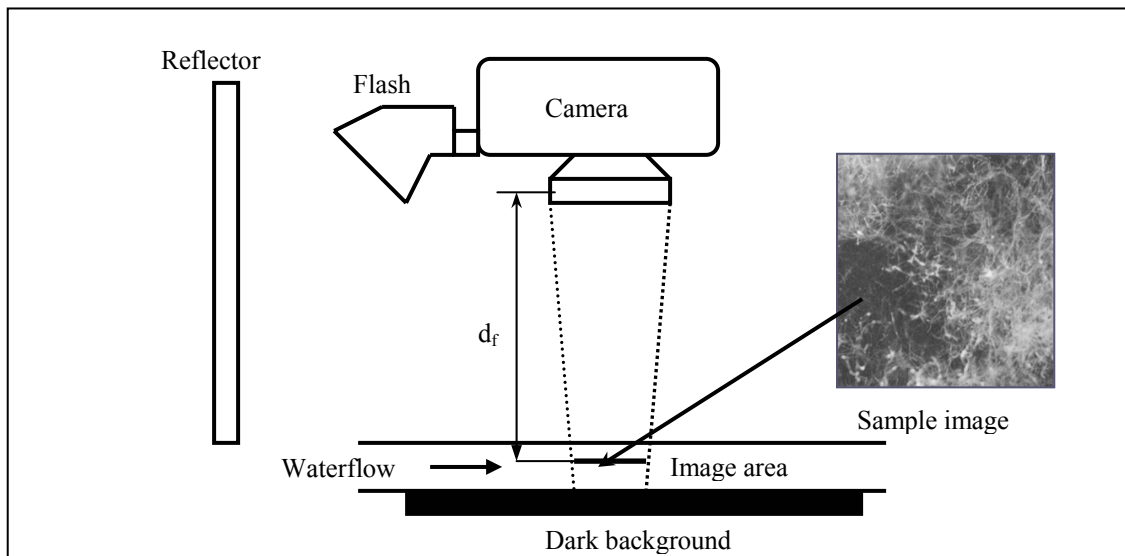


Fig. 31. Imaging apparatus and configuration.

Figure 31 shows the configuration for the image-capturing experimental setup. A 35mm conventional camera was used to capture the image of moving fibers inside water flow. A Vivitar-283 camera flash was used to provide illumination to the captured images. Using an appropriate flash setting, the flash was capable to freeze the water

flow image up to 1/30,000 seconds to minimize unnecessary image blurring. The sharpness of the fiber image becomes important when applied to the current texture analysis in which the results depend on how pixels are related and compared to the neighboring pixels. Any blurring problems may cause the inaccuracy of pixel gray values and, moreover, will cause the miscalculation of the texture/dispersion values. With the average flow velocity of 0.3 m/s used in this study, the amount of blurring detected was 10 μm ($1/30,000 \text{ s} \times 0.3 \text{ m/s}$). Compared to fiber length and diameter, this blurring is expected to give a minimal effect to texture analysis. A Sigma 50 mm macro lens was used to give good magnification and detail of the fibers. The camera was set at shutter speed of 1/60 second and F-stop of 5.6 to provide enough depth of field of the image with the distance (d_f) from camera lens to water channel was set to be 0.20 m. The film speed used was ASA 400 that gave relatively sharp image but at the same time was able to capture enough light. The reflector of white plain paper and the dark background of black plain paper were used to achieve uniform lighting around the image. During the picture taking, the surrounding area of the channel was set to be as dark as possible to eliminate interference from exterior lighting. The lighting uniformity was calibrated by measuring the grayscale intensity of image taken with no fibers inside the water flow. With some samples, it was found that no significant variation existed in grayscale values.

The actual captured area was 38x38 mm^2 . The images were printed with magnification of 2.5, which brought the smallest fiber entity (fiber diameter) to be about 37.5 μm (15 $\mu\text{m} \times 2.5$). Once all the pictures were taken and developed, scanning process was used to convert the images into digital images. These images were scanned at a resolution of 295 pixel/cm. With the scanning resolution above, the pixel size is approximately about 33 μm . At this resolution, it is possible to have pixel sizes (33 μm) that are smaller than the fiber diameter size in the image (37.5 μm) and at the same time to have minimum time to process them. These digital images were then processed into gray images and then their dispersion levels were measured using the texture method as described in Chapters I and II.

Investigation of the use of Particle-Image-Velocimetry concept

Prior to conducting the current experiments, the use of laser as the illumination source as an alternative way to investigate the fiber dispersion was explored. The use of laser was expected to give better image. Unlike regular light, laser has monochromatic light that is more powerful and coherent. The proposed methodology was very similar to the one used in particle-image-velocimetry (PIV) concept as shown in Fig. 32, where a thin sheet of laser light was exposed to the water flow, and a camera shot the image right at the top of the laser sheet.

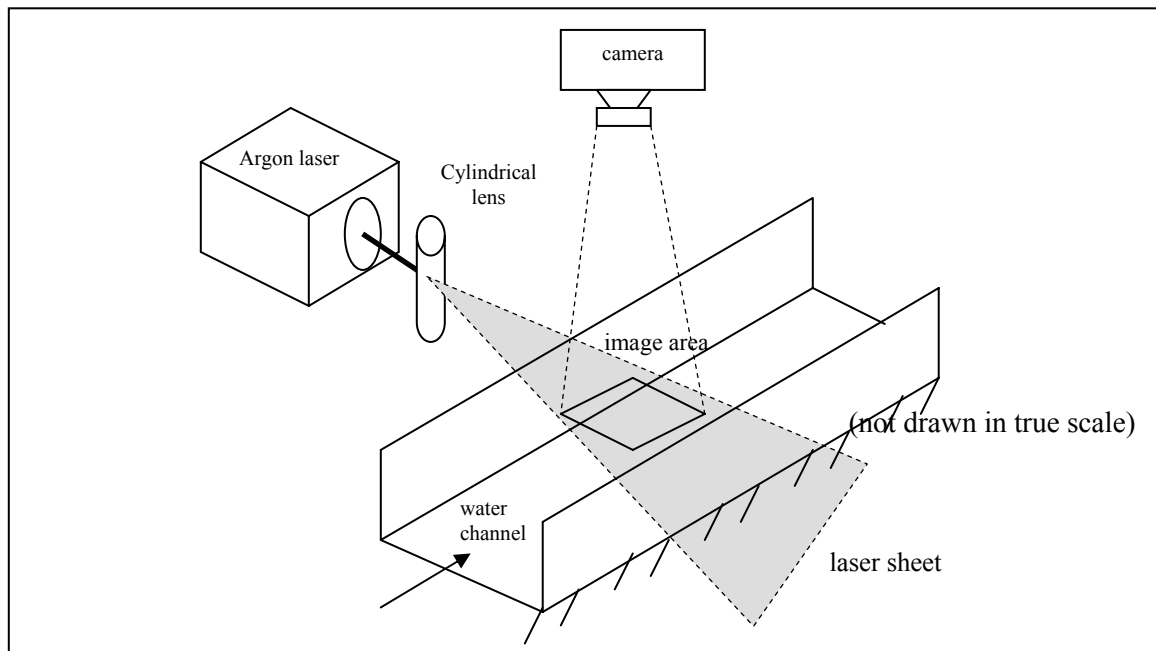


Fig. 32. Apparatus configuration using PIV concept.

The main problem appeared when the water flow started to be filled with higher fiber consistency (approximately at 0.2%). The presence of a large amount fiber aggregation made the laser beam scattered resulting in a non-uniform lighting around the photo area and the fiber color intensity varied from one place to another. Sample images were shown in Fig. 33 at different consistencies. Figures 33b and 33c gave some observable spots where discrepancy in light intensity appeared. Higher consistency fiber solution blocked the laser beam and scattered it. Obviously this problem is almost

unavoidable and unfavorable for investigating the dispersion level at high fiber concentration. The study then settled with the regular camera flash since there was no significant amount of light scattering appears when camera flash was used.

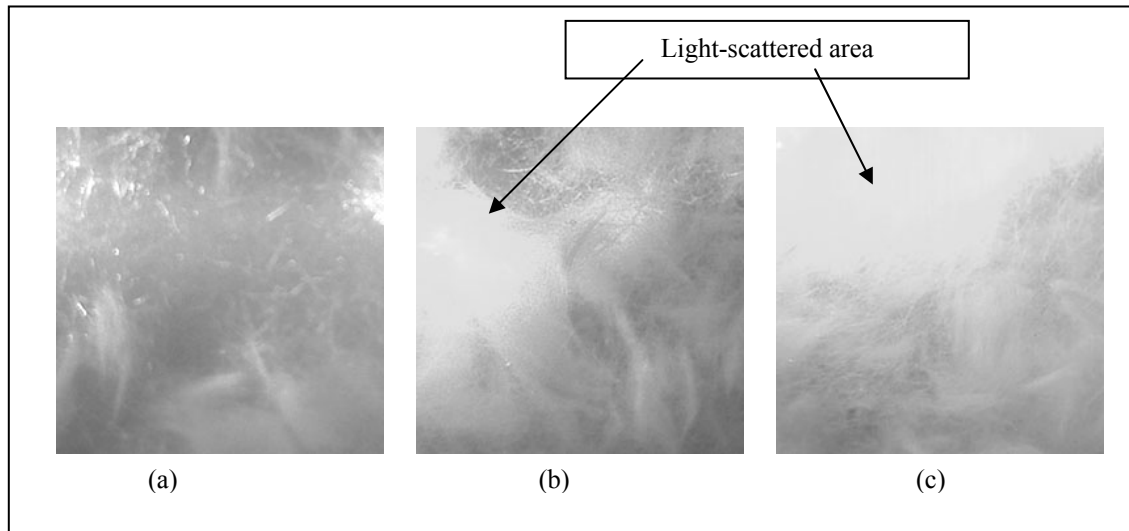


Fig. 33. Sample images using PIV concepts: (a) $C = 0.05\%$, (b) 0.2% , (c) 0.25%

4.5. Two-factorial design

A factorial design is used to evaluate two or more factors simultaneously. The treatments are combinations of levels of the factors. The advantages of factorial designs over one-factor-at-a-time experiments are that they allow main effects and interactions to be detected. They also minimize number of samples required and time consumed for analysis. A two-factorial design consists of 2^k experiments where k is the number of factors each with a high and low value/level. The relevant statistical effects of each factor are found by comparing the results from all the experiments with the high value of a factor to the results of all the experiments with the low values. For three-factor analysis, the four experiments with a high value of one factor are compared to the four experiments with the low value. In this manner, it is also possible to quantify higher order (or combined) effects. At the end the main effects of each parameter and interactive effects between parameters are calculated and compared with a statistical number. Main effect is the simple effect of a factor on a dependent variable. It is the

effect of the factor alone averaged across the levels of other factors. An interaction is the variation among the differences between means for different levels of one factor over different levels of the other factor. An interactive effect tells if the other factors influence the main effect result. If there is a significant interactive effect, then it is not certain that a main effect is due solely to the raising or lowering of a factor level. Complete details of two-factorial design setup can be found at most of statistics textbook such as in [55] and are presented in Appendix C.

4.6. Operating parameters

A two-level-factorial design was implemented in these experiments to compare the effects of three different factors on the dispersion level. In this context a factor is an experimental variable, and a result is the quantitative measure of the parameter of interest. In this study the factors used were fiber aspect ratio (length/diameter), fiber concentration, and fluid velocity (Reynolds number), and the result was the texture number. These three factors were selected because they have been considered as important parameters that are critical to formation of fibers in paper. Literature also provide limited information and data to compare with the results of this study

Figure 34 describes the cubical diagram of these three parameters for the experiment. Each corner inside circle represents the experiment with combination of low (-) and high (+) parameters, while the middle point (000) represents the experiment with combination of the middle values of all three parameters, i.e.(- - -) represents the experimental setup run at lower velocity, lower concentration, and lower aspect ratio.

The values of low and high for each parameter used are shown in Table 4. As mention in section on fiber properties, the lengths of the two types of fibers considered in this study are 6.0 ± 0.10 mm (0.25 ± 0.01 "") and 3.0 ± 0.15 mm (0.125 ± 0.01 "") with a diameter of 15 ± 0.5 μ m for both fibers. These yield the aspect ratios (length/diameter) of 400 and 200 respectively.

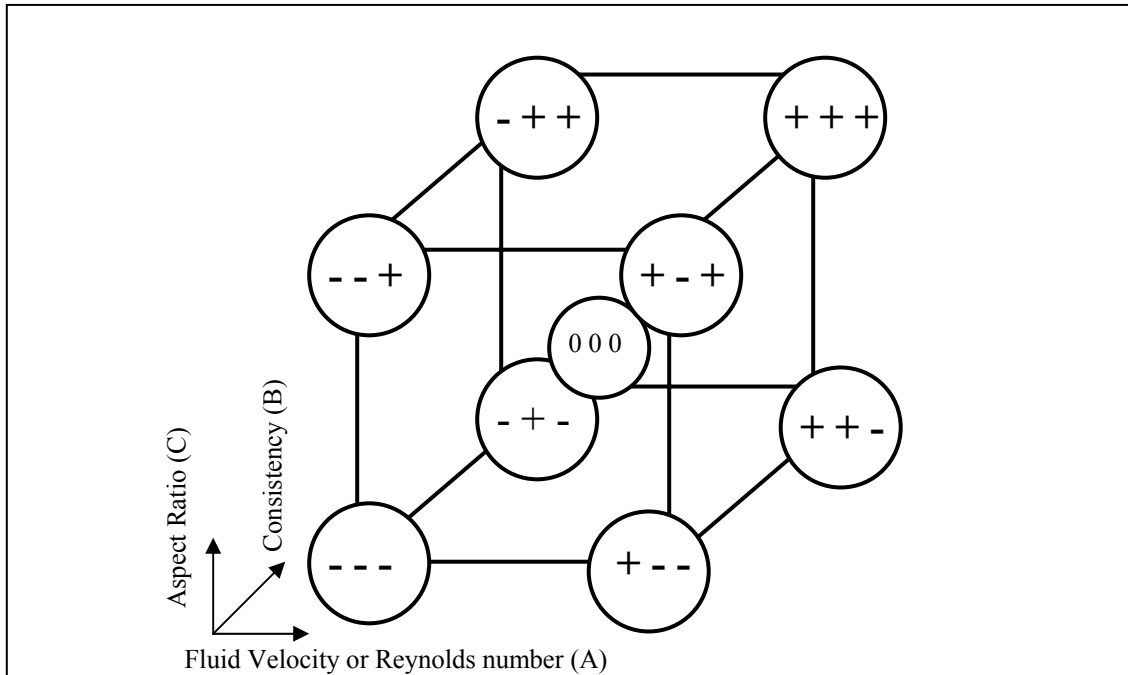


Figure 34. Arrangement of experimental settings.

Table 4. Mean and standard deviation of low and high values of each parameter used for experiments.

Parameter	Low	High
Fluid velocity	0.20 ± 0.0074 m/s	0.40 ± 0.0072 m/s
Consistency/concentration	$0.10\% \pm 0.0125\%$	$0.40\% \pm 0.0133\%$
Fiber Aspect Ratio	200 ± 2.35	400 ± 3.89

The lower limit velocity is determined by the piping and pump configuration. Below flow velocity of 0.2 m/s, the system was unable to feed enough water to be pumped at the height of the channel. The water channel is located about 1.25 m above the pump, and in order for the water get pumped to that height, the pump has to be operated at a certain minimum amount of power and water. This limitation led to minimum flow velocity of approximately 0.2 m/s. The upper velocity of 0.4 m/s was determined by the appearance of ripples at the flow surface. These ripples appeared on the images and distorted the image analysis. Another concern on running the pump at

the maximum capacity was due to substantial vibration of water channel. This vibration clearly gave a safety concern during the experiment.

The lower concentration was selected because at consistency below 0.1%, the solution is so dilute that the majority of fibers in suspension were not in continuous contact [22]. To form local network structures (flocs) fibers must collide and then remain in contact. Collisions occur when fibers are present in sufficient number and have a relative velocity between them. Below 0.1% then, the study would not show the flocculation process of fibers. The upper consistency was limited by the capacity of pump and piping. At consistency higher than 0.4%, the fibers tend to clog inside the pipe, stopping the pump from operation.

Due to the lack of resource to have an appropriate fiber size, the middle point of the two-factorial design (denoted as 000 in Fig. 34) was not conducted. While the middle point results are still important to have all interaction constants calculated, the current results are adequate to investigate how the operating parameters will affect the fiber dispersion. The main and interaction effects can still be evaluated properly. In order to have reliable results, for each condition, ten random runs were conducted. The mean (σ) and standard deviation (μ) of each condition were ultimately calculated and presented in the Results and discussion section.

4.7. Results and discussion

Figure 35 shows sample images for each condition. Unfortunately at higher concentration, the images show more blurring than expected. This is caused by the part fibers that were flowing above water surface. However to ensure all the images taken get the same treatment, all these images were continued to be used. Different treatment like image enhancement and lens configuration can cause each set of image has different of lighting intensity. Visual inspection indicates that even without any blurring, the images will have small amount grayscale variation due to significant amount of fiber aggregation appears on the images.

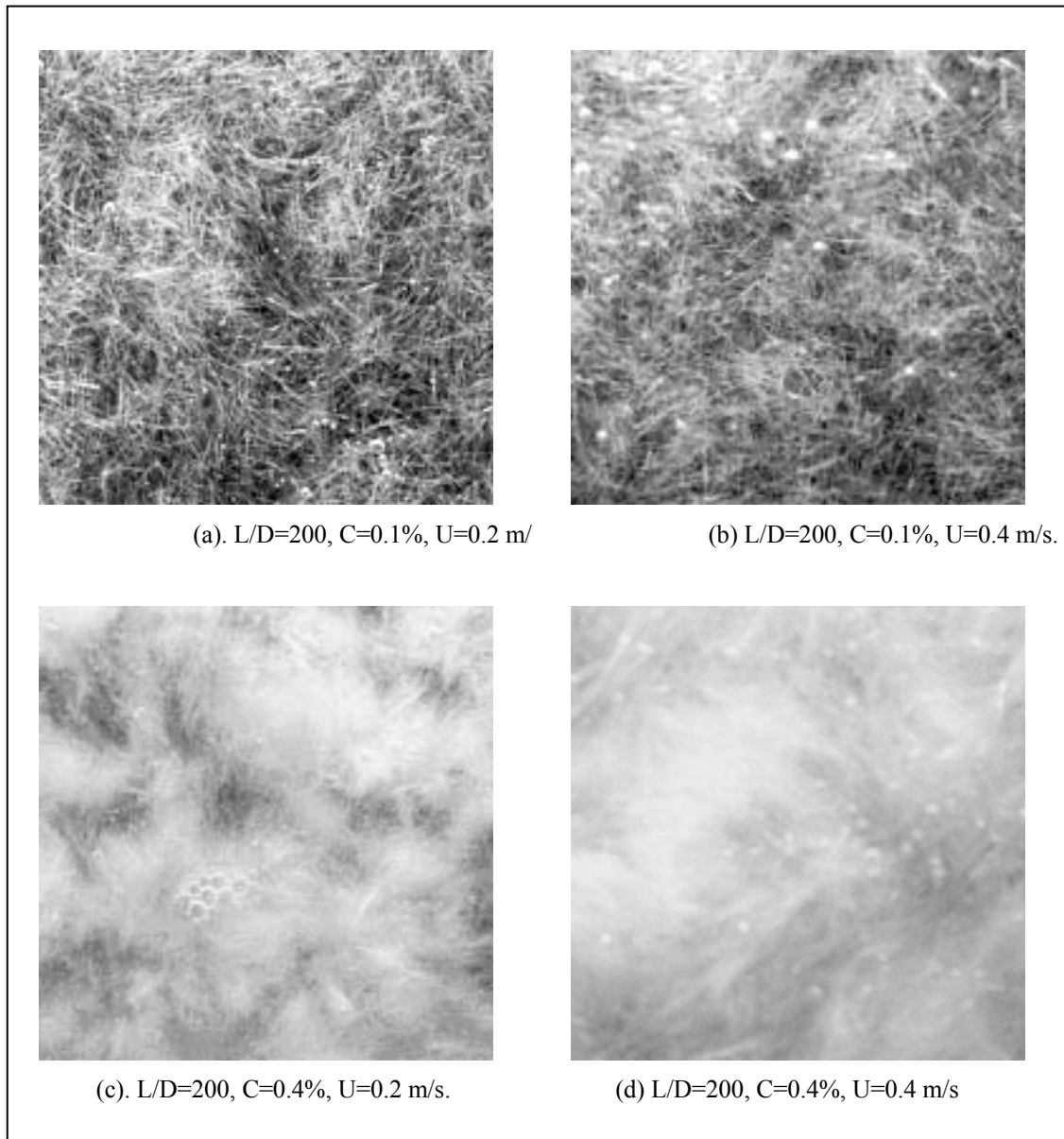


Fig. 35. Sample image at different operating conditions.

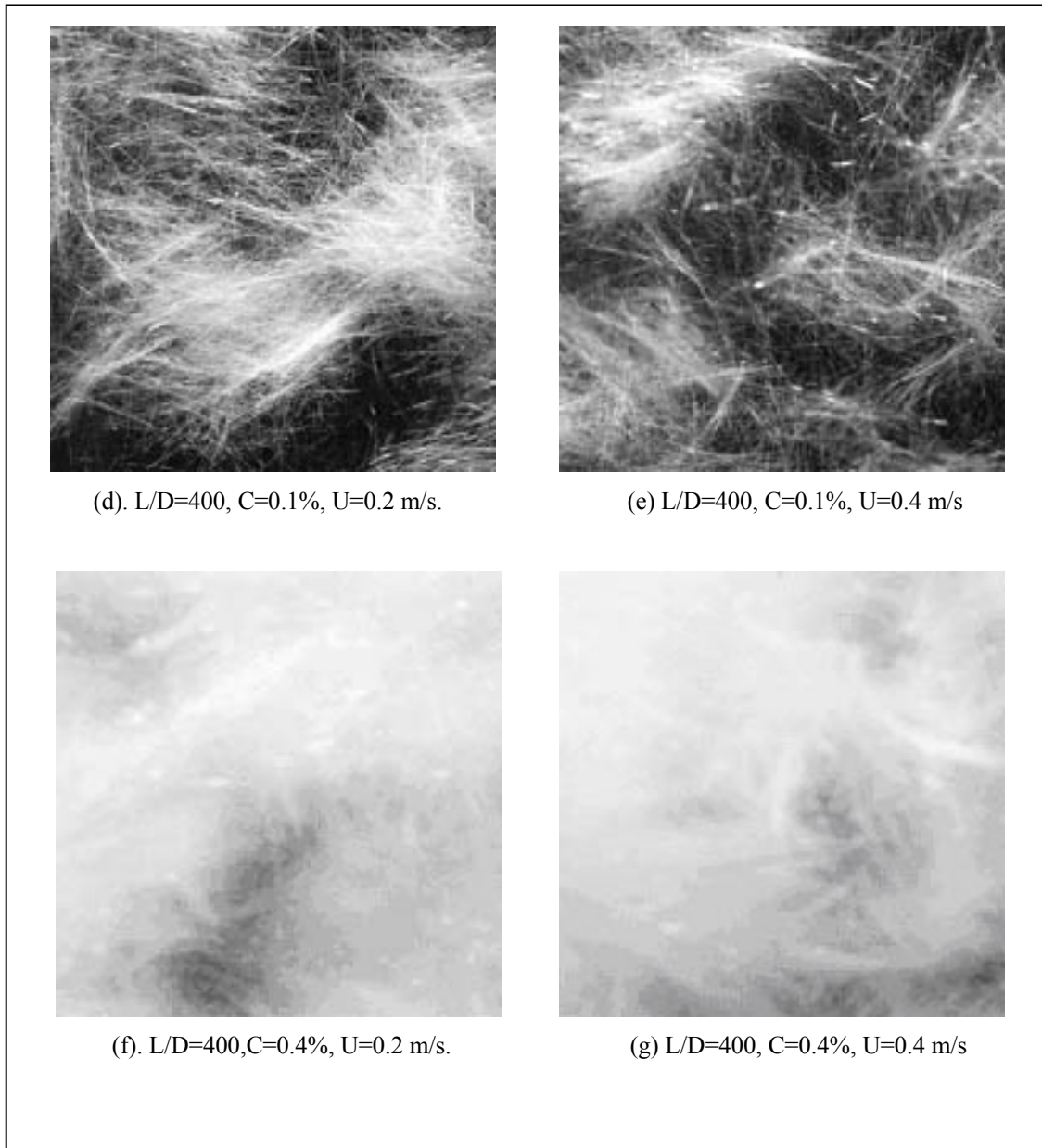


Fig. 35. (continued)

Analysis using BeghELLO et al. [25-28] method

An attempt was made to analyze the image results using imaging technique developed by BeghELLO et al. [28]. BeghELLO et al. [28] had conducted various studies on the fiber flocculation as some of their method and results have been mentioned and discussed in Chapter III [25-28]. In their study, they used the FFT concept to obtain flocculation size as a measure of fiber dispersion. The flocculation size can be then calculated based on the mean value of the wavelength graph of FFT results. The effort to use their method unfortunately gave unsatisfactorily results.

Table 5 is the calculated results using BeghELLO et al. [28] procedure. Combining the mean and standard deviation, the closeness can be observed within $[\mu+(1)\sigma]$ range values. Ideally, the results between two different conditions should have enough range in order to discriminate them. A problem definitely will arise when applying the operating conditions that fall within the current operating conditions, for instance, at the middle value of $L/D=300$, $C=0.25\%$, and $N_{Re}=34000$. This closeness in the result makes a conclusion that the method became unreliable in this study.

Table 5. Results analysis using BeghELLO's procedures.

	Case 1: L/D = 400 C = 0.10 % $N_{Re} = 53000$	Case 2: L/D = 400 C = 0.10 % $N_{Re} = 15000$	Case 3: L/D = 400 C = 0.40 % $N_{Re} = 53000$	Case 4: L/D = 400 C = 0.40 % $N_{Re} = 15000$
Mean (μ)	1.70 cm	1.76 cm	1.72 cm	1.75 cm
Std. Dev. (σ)	0.0785 cm	0.0673 cm	0.0410 cm	0.0305 cm
	Case 5: L/D = 200 C = 0.10 % $N_{Re} = 53000$	Case 6: L/D = 200 C = 0.10 % $N_{Re} = 15000$	Case 7: L/D = 200 C = 0.40 % $N_{Re} = 53000$	Case 8: L/D = 200 C = 0.40 % $N_{Re} = 15000$
Mean (μ)	1.64 cm	1.70 cm	1.70 cm	1.71 cm
Std. Dev. (σ)	0.0363 cm	0.0242 cm	0.0318 cm	0.0261 cm

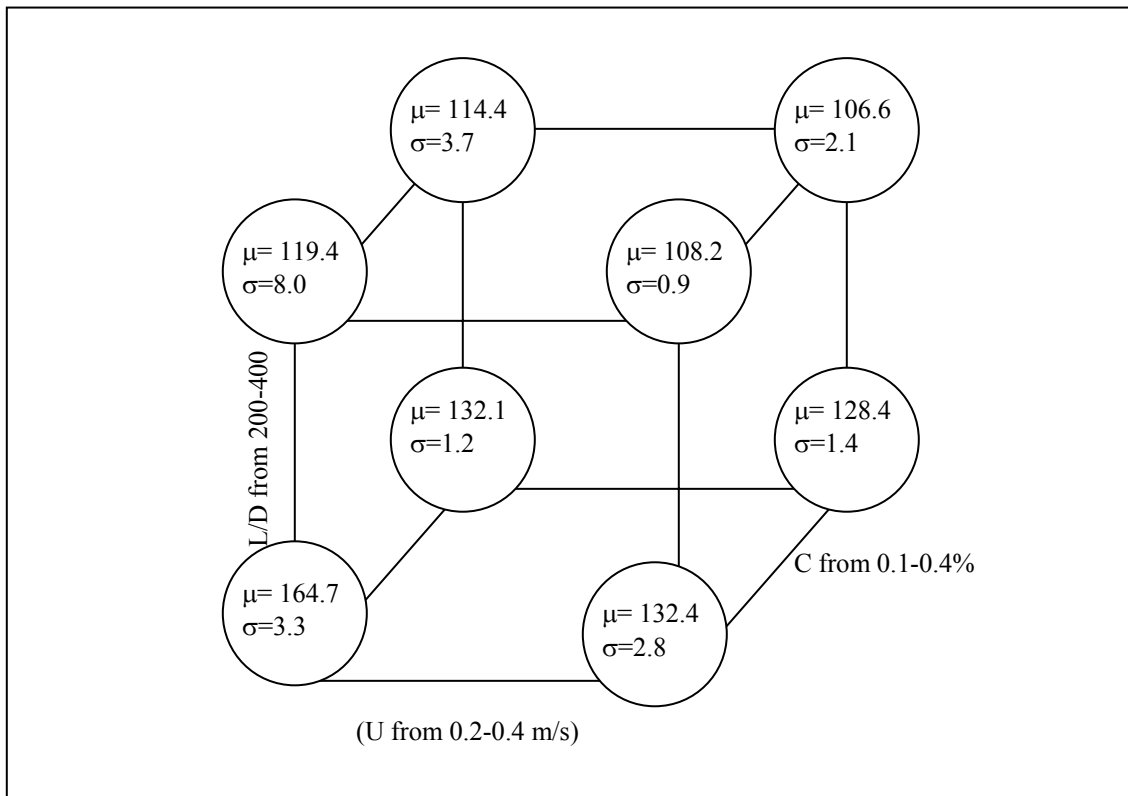


Fig. 36. Mean and standard deviation of experimental results.

General Results

Figure 36 shows the cubical results of the study. The numbers inside the circles indicate the mean (μ) and standard deviation (δ) of dimensionless texture number as proposed by Ganesan and Bhattacharyya [3].

The effect of three parameters can be summarized as:

- Increasing consistency decreased texture/dispersion level
- Increasing aspect ratio decreased texture/dispersion level
- Increasing velocity decreased texture/dispersion level

Main and interaction effect analysis

Table 6. Two-factorial design analysis results.

	Factor	Calculated Effect Value	Significances
Main Effects	Fluid Velocity (U)	$E_1 = -13.70$	Yes
	Fiber Consistency (C)	$E_2 = -10.75$	Yes
	Fiber Aspect ratio (L/D)	$E_3 = -27.30$	Yes
Interactive Effects	U and C	$E_{12} = 7.95$	Yes
	U and L/D	$E_{13} = 4.30$	Yes
	C and L/D	$E_{23} = 7.55$	Yes
	U,C, and L/D	$E_{123} = -6.35$	Yes
	Average texture number of all corners	$\mu = 125.76$	

Table 6 shows the statistical results of two factorial design analyses. The “Calculated Effect Value” in the third column represents the statistical magnitude values of how each individual (main) and combined (interactive) parameter will affect the dispersion level. These numbers were then compared to the minimum value tabulated at statistical table of t-distribution. For this case, the minimum value obtained at level of confidence of 0.005 is 3.5. If the calculated effect value is higher than this tabulated number, the significant effect for that particular parameter/s was said to be observed, and it is indicated as “Yes” otherwise “No” in “Significances” column in Table 6. Table 6 shows that all the factors have significant effect. These values represent how the factor or combined-factors can influence the texture numbers and furthermore the dispersion results. From Table 6 and at Figure 36, it can be observed that all main factors have negative effect values that indicate that as the value of parameter increases, the experimental results decrease. The higher effect value (in absolute value) means that the

particular factor or combined-factor will be more important in affecting the dispersion level. Since the interactive effect values are relatively smaller than the main effect values, the interactions between factors play less significant role compared to main effects. A change in dispersion number is then mainly due to a change of one factor, not a combination with the other factors. The most significant main effect is made by the aspect ratio (L/D), while the concentration (C) is the least. If someone has to choose between these three parameters with changing each of these three parameters cost about the same, then the choice will be changing fiber aspect ratio solely without any combination with other parameters. As shown in Table 6, aspect ratio would bring the most effective way to increase fiber dispersion.

The dispersion/texture response can be written as

$$Y (\text{Texture Number}) = \mu - E_1/2 x_1 - E_2/2 x_2 - E_3/2 x_3 + E_{12}/2 x_1x_2 + E_{13}/2 x_1x_3 + E_{23}/2 x_2x_3 + E_{123}/2 x_1x_2x_3 \quad (15)$$

where x_1 , x_2 , and x_3 are dimensionless fluid velocity, fiber concentration, and fiber aspect ratio respectively, ranging from -1 (low) to 1 (high). Using results presented in Table 5 and Eq. (15), the texture response is:

$$Y = 125.76 - 6.85 (U) - 5.38 (C) - 13.65 (L/D) + 3.98 (U) (C) + 2.15 (U) (L/D) + 3.78 (C) (L/D) - 3.18 (U) (C) (L/D) \quad (16)$$

This response equation then can be used to predict the dispersion level at given fluid velocity, consistency and aspect ratio. Figure 37 describes the three-dimensional graphical representation of Eq. (16) for each of constant parameter.

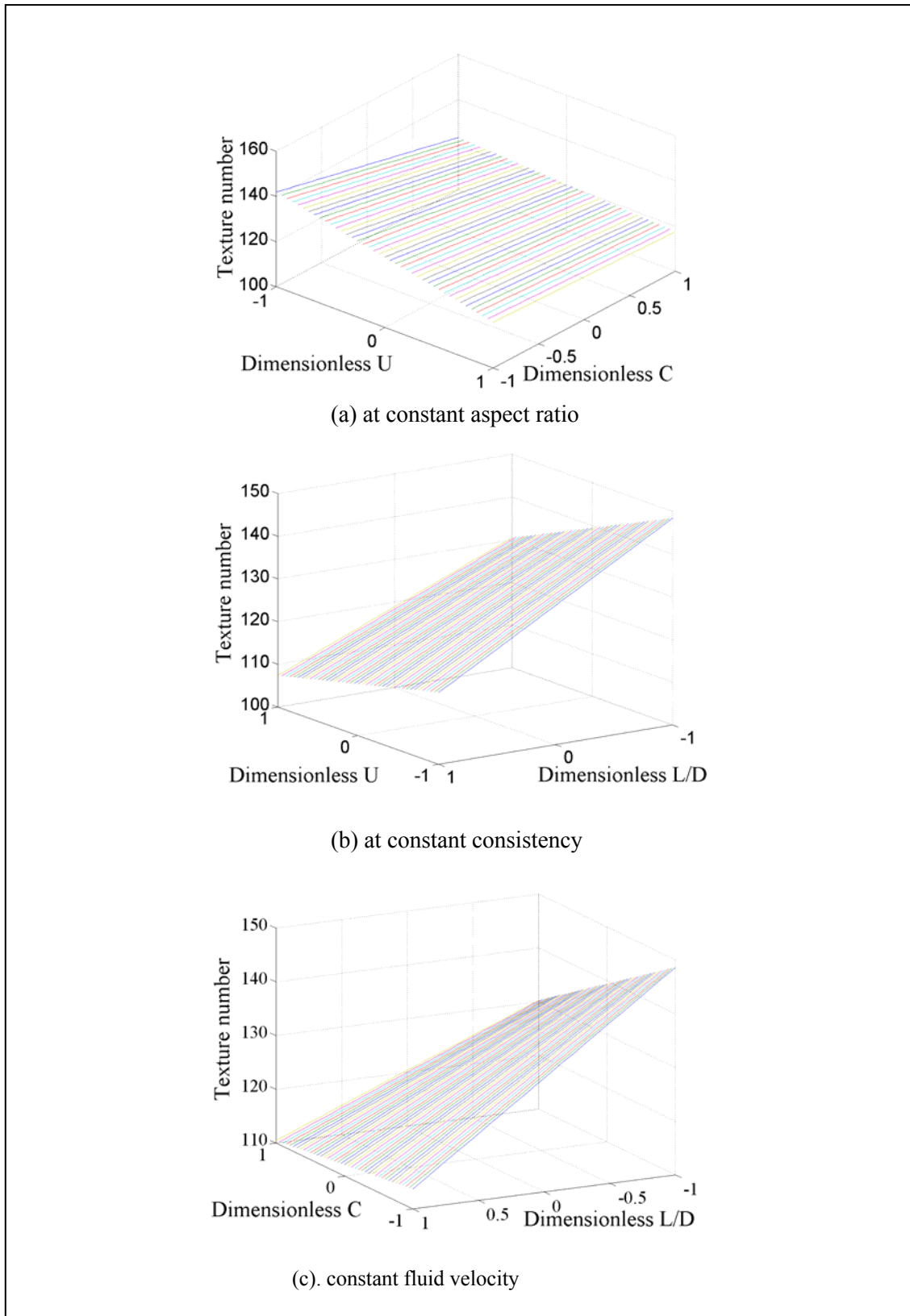


Fig. 37. Three-dimensional description of two-factorial design prediction.

Consistency effect

The comparisons of consistency and aspect ratio of current results and the literature can be presented in Fig. 38. Figure 38a is the current study results with its predicted values using Eq. (16) and Fig. 48b was presented previously as Fig. 11. Figure 38b includes the published study by Kerekes and Schell [24] and Beghelli et al. [25]. Crowding factor as discussed in Chapter III combines both consistency and fiber aspect ratio into a dimensionless number that describes the number of fibers (crowdedness of fibers) that can be packed inside a sphere that has a diameter equivalent to the fiber length. Higher crowding factor will represent more contacts among individual fiber that lead to more fiber entanglements (floc). The current study covered better range of crowding factor mainly because of larger aspect ratios used. Table 7 shows the corresponding crowding factor for each condition of consistency and aspect ratio. The volume concentration was calculated using density of water of 1000 kg/m^3 and Nomex density is 1370 kg/m^3 .

Table 7. Corresponding crowding factor for different consistency and aspect ratio.

Consistency	L/D	C_{vol}	Crowding factor	Texture # U=0.2 m/s	Texture # U=0.4 m/s
0.1%	200	0.075 %	20	164.7 (point a)	132.4
0.1%	400	0.075 %	79	119.4 (point b)	108.2
0.4%	200	0.3 %	79	132.1 (point c)	128.4
0.4%	400	0.3 %	315	114.4 (point d)	106.6

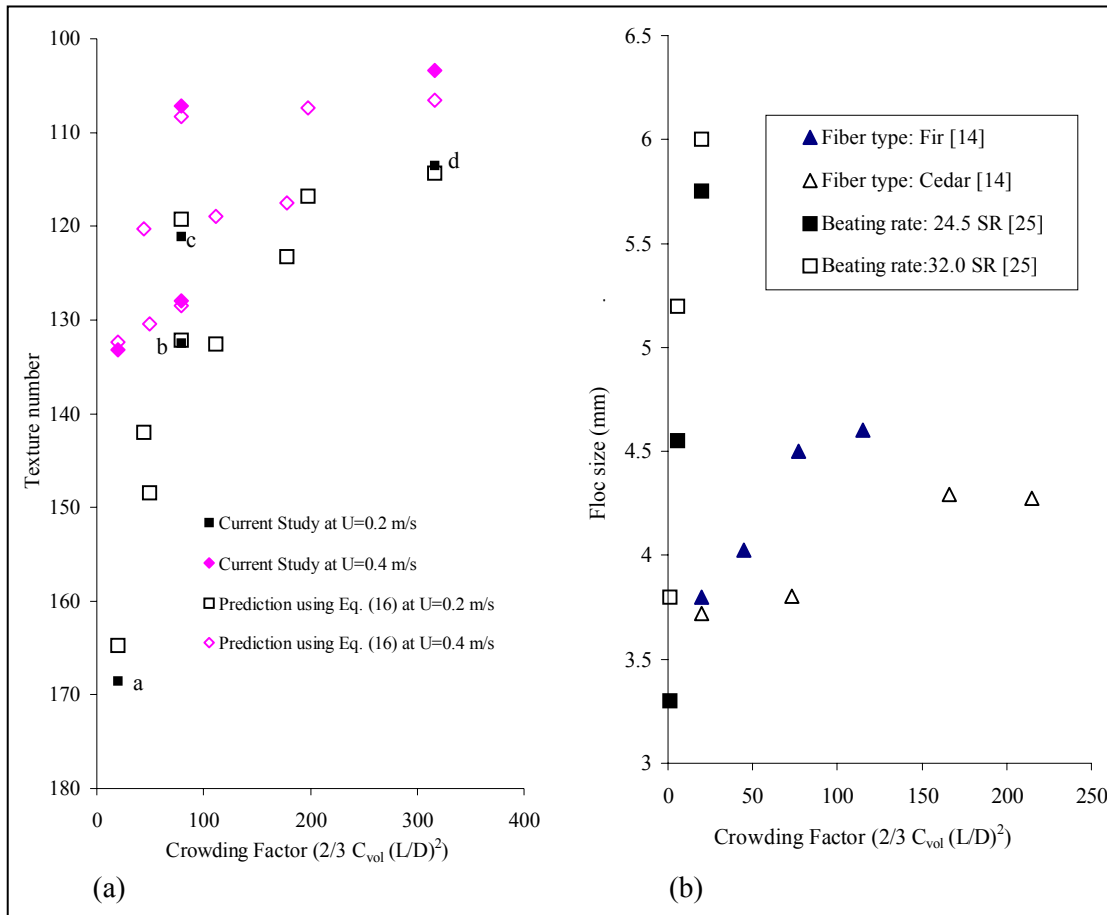


Fig. 38. Comparison of consistency and aspect ratio of current results with literatures.

The results in Fig. 36 and Fig. 37a show that lower consistency gives better texture and distribution of the fibers. Initially at lower consistency of 0.1%, the water flow is able to distribute the fiber easier. In this lower consistency, more water flow is capable to penetrate to fiber network, causing imbalance in flocs structure, and finally the rupture of fiber entanglement become more imminent. As the consistency increase, more fibers are involved in contact and entanglement with each others causing the growth of larger and stronger fibers flocs that are difficult to be broken down into smaller entities by water flow.

Fluid velocity has different degree of contribution at low and high consistencies. This can be seen as the difference of texture number values between higher and lower

velocities at higher consistency is smaller than the difference at lower consistency. Higher consistency fiber flocs have better resistance to any change of fluid velocity. These results agree with the experimental conclusion of Kerekes and Schell [23,24] as shown at Fig. 38b. They found that the higher consistency increases the flocculation by increasing the collision frequency of fibers inside the suspension. Using fiber rayon, Beghelli and Eklund [25] reached similar conclusion as also shown in Fig. 38b. The experimental results and their conclusion also expectedly agreed with the results from computer-generated images as discussed in Chapter V. The complete detail of experimental parameters used by published literature is presented in Appendix E.

Aspect ratio effect

Lower aspect ratio (L/D) gives better texture and distribution of the fibers as shown in Figs. 36 and 38. Longer fibers will have better contact and entanglement with each other, while the shorter fibers when they get flocculated, they will get distracted easier by the flow that leads to a better distribution of fibers. Shorter fibers are also more mobile and easier to avoid any entanglement with other fibers or aggregated fibers. Using various nylon and pulp fibers Kerekes and Schell [23,24] also came up with a similar conclusion as shown in Fig. 38. Furthermore, the study by Beghelli and Eklund [25], as they came with similar conclusion, noted that the longer fibers might have better flexibility and this flexibility exerts a large influence on flocculation process by building more entangled networking.

While fiber diameter was kept constant throughout the current study, some observation can be made on the effect of this variable using the work of earlier researchers. Kerekes and Schell [23] indicated that any increase in fiber diameter creates more fiber bending. More fibers bending create smaller flocs or better dispersion by reducing their "effective length". Their conclusion on fiber diameter effect was parallel with the results that used aspect ratio or crowding factor as main parameters. The increase in fiber diameter will mean the decrease in aspect ratio and crowding factor, and also the fiber flocculation, as shown in Fig. 38. More details on the operating parameters of published results are shown in Appendix E.

An interesting observation was made during experiment related to the effect of aspect ratio to flocculation. During the experiment the fibers with higher aspect ratio value tended to make the clog problem inside the pipe easier than when the smaller aspect ratio fibers were used. While this phenomenon is not related directly to fiber dispersion study, this clog problem shows that the higher aspect ratio fibers lead to more entanglement and bonding within fibers.

Difference degree of effect of crowding factor

While the aspect ratio and consistency parameters can be presented either individually or as a combined parameter in crowding factor, it is important to recognize that changing the crowding factor by changing the aspect ratio does not produce the same effect as changing the crowding factor by changing the suspension consistency. Kerekes and Schell [25] believed that crowding factors alone is not adequate to characterize the flocculation level. At the same crowding factor, changes in fiber length yield different results than changes in consistency. This is the main reason for the current study focusing on these two factors individually instead of just combining them into a single crowding factor.

This difference in effect of aspect ratio and consistency can be observed in the current study results presented in Fig. 38a. and Table 7. At constant fluid velocity line in Fig. 38a, there is significant result difference in texture numbers at location with similar crowding factor numbers but with two different operating conditions. At the case of fluid velocity of 0.2 m/s, for instance, as described in Fig. 38a and Table 7, at point c ($C=0.4\%$ & $L/D=200$) has the texture number of 132.1. On the other hand, point b ($C=0.1\%$ & $L/D=400$) has texture number of 119.4. Although both conditions have similar crowding factor of 79, their corresponding texture numbers are significantly different. This causes the slope between point a ($C=0.1\%$, $L/D=200$) to point c, being steeper than the slope between point a to point b. Similarly, the slope between point b to d ($C=0.4\%$, $L/D=400$) is steeper than the slope from point c to d. This observation indicates that the fiber aspect ratio is more dominant component in crowding factor compared to consistency within the ranges of study. Same phenomenon was also

observed at the case of fluid velocity of 0.4 m/s. This conclusion support the fact that crowding factor has the fiber aspect ratio in squared term compared to consistency term. The conclusion also agrees with the conclusion drawn from two-factorial design analysis which has been discussed previously. While the crowding factor may not represent correctly the degree of each factor/parameter affect the flocculation level, but, nevertheless, because of the strong dependence on fiber dimensional properties (L/D) and its capability to describe the fibers ability to move inside the fluid flow, the crowding factor is useful parameter for characterizing fiber flocculation.

Velocity effect

The comparisons of fluid velocity of current results and the previous literature are presented in Fig. 39 that has been presented previously as Fig. 15 but with no current study results. The predicted values using Eq. (16) are also shown in Fig. 39. The results from Takeuchi et al. [31] and Jokinen and Ebeling [29] were presented in form of flocculation change percentage in Fig. 39b and results from Hourani [34] in form of floc size in Fig. 39c.

The results of current study in Figs. 36 and 39 show that lower fluid velocity gives better texture and distribution of the fibers. The results agree with experimental data of Hourani [34] using softwood fiber a length of 4 cm. Unfortunately they disagree with the results shown by Jokinen and Ebeling [29] and Takeuchi et al. [31]. Using laser light transmission to measure dispersion at velocity of 0.15-0.6 m/s, Jokinen and Ebeling [29] found the velocity tends to increase dispersion level of the fibers. Similarly, Takeuchi et al. [31] achieved similar results as shown in Fig. 39. However, Hourani [34] also found conflicting results of his study. Using the hardwood fiber of 1 cm in length, he found that the floc size decreases with fluid velocity as shown in Fig. 39b. Meanwhile with softwood fibers, he found that the floc size increases slightly with fluid velocity.

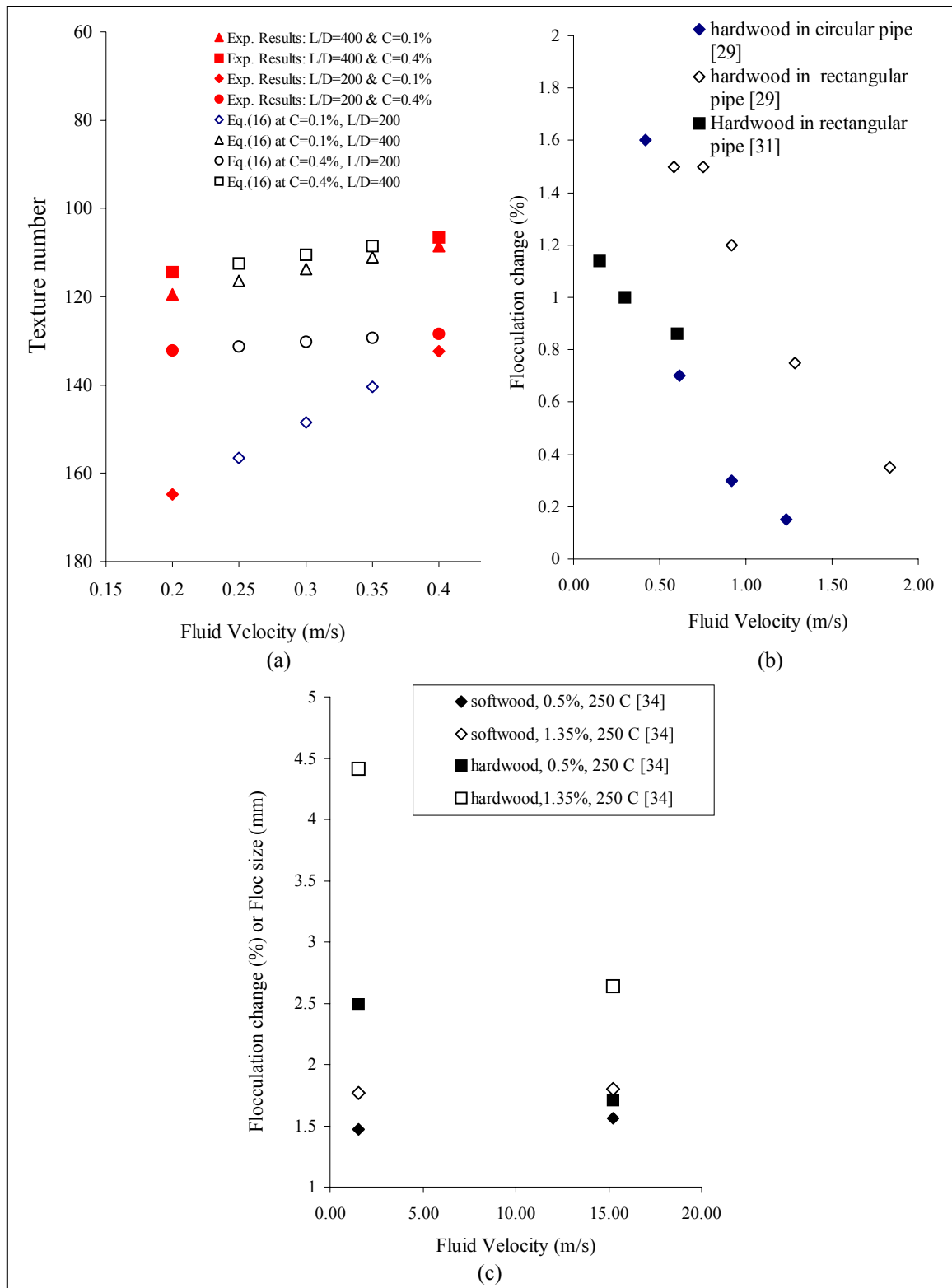


Fig 39. Comparison of fluid velocity effect of current study results with published results in literatures at two different conditions: constant velocity (b and c).

Hourani [34] believed that the velocity effect is more complex due to different mechanisms. Vortices generated within fibers may favor flocculation while shear may break flocs. He suggested that these two mechanisms are dependent on consistency and fiber properties. It is very possible then that if either the velocity is increased or decreased from the originally set, the outcome of the experiment will be different depending on the other properties of fibers and consistency [34]. The experimental conditions and parameters of previous researchers are given in Appendix E.

Additional observation of velocity effect

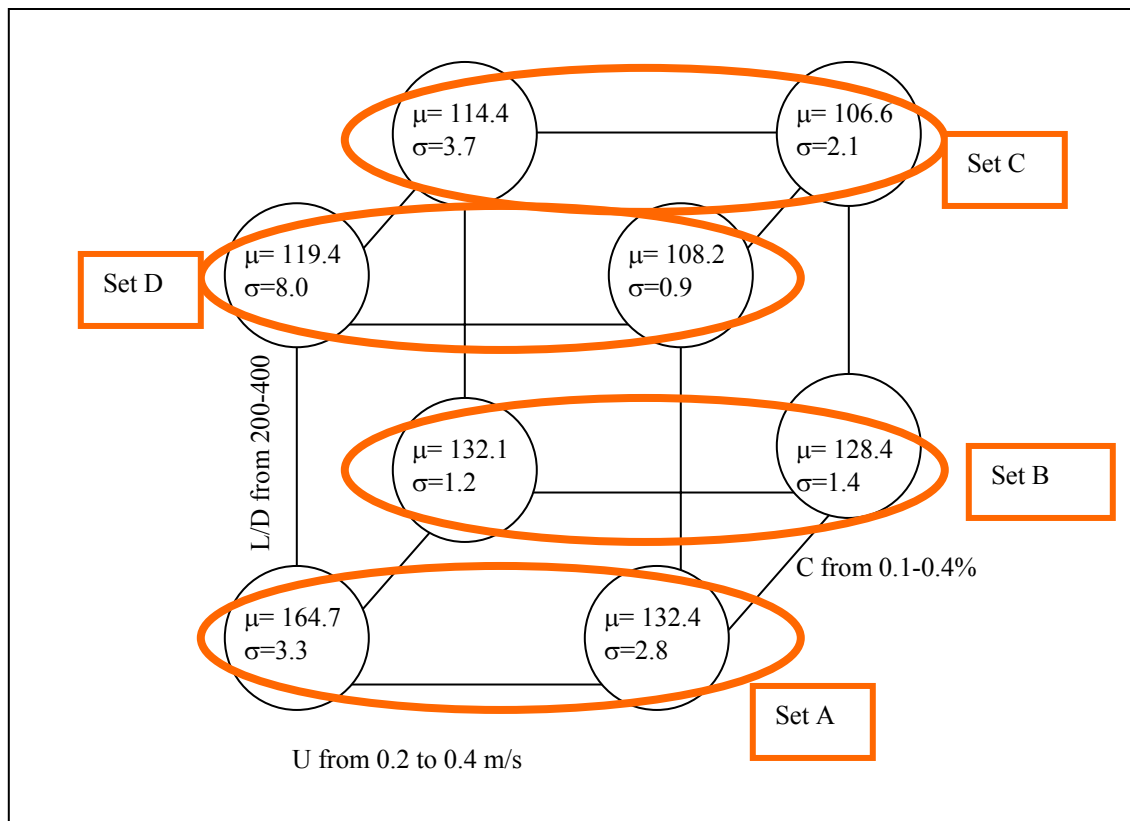


Fig. 40. Four set configurations for further velocity study.

Due to disagreement with several data published in literature, further studies were made to investigate fluid velocity effect to fiber dispersion. Four experimental parameters based on the conditions in two-factorial study were set as shown in Fig. 40 as sets A to D with varying velocity. For each set, six data were taken. The results at each corner of sets A-D were compared to the original results at Fig. 36. The differences between original results were found to be insignificant compared to the new results as described in Table 8. Figures 41 to 44 show the sample images taken and Figure 45 shows the dispersion results.

The results show that at all four cases, the texture number decreases as the velocity increases. As mentioned above these results disagree with results from other researchers. The difference might occur due to velocity range used, channel type, and fiber type. The velocity range used for current study is about 0.2 to 0.4 m/s. This range might not well served as other researchers have used. Jokinen and Ebeling [29] used light transmission to measure dispersion at fluid velocity of 0.15 to 0.6 m/s. Takeuchi et al. [31] studied the flow velocity effect on the fiber flocculation at the range 0.5 to 2 m/s. The velocity range used might not have enough strength to disrupt the formation of that observable by the imaging techniques. The micro eddies occurrence within the fibers and flocs might also affect further the tendency of fibers to form flocs. However, the upper velocity used might not have enough inertia to disrupt the formation of fibers that are already created from the upstream of the channel

Table 8. Results of additional study of velocity effect.

Set A: $l/d = 200$ & $C = 0.1$ %

U in m/s	Result from Fig. 36	Results from additional study
0.2010±0.0074	164.7±3.3	168.5±3.5
0.2502±0.0054	n/a	153.4±3.1
0.3001±0.0067	n/a	142.6±2.8
0.3504±0.0071	n/a	139.4±2.5
0.4005 ± 0.0072	132.4±2.8	133.2±3.2

Set B: $l/d = 200$ & $C = 0.4$ %

U in m/s	Result from Fig. 36	Results from additional study
0.2010±0.0074	132.1±1.2	132.5±2.5
0.2502±0.0054	n/a	130.4±1.6
0.3001±0.0067	n/a	130.1±4.4
0.3504±0.0071	n/a	130.0±2.4
0.4005 ± 0.0072	128.4±1.4	128.0±3.5

Set C: $l/d = 400$ & $C = 0.4$ %

U in m/s	Result from Fig. 36	Results from additional study
0.2010±0.0074	114.4±3.7	113.5±2.6
0.2502±0.0054	n/a	112.1±1.6
0.3001±0.0067	n/a	108.4±3.7
0.3504±0.0071	n/a	106.1±2.5
0.4005 ± 0.0072	106.6±2.1	103.4±5.1

Set D: $l/d = 400$ $C = 0.1$ %

U in m/s	Result from Fig. 36	Results from additional study
0.2010±0.0074	119.4±8.0	121.1±1.9
0.2502±0.0054	n/a	120.3±3.4
0.3001±0.0067	n/a	120.1±2.2
0.3504±0.0071	n/a	117.5±4.1
0.4005 ± 0.0072	108.6±0.9	107.2±1.7

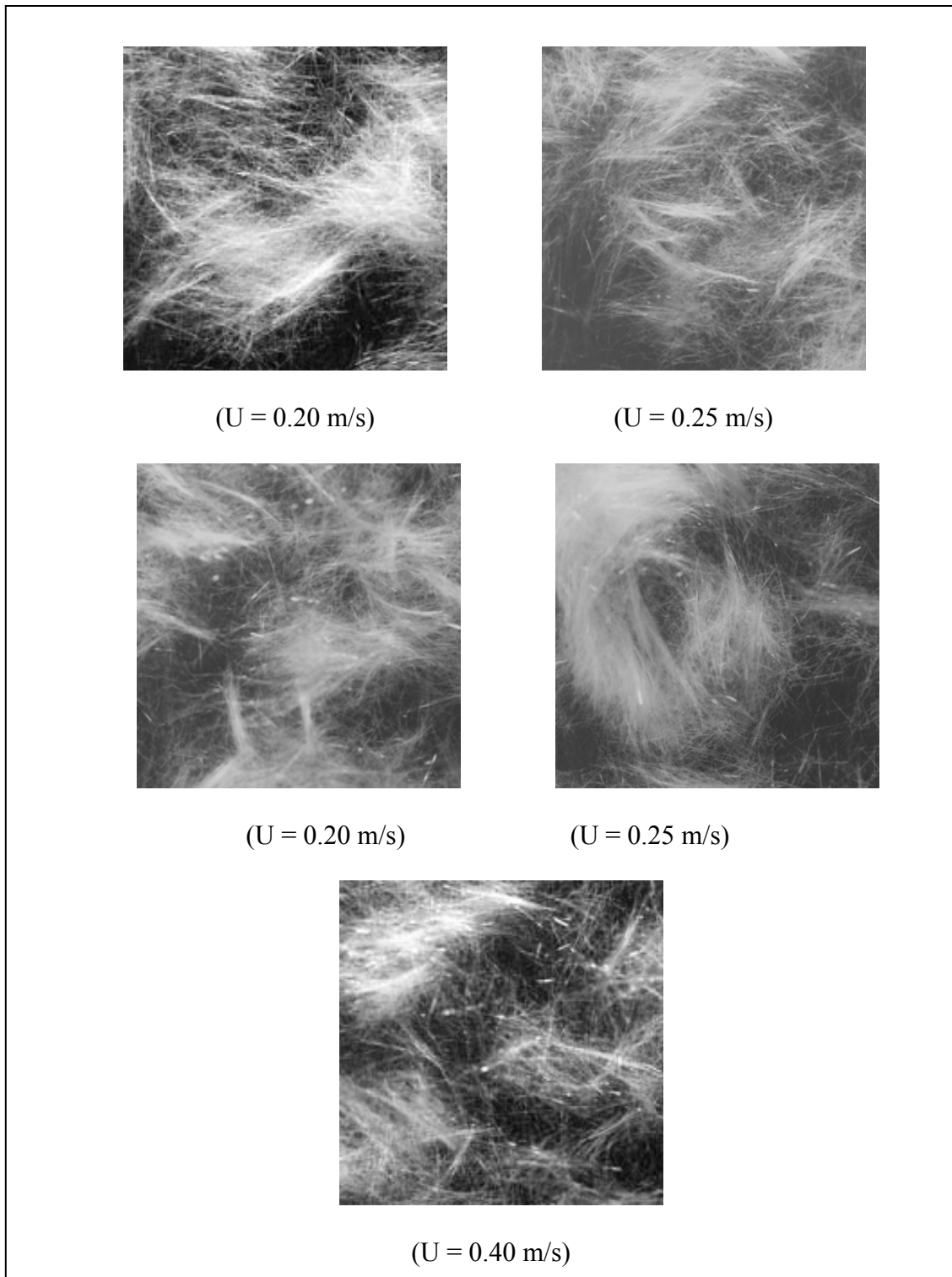


Fig. 41. Sample images taken with different velocities at $C=0.1\%$ and $L/D=400$.

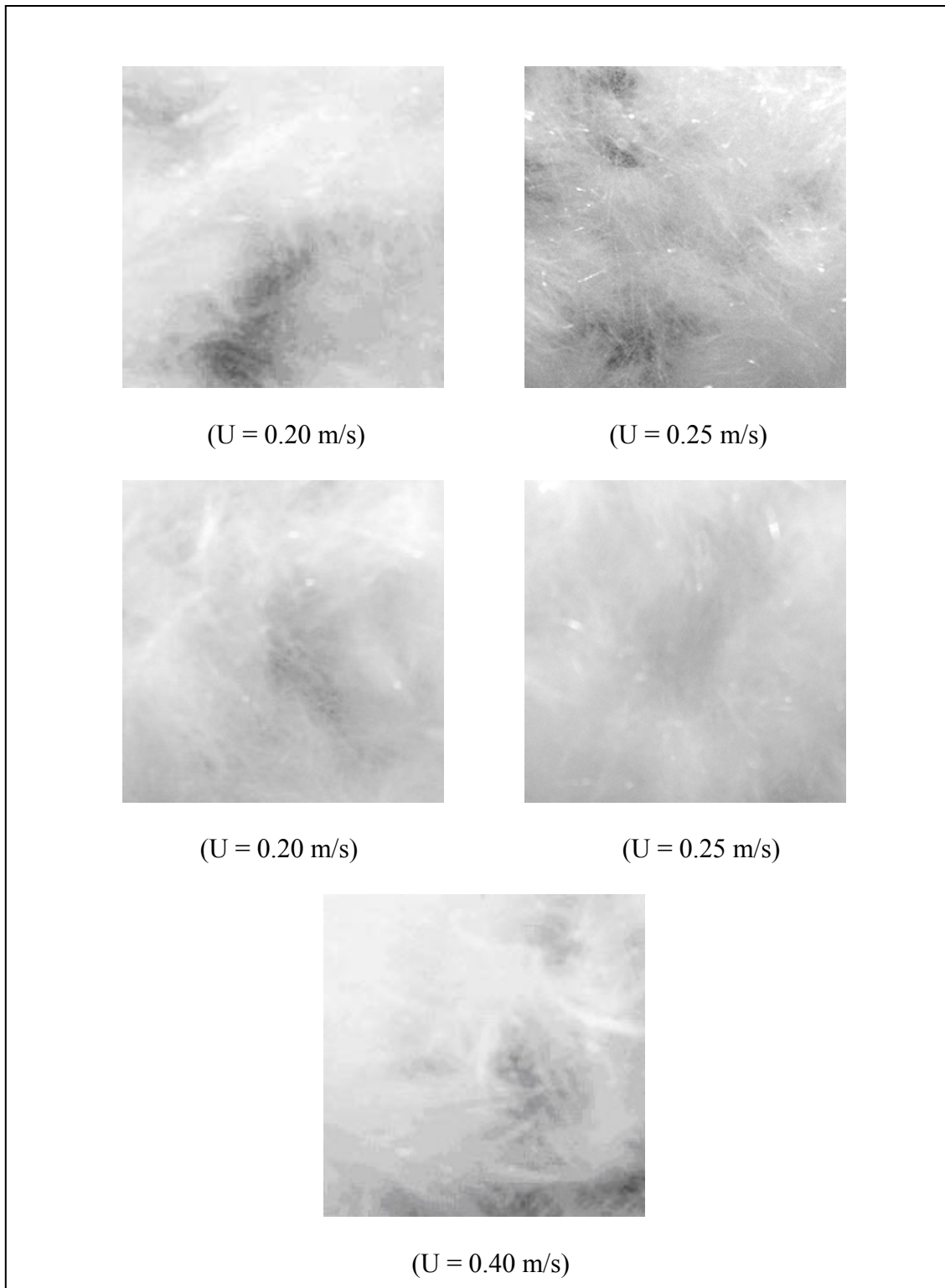


Fig. 42. Sample images taken with different velocities at $C=0.4\%$ and $L/D=400$.

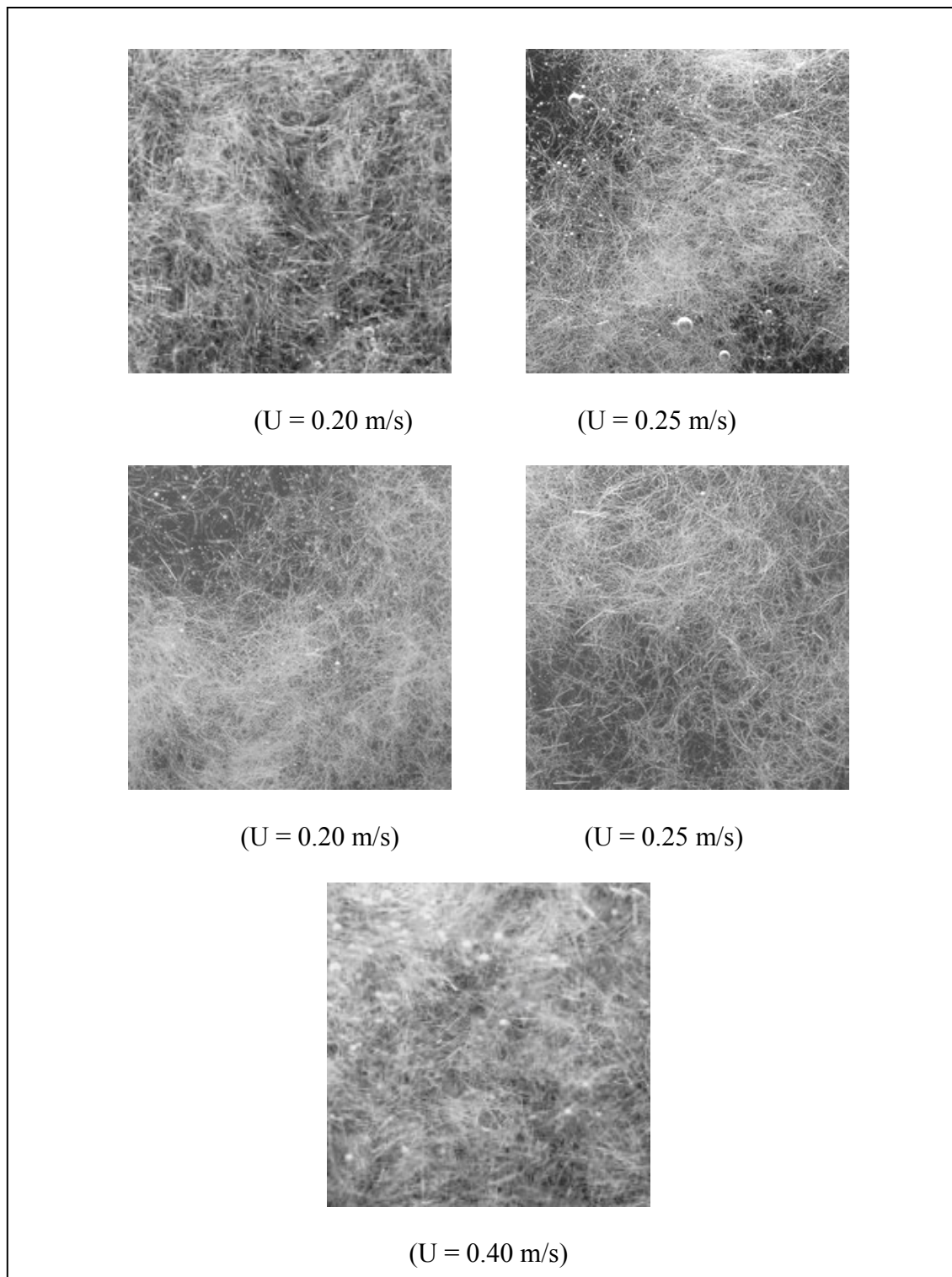


Fig. 43. Sample images taken with different velocities at $C=0.1\%$ and $L/D=200$.

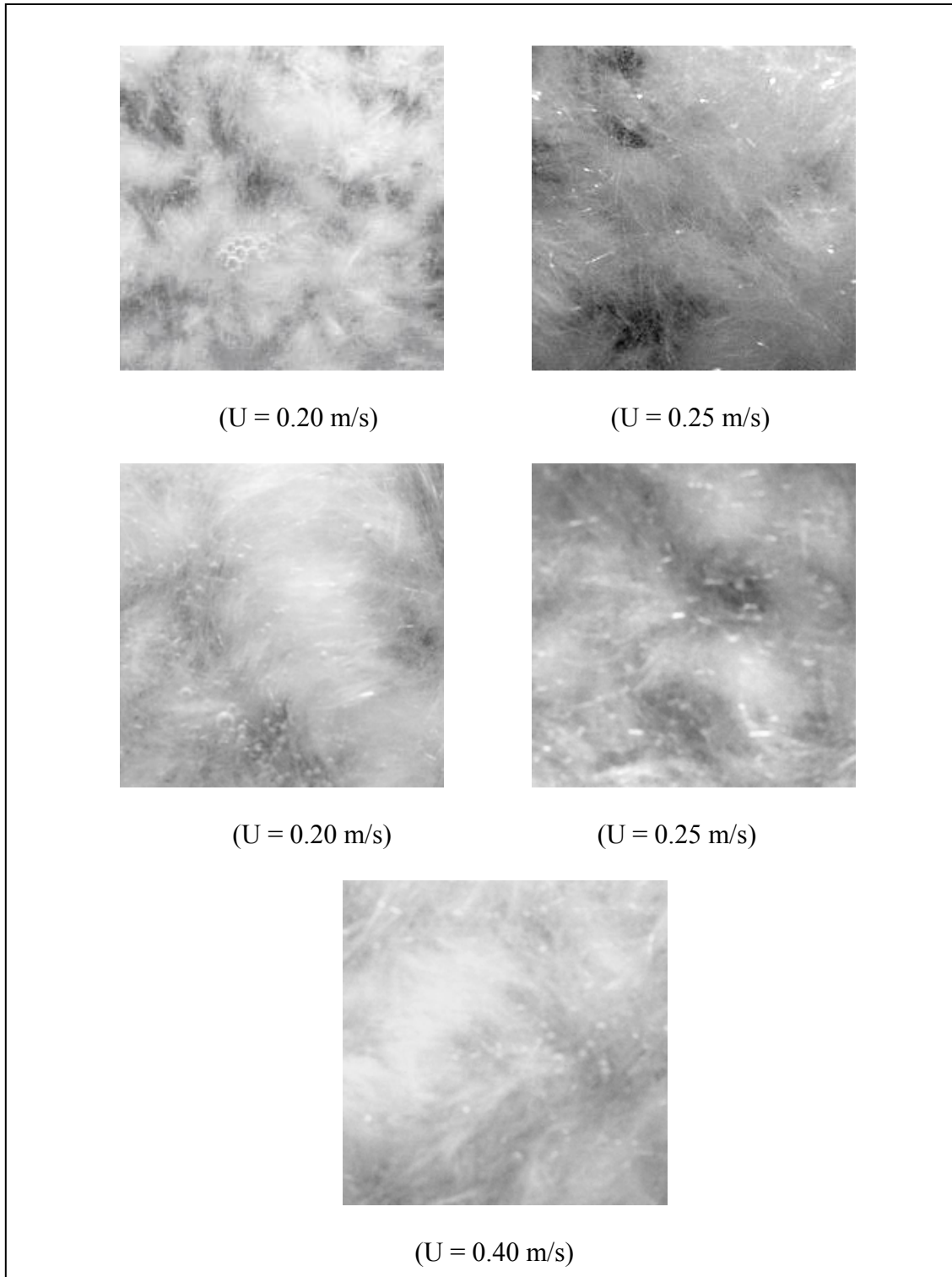


Fig. 44. Sample images taken with different velocities at $C=0.4\%$ and $L/D=200$.

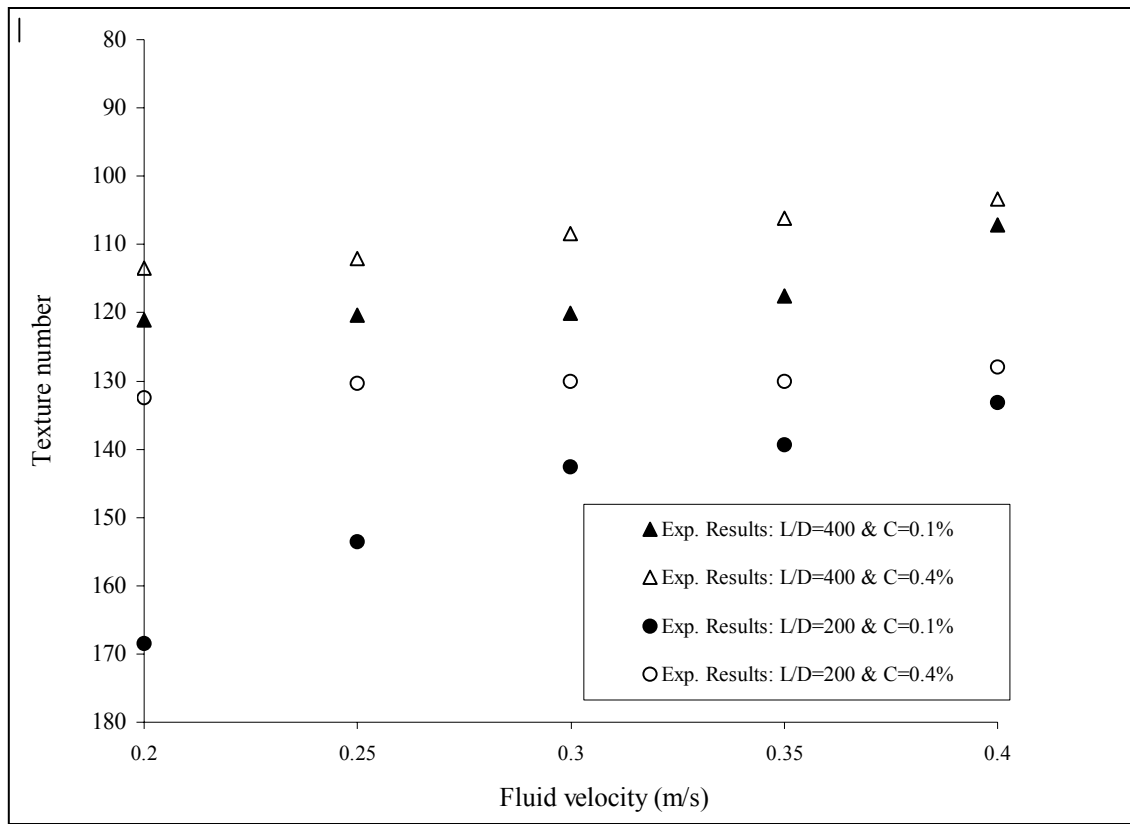


Fig. 45. Experimental data of fluid velocity as a function of texture number.

Reynolds number analysis

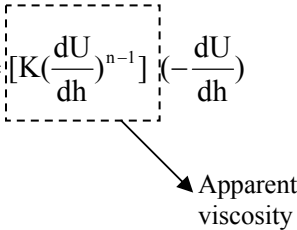
In order to understand the relation between fibers and fluid properties, the study was expanded to Reynolds number analysis. This number represents relative significance of the viscous effect compared to the inertia effect. It signifies the fluid velocity, fluid viscosity, and the channel shape and size effect. During flocculation process, as the fibers exist inside fluid flow, the Reynolds number reflects the ability of a fiber to follow fluid streamline. A small Reynolds number indicates a dominance of viscous forces and therefore an increasing tendency of fibers to follow the fluid (24).

In this study, the velocity results can be represented also in terms of Reynolds number (N_{Re}) for an open channel [53].

$$N_{Re} = U D_h / \nu \quad (17)$$

where U is the fluid mean velocity, D_h is the hydraulic diameter ($=4A/P$; where A is cross-section flow area, and P is wetted perimeter), and ν is the fluid kinematic viscosity ($=\rho/\mu$, with ρ is fluid density and μ is fluid dynamic viscosity). To calculate Reynolds number, the viscosity of fluid was measured using rotational viscometer by Cole-Parmer model 98936. The measurement was made at room temperature of 21° C and was assumed that there was no significant change of fluid properties. The fibers are also assumed to be uniform distribution during the measurement to ensure consistent measurement. Figures 46 and 47 describe relative viscosity of $L/D=400$ and 200 respectively as a function of shear rate at different consistencies. To describe the non-newtonian fluid behavior, the power-law fluid relation is used:

$$\tau_{rz} = \left[K \left(\frac{dU}{dh} \right)^{n-1} \right] \left(- \frac{dU}{dh} \right) \quad (18)$$



Where τ_{rz} is the shear stress, dU/dh is the shear rate, and constants K and n are determined based on the solution behavior. Using trendline generated and shown in Figure 46 and 47, the values of K and n can be determined.

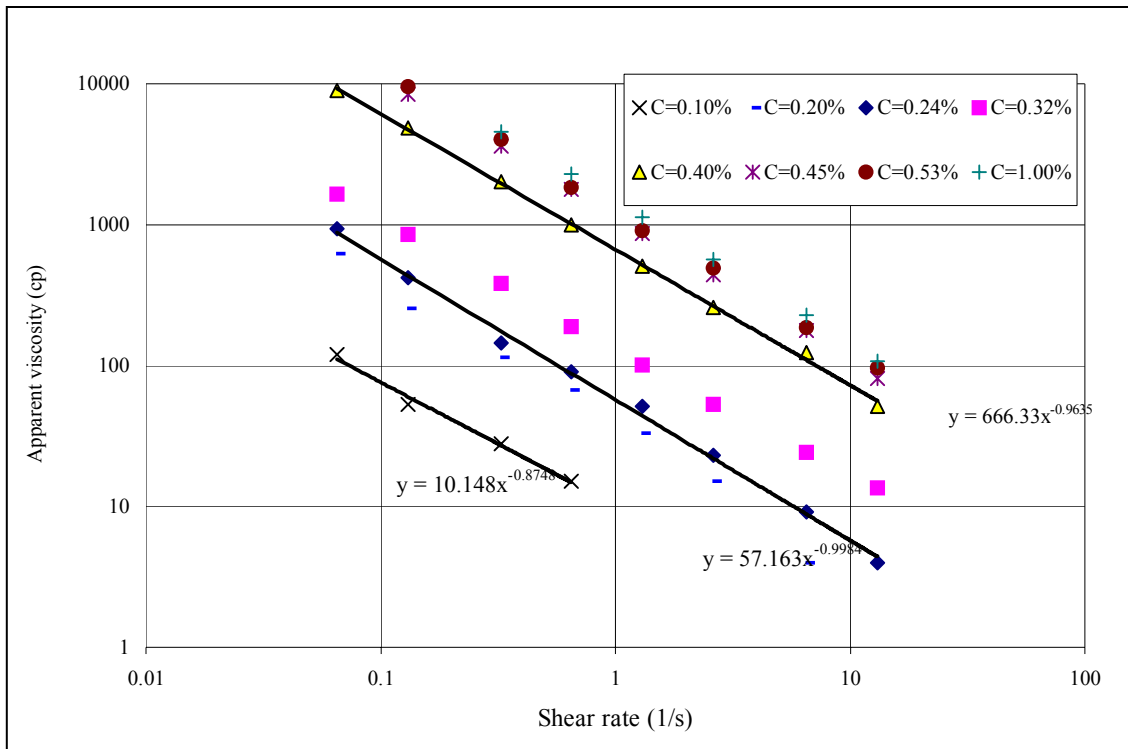


Fig. 46. Variation of apparent viscosity with shear rate for $L/D=400$.

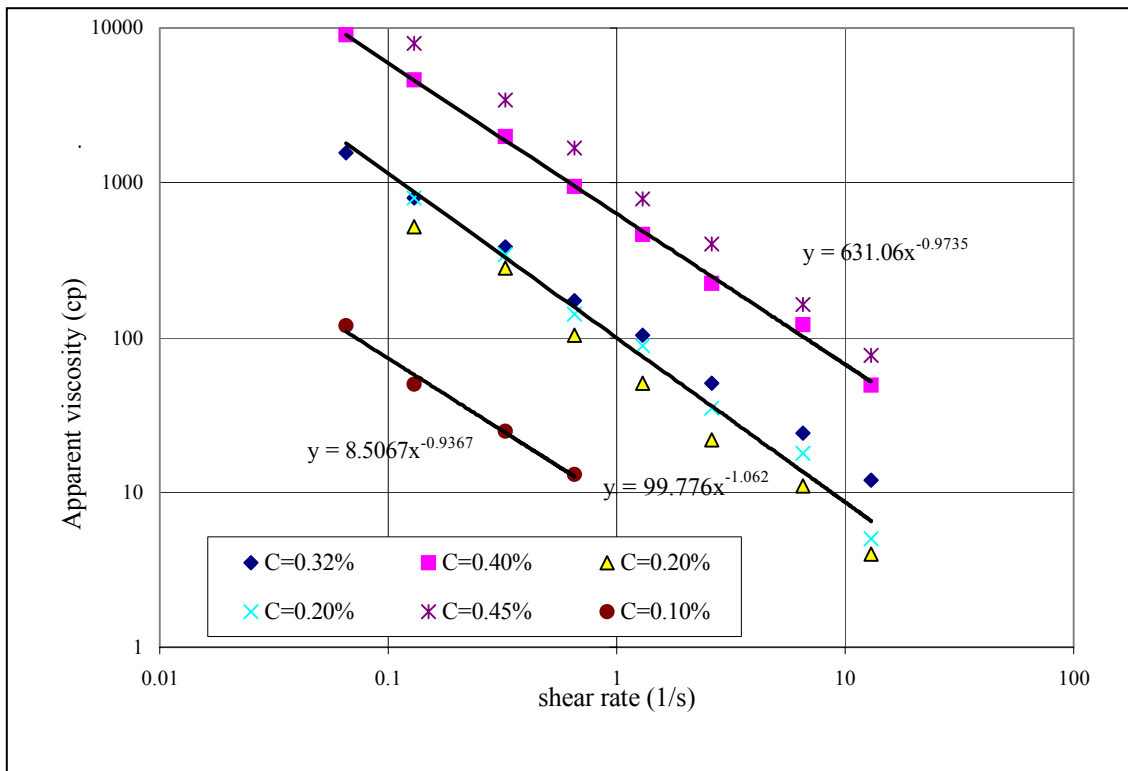


Fig. 47. Variation of apparent viscosity with shear rate for $L/D=200$.

The shear rate of experimental water flow can be determined by assuming that the fluid velocity (U) acts as surface fluid velocity and assuming that velocity profile follows linear relation as described in Fig. 48

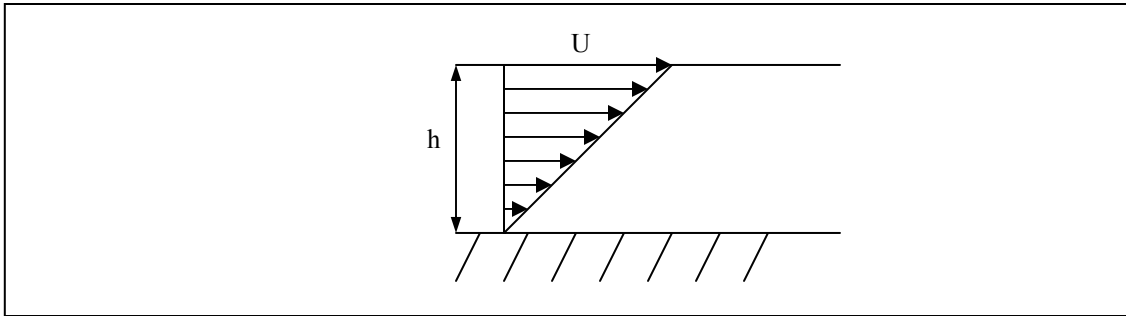


Fig.48. Assumed velocity profile.

Using constants K and n from equations shown in Figs. 46 & 47 and assumption mentioned above, the shear rate and viscosity of the water channel can be calculated and shown in Table 9.

Table 9. Calculated dynamic viscosity (μ) at experimental fluid velocity.

Velocity (u) in m/s	Water depth (h) in m	Shear rate in (1/s)	Viscosity (cp) At $L/D = 400$, $C=0.10\%$	Viscosity (cp) At $L/D = 400$ $C=0.40\%$	Viscosity (cp) At $L/D = 200$ $C=0.10\%$	Viscosity (cp) At $L/D = 200$ $C=0.40\%$
0.2	0.021 m	9.52	1.41	76.00	1.03	70.37
0.4	0.040 m	10	1.35	72.48	0.98	67.08
At $C=0.20\%$ average viscosity = 1.19 cp						
At $C=0.40\%$ average viscosity = 72.24 cp						

Table 9 shows that the flow velocity and aspect ratio have minimal effect to the change in viscosity while the consistency has significant effect to change in viscosity. It can safely conclude that the viscosity will depend solely on consistency of the solution. To calculate fluid density, Eq. (19) was used and its derivation is given in Appendix F.

$$\rho_{\text{mix}} = \frac{\rho_w \rho_f}{\rho_f (1 - C) + \rho_w C} \quad (19)$$

where ρ_w is water density (=1000 kg/m³) and ρ_f is fiber density (=1400 kg/m³). At $C=0.02\%$ and 0.04% , the densities were calculated to be 1000.57 kg/m³ and 1001.43 kg/m³ respectively.

Since the viscosity is assumed to depend solely on the consistency, then Reynolds numbers would depend on fluid velocity and consistency. Figure 49 describes the variation of texture number based on Reynolds number. The results show the Reynolds number as a combined factor has minimal effect to flocculation. It is due to that viscosity (or consistency) and velocities of the current study have an opposite effect to flocculation as shown in Figs. 38 and 39 previously.

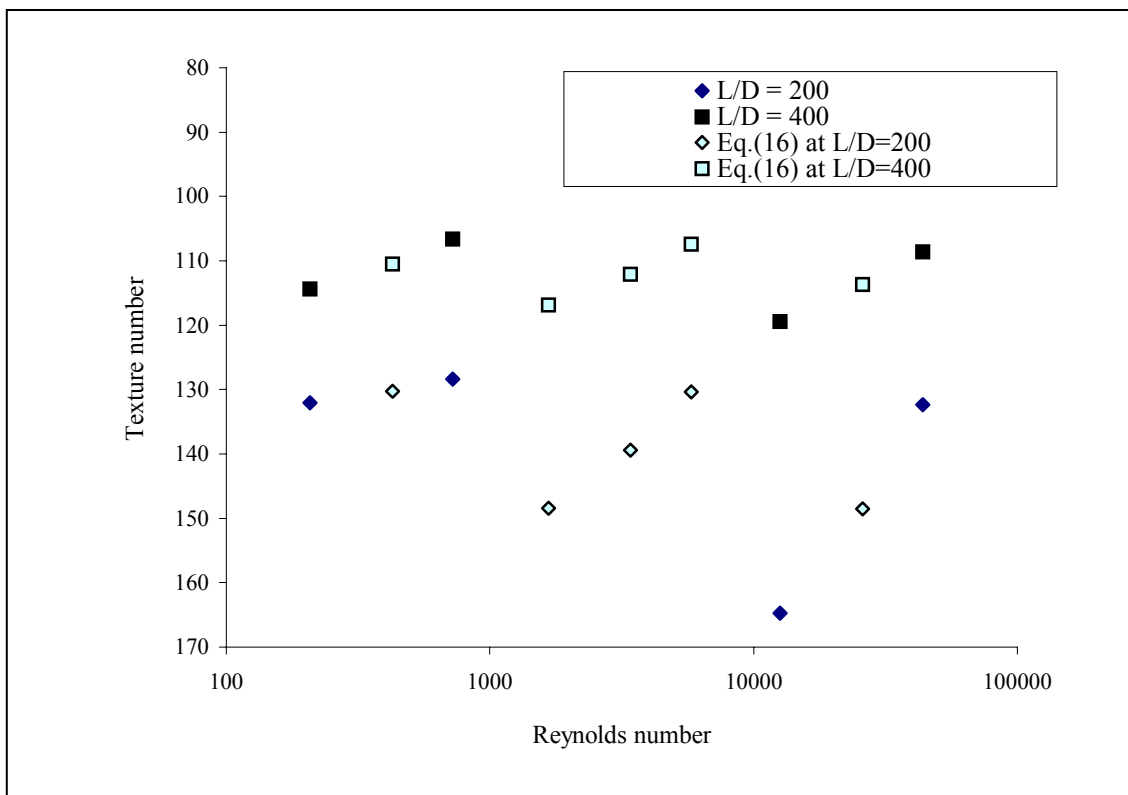


Fig. 49. Texture number variation based on Reynolds numbers.

While the current study on velocity effect has disagreement with the results shown by Takeuchi et al. [31] and Jokinen and Ebeling [29], it is necessary to observe a different case where fluid viscosity is changed by using different type of liquid viscosity keeping other variables to be constant. BeghELLO et al. [26] conducted experiment by using constant values of velocity at 1 m/s and consistency of 0.3% and varied the viscosity by adding the sugar into solution. Figure 50 has been shown previously in Fig. 16 but with no current results and in term of viscosity instead of Reynolds number. The current results showed that flocculation increases as the Reynolds number increases. Similar conclusion was also shown by results of Soszynski and Kerekes [42,43].

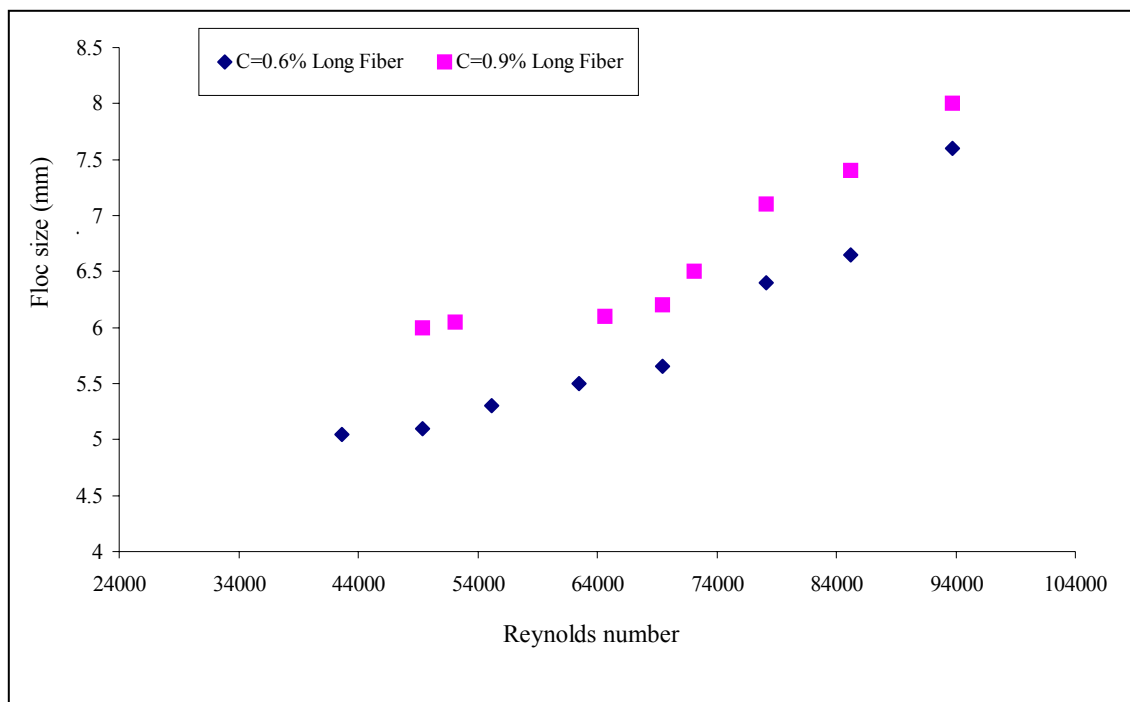


Fig. 50. Experimental data from BeghELLO [26] with constant fluid velocity and consistency.

The effect of Reynolds number in case of varied liquid viscosity was further explained more by Zhao and Kerekes [35]. They postulated that low Reynolds number creates more orderly flows as results of high viscous shear on fibers. This low Reynolds number decreases the relative motion between the fibers and enhances their ability to follow the fluid flow. This tends to diminish flocculation as anytime the fiber

flocculation occurs, the higher viscous forces on fibers would tend to disperse them. The higher Reynolds number tends to contribute the irregularity in fiber orientation and make the fibers less distributed/dispersed

The result shows that as the Reynolds number increases (with decrease in viscosity) the flocculation level increases. This conclusion contradicts with the conclusion drawn previously in Fig. 39b and c, which shows that as the Reynolds number increases (with increase in velocity), the flocculation level tends to decrease. The contradictory between fluid velocity and viscosity effects may be explained by Hourani [33], who noted that the mix results might depend on the fiber consistency and properties.

The shape, size, and type of channel may also contribute to make differences in results since they are integral parts of Reynolds number calculation. Previous researchers such as Jokinen and Ebeling [29] and Takeuchi et al. [31] used a closed channel that definitely has different flow characteristics from the open channel used in current study. Three-dimensional flow analysis also is another component that may be necessary to improve the accuracy of measurement instead of using one-dimensional assumption. The type of fibers used in current experiment also might contribute to the disagreement in results. The synthetic fibers used in this study have different properties in terms of flexibility and curliness compared to cellulose fibers used by Jokinen and Ebeling [29] and Takeuchi et al. [31]. Unfortunately, with limited resources, the current study was not able to verify these factors.

Non-Dimensional analysis

Undoubtedly, it is often difficult to investigate the flocculation factor effects when these factors are combined and used together. They may have different results depending on the value range of parameters. Crowding factor and Reynolds number as discussed above, combine two or more individual factors into single dimensionless numbers. While both are compact and convenient, they may not provide good approximation on the degree of how each of individual factors affects the flocculation/dispersion level.

From previous discussion on crowding factor and two factorial design analyses, clearly, there is a need to accommodate aspect ratio that has the biggest role in achieving the fiber dispersion. From Table 6, it can be seen that fluid consistency has the lowest influence to dispersion. However, the fluid consistency may have the second highest effect after fiber aspect ratio, considering that the fluid velocity experimental results have conflicting conclusion with literature. In study by Hourani [33], the conflicting result on fluid velocity effect also appeared. Fluid consistency experimental results also show good agreement with the previous studies conclusion. With above reasons, it is wisely to conclude that fluid consistency effect outweighs the fluid velocity effect.

Since fluid velocity is not a dimensionless number, the current study use Reynolds number as the way to accommodate the velocity effect. Reynolds number in our study, however, has a minimum role as shown in Fig. 49 previously. The reason is that Reynolds number depends on many factors that sometimes, as discussed and shown earlier, are contradicting to each other. Using Reynolds number also will include the effect of fluid consistency to the viscosity of solution, and the water channel size and shape. However, since the water channel shape and size are unmodified throughout the experiment, their effect to fiber dispersion cannot be investigated

Figure 51 gives an alternative on how a new dimensionless number can be developed. The numbers were given based on experimental data analysis and its corresponding two-factorial design results. The equation on x-axis $[(L/D)^6(C)^4(N_{Re})]$ of Fig. 51, provides the good approximation of the effect of these three parameters used. This equation was made based on trial-and-error method to get closest approximation to the current experimental results. The correlation coefficient (R^2) value is also given to give closeness of the trendline to the real data. This dimensionless equation clearly gives fiber aspect ratio the biggest role followed by fluid consistency, and fluid velocity (or Reynolds number) .

Attempts to use this dimensionless number for other researchers results were made. Unfortunately, they cannot be done due to lack of information especially on the relation between viscosity and consistency of the fiber solution, and shear rate used during their experimental studies. Relation between viscosity and consistency through

Power-Law as described by Eq. (18) can become a different subject of study, since the relation of viscosity results can be different, under different fiber distribution and configuration. Shear rate calculation can be also complicated since to determine a correct velocity profile is difficult to do especially with the turbulent flow and the presence of fibers inside the flow.

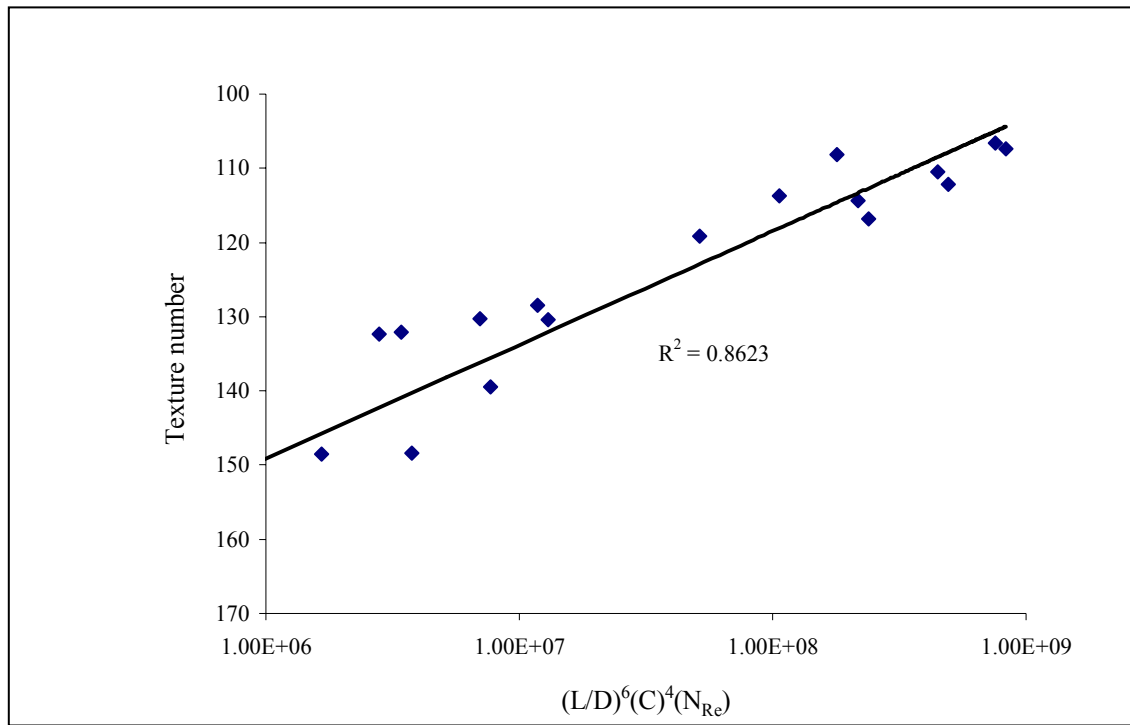


Fig. 51. Dimensionless variable to describe degree of effect of each parameter.

4.8. Summary

Understanding the mechanism and physics of fiber dispersion is very important in many industries such as paper and powder industries. Various measurement techniques have been proposed but none appears to be widely accepted by many researchers. Early attempt to use laser as illumination source similar to technique in PIV gave unsatisfactorily results at high consistency. A different technique in measuring fiber flocculation size using FFT concept by Beghelli et al. [28] was also applied.

Unfortunately the method failed to yield satisfactory results as their flocculation size at each operating condition came too close to each other.

The dispersion method proposed was originally made to measure the texture level of the image, but then proved to be useful to measure the dispersion too as developed by Ganesan and Bhattacharyya [11]. The results showed a satisfying result in identifying the level of dispersion. Two-factorial design was used to determine the critical parameters in fiber dispersion. Dispersion analysis yields that the increasing value for each factor will cause the decrease in dispersion level or increase in flocculation level. The results showed that two factors (aspect ratio and concentration) results have good agreement with the literature. The other factor (fluid velocity) results agreed with conclusion shown by Hourani [33,34] but had disagreement with results shown by Jokinen and Ebeling [29] and Takeuchi et al. [31]. This disagreement can be caused by various factors but notably are the size and shape of water channel. Fiber properties may also contribute to the difference. The analysis using crowding factor concept and two-factorial design analysis yielded that aspect ratio contributes heavily compared to the other two parameters. Two-factorial design analysis also indicated that the individual factors had larger effect to dispersion compared to the combined or interaction factors effects.

Reynolds number analysis was generated to study the relationship between fiber and fluid flow properties. Analysis and comparison with other studies indicated that Reynolds number may have contradicting effect due to the difference in effect of fluid velocity and viscosity. These conflicting results indicated that Reynolds number effect as combined factor have more complicated effect than when it is broken down into individual factors.

To accommodate properly the degree of each factor affecting the dispersion level, a dimensionless variable was proposed. This dimensionless variable consisted of not only the three main factors studied, but also the supporting parameters such as fluid viscosity and channel size and shape.

As these three factors were selected for the experimental study for the fact that they were most studied previously, it will be very intriguing to see how other parameters

such as beating rate, fiber flexibility, and chemical factors would affect the fiber dispersion. A significant improvement of fiber flocculation research also can be achieved by more developments in digital imaging technique and understanding.

CHAPTER V

COMPUTER-SYNTHEZIZED IMAGE ANALYSIS

5.1. Introduction

Computer-synthesized images that simulate real cylindrical-shaped fiber distribution were developed. These images were used to idealize the situation where concentration/density and local aggregation of fibers were controlled while letting each individual fiber location and orientation to be random. The images were analyzed to test the effect of fiber concentration and local aggregation using the texture level measurement that had been introduced and described above in Chapter II. Comparison was then made between results from the water channel experimental study (in Chapter IV) and computer-synthesized image study

5.2. Image Preparation

In order to get a close approximation to the fiber used in fiber dispersion experiment in fluid, the image of a single fiber and its dimension shown in Fig. 52 was proposed to use. The aspect ratio then is calculated to be 120. While this number is relatively lower compared to the ones used in the current water channel experiment (200 and 400), the number is well within the fiber aspect ratios used by previous researchers, [23,24,26-29]. The other reason is that the most important factor to achieve a reliable dispersion analysis is to generate image pixel size that is smaller than the fiber entity, which, in this case, is fiber diameter. Smaller pixel size will yield better accuracy of image representation. On the other hand, the lengths of fiber can be varied within a reasonable number of real fiber sizes and they will still work fine to satisfy the purpose of the study.

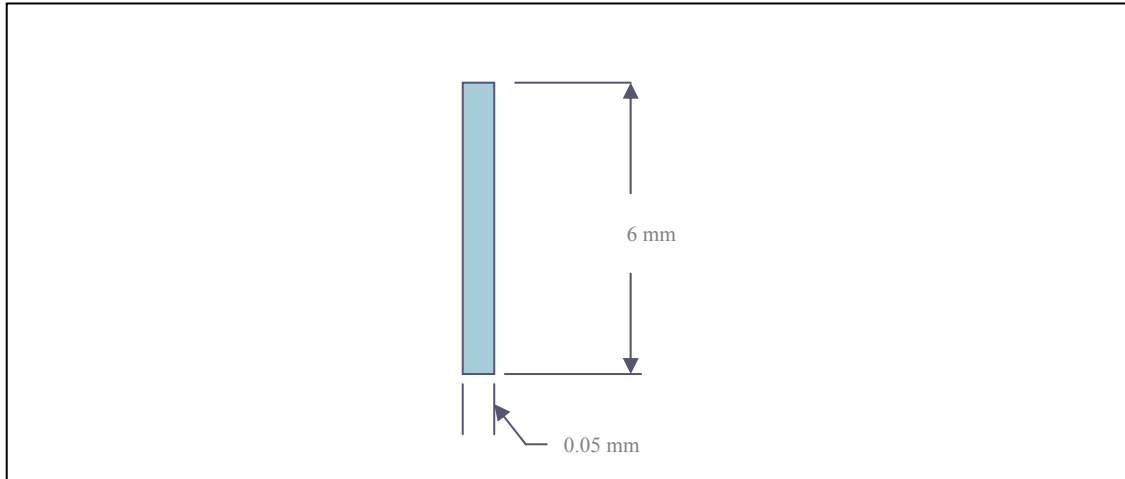


Fig. 52. Single fiber dimension.

To fulfill pixel requirement mentioned above and at the same time to minimize computing time, the image pixel size was selected to be 40 pixel/mm or 1 pixel equals to 25 μm . To generate image, initially computer program written in Matlab was developed. This code allows the orientation and location of a single fiber set to be random. The Photoshop software was then used to control fiber concentration and local aggregation depending on different cases studied. The total resolution of image is 2880x2880 pixels or 7.2x7.2 cm^2 using pixel size of 25 μm .

Unlike images produced in water channel experiment, the computer-synthesized image will be binary images containing pixels colored with only either black or white color. The white color represents the color of fibers while black color is the void background of water. Once a complete image produced, its dispersion level was measured using the procedure explained in Chapter II. Because of containing only two opposite color: black and white, the texture measurement results, in general, will have higher values compared to the results produced from water channel experiment/study. The texture measurement technique yields higher number when more contrast areas exist inside the image.

5.3. Case studies

Four different cases have been observed: two cases with varying density, and the other two with constant density. In general (except Case 1), the images will be divided into smaller and uniform-in-size squared blocks. Half of blocks will consist of more fibers compared to the other half. These blocks will be called as higher density blocks while the other half will be called lower density blocks. The exact number, configuration, and sample images for each case will be discussed in Results and discussion section. The summary of condition for each case is shown in Table 10.

Table 10. Summary for each case for computer-synthesized image texture analysis.

Case	Fiber density	Number of blocks	Higher density block	Lower density block
1	Varied	Constant	Constant	Constant
2	Varied	Constant	Constant	Varied
3	Constant	Varied	Varied	Constant
4	Constant	Constant	Varied	Varied

5.4. Results and discussion

a. Case 1

The objective of Case 1 was to observe the texture or dispersion level with the increase of fiber density with uniform distribution. In respect to water channel experiment in Chapter IV, this idealized situation can be achieved by adding the fibers concentration inside the water channel using assumption that the fibers are constantly well-distributed inside channel. The sample images used in testing are shown in Fig. 53. The results in Fig. 54 show that as the fiber densities are increased, the texture number was also increased up to an optimum point before it was finally decreased. The increase was due to more gray variation which is caused by more fibers appearance on the image. However, as more fibers were added into the images, the area became more crowded and the variation of grayscale finally is decreased. This decrease then caused the texture number to decrease too. From Fig. 53, can be also observed that as the fiber density

increased, the fibers started to overlap or contact to each other and caused the change of grayscale variation becomes less. While overlapping fibers might start to occur at low concentration, the probability or chance of occurrence is considered low compared to the overlapping at higher concentration. The rate of change of overlapping fibers occurrence is shown in Fig. 54 as the slope becomes less steep at higher density starting at fiber density of 2880. As the concentration of fibers increase to fill the whole image area, the texture number is expected go back to zero since at that case, no grayscale variation is expected to appear on the image therefore no texture will be exist either.

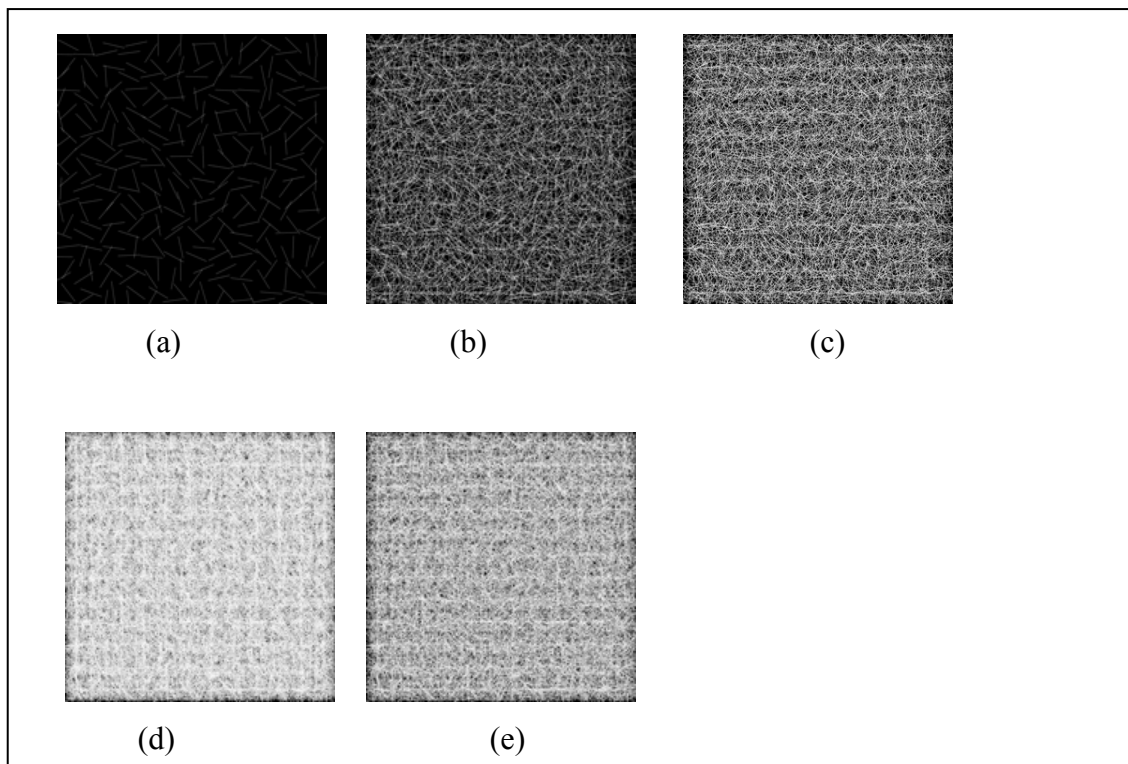


Fig. 53. Sample images with different densities used in Case 1: (a)288, (b)5760, (c) 10080 (d)20160, and (e)30240 fibers.

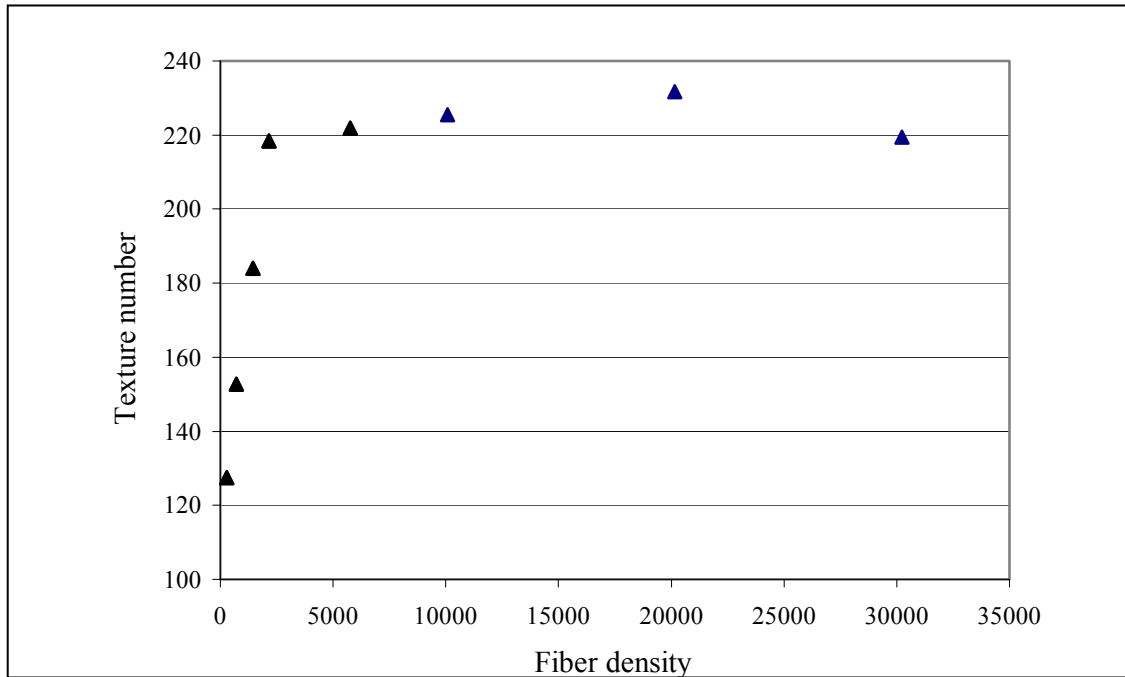


Figure 54. Variation of texture number with fiber density.

b. Case 2

Similar to Case 1, Case 2 also has varying fiber density. However, in Case 2, the images were divided into 8 by 8 blocks with higher and lower density small blocks with each block has a size of 360x360 pixels. The numbers of fibers at the higher density blocks were kept to be constant at 315 fibers/small blocks while at the lower density blocks, they were varied from 0 to 315 fibers/small blocks as shown in Fig. 55.

The higher density blocks can be imagined as groups of flocs or concentrated fibers inside the water channel experiment, while the lower density blocks contain water only. Furthermore, these constant higher density blocks may follow the arrangement of static equilibrium concept in flocculation which has been discussed in section 3.5 part a. In static equilibrium, the flocs will not be dispersed once they are created inside the flow. This concept also tells that there is a limit on the amount of fibers that can be bonded by the flocs. Case 2 tries to idealize this situation by using the higher density blocks as flocs that have already the maximum fibers bonded, and lower density blocks as the area outside flocs that keep receiving the fibers.

The objective of this part is to see how the texture analysis on the changing density with non-uniform distribution. Similar to Case 1, the results in Fig. 56 show that the texture number increases as the density increases due to the fact that more fibers at lower density block causes more grayscale variation of the image.

If the fiber density keeps increasing, the texture number is expected to decrease ultimately (similar to Case 1). The number of fibers inside the higher density blocks and total number of blocks can selected arbitrarily since the conclusion of the results will be qualitatively similar.

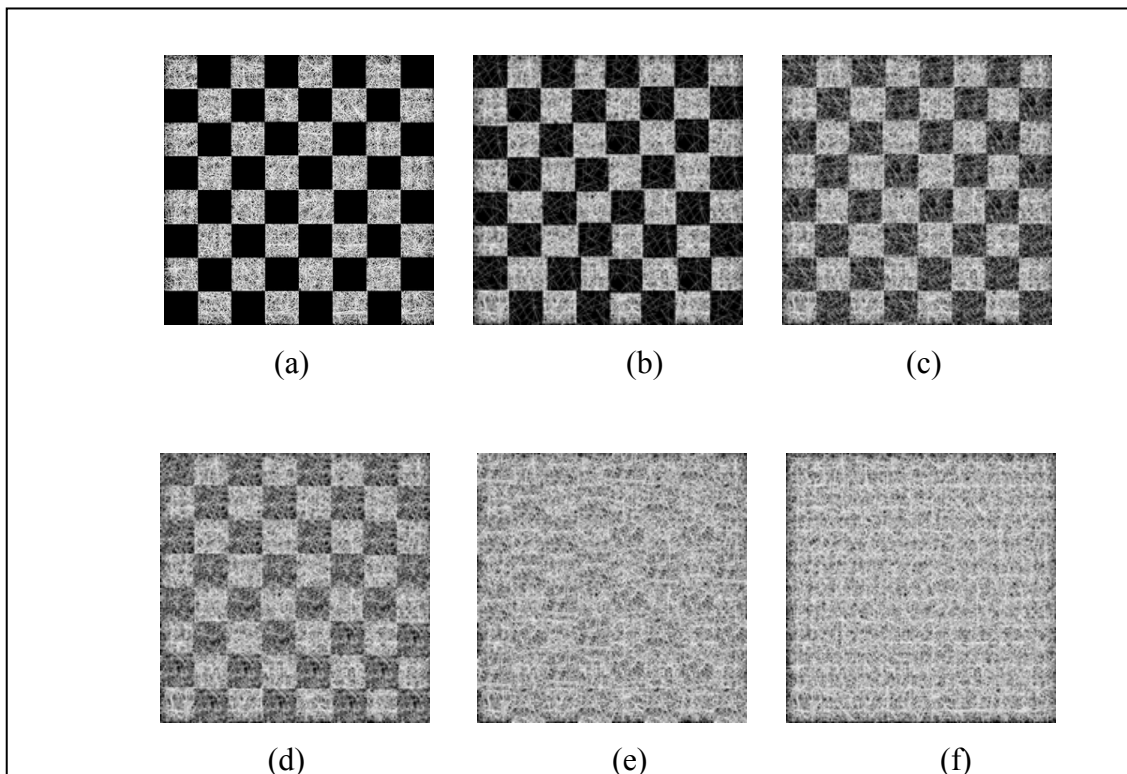


Fig. 55. Sample image used in Case 2 with constant higher density blocks at 315 fibers/small block and varied lower density blocks: (a) 0, (b)23, (c)80, (d)158,(e) 269, and (f) 315 fibers/small blocks.

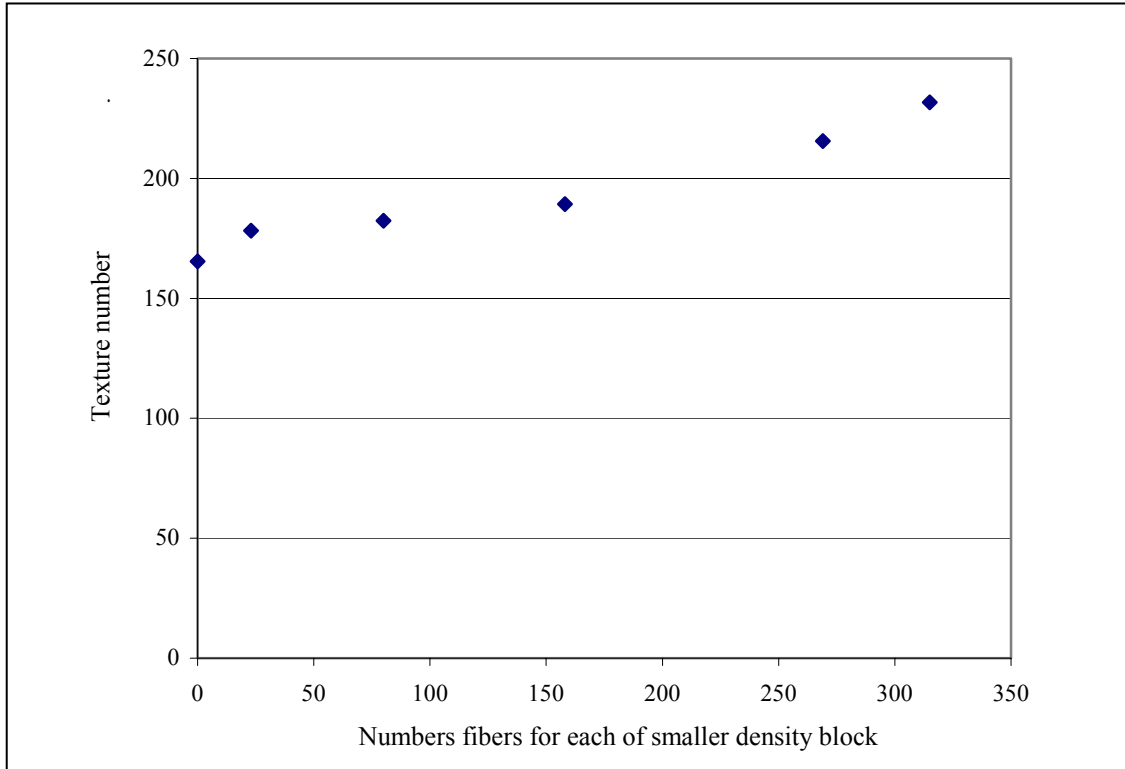


Fig. 56. Variation of texture number with fiber density of smaller density blocks.

c. Case 3

The dispersion analysis on constant fiber density with two different configurations is shown in Cases 3 and 4. Unlike the Case 2, Cases 3 and 4 can be related to the dynamic equilibrium concept introduced by Mason [18] and have been discussed in section 3.5 part a. In dynamic equilibrium, Mason [18] believed that inside the flow, the flocs repeatedly undergo forming and dispersion process. However the exact mechanism of dynamic equilibrium was not well known in literature. Two possible mechanisms to dynamic equilibrium were proposed and idealized in Cases 3 and 4.

First proposed mechanism is that once a floc is created, it starts to be broken up into two smaller pieces and the process occurs repeatedly until finally that floc is totally dispersed. This mechanism is described in Fig. 57. As mentioned above, the process is

reversible, meaning that the process keeps repeating from floc to dispersed fibers and from dispersed fibers to flocs. This concept was simulated in Case 3.

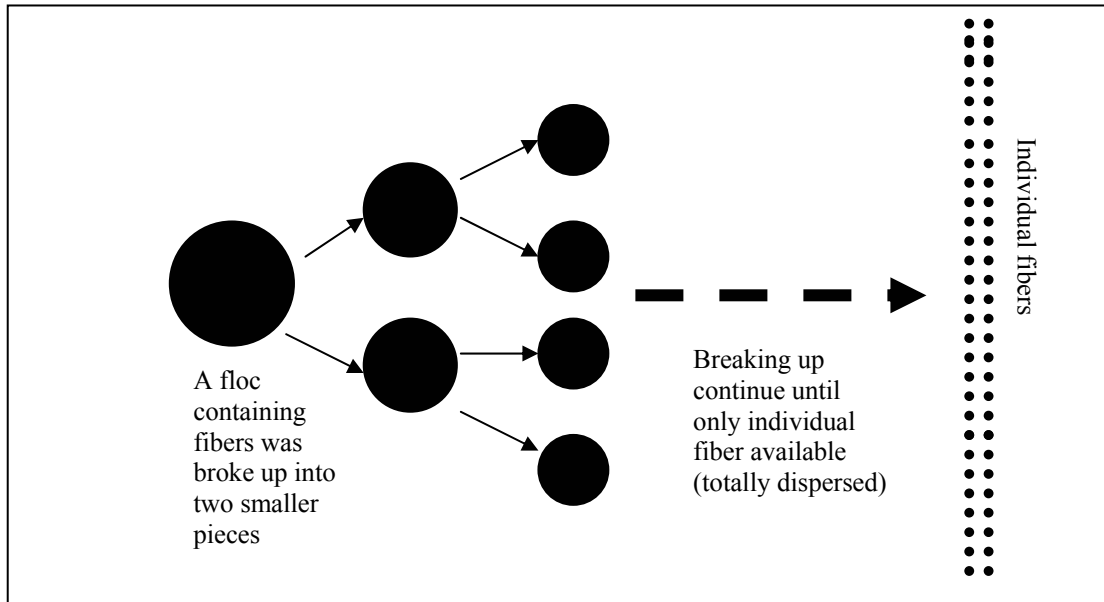


Fig. 57. First proposed mechanism of dynamic equilibrium.

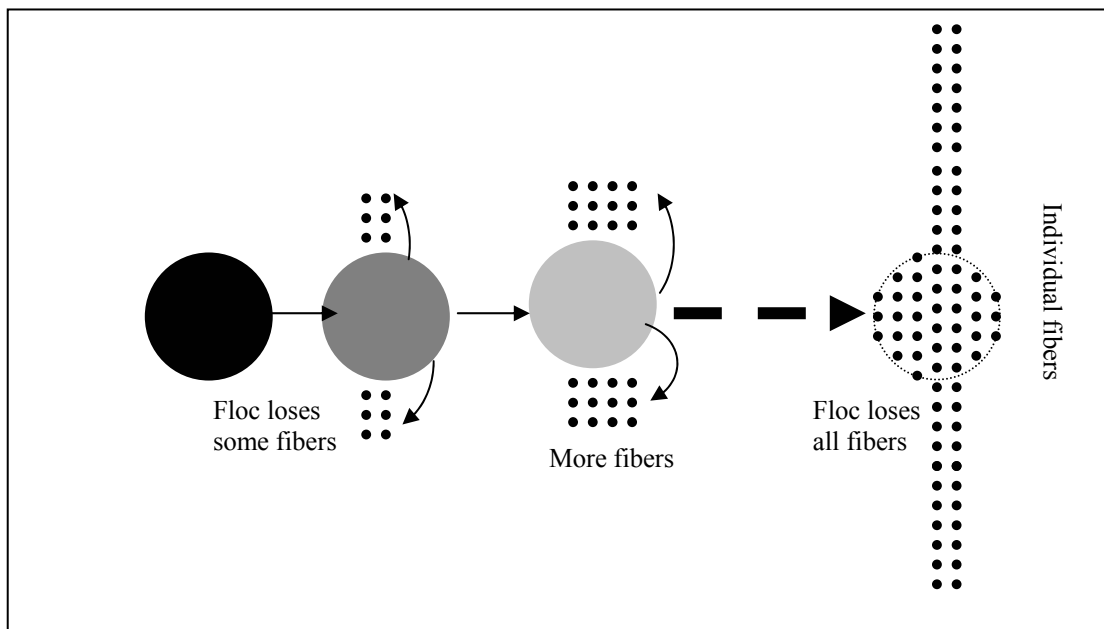


Fig. 58. Second proposed mechanism of dynamic equilibrium.

The second mechanism is that a floc once created, instead of being broke up into two pieces, that floc loses the fiber one by one to the flow until finally the floc loses all the fibers and gets totally dispersed. This mechanism is described in Fig. 58. Again, this process is reversible from fully dispersed to all flocs condition due to dynamic equilibrium concept. This mechanism was simulated in Case 4.

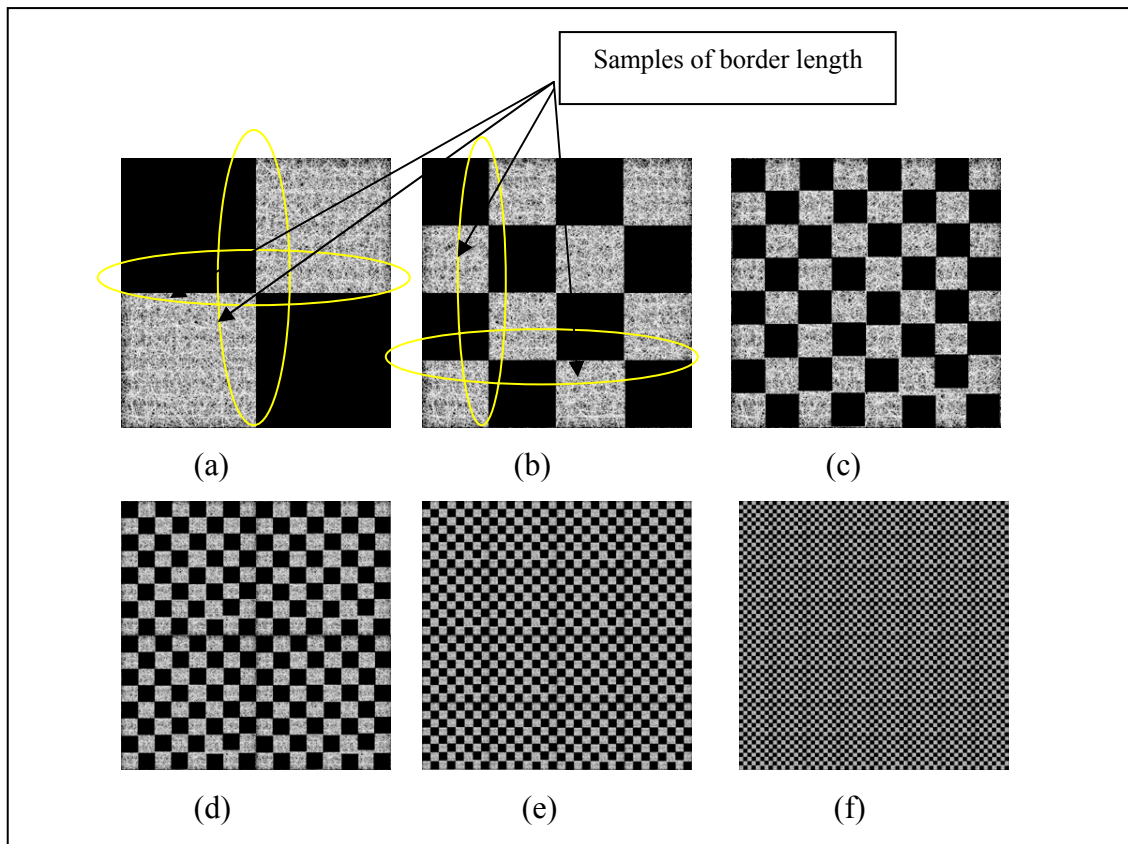


Fig. 59. Sample images used for case 3 with 6 different blocks: (a) 2x2; (b) 4x4; (c) 8x8; (d) 16x16; (e) 32x32; (f) 64x64.

On Case 3, the total number of small block was varied from 2x2 to 128x128 blocks. The whole fibers at higher density blocks were kept to be constant at 10080 fibers while no fibers exist at lower density blocs as can be seen at Fig. 59. The higher density blocks can be treated as flocs that are losing their sizes as described in Fig. 57. It

was found as shown in Fig. 60, that as the number of blocks is increased, the texture number is also increased. Observing the length of borders that are just imaginary lines existing between the higher and lower density small blocks can explain this increase. As the border length increases, the grayscale variation between lighter and darker regions will exist more and cause the increase of the texture number and dispersion level. If the number of blocks is increased to infinite while keeping a constant fiber density, the expected result will similar to the results from Case 1 at fiber density of 10800 fibers (Fig. 53c). Any small discrepancy may also came from the fact that each image from the Fig. 59 still has different image configuration due to the random single fiber location and orientation.

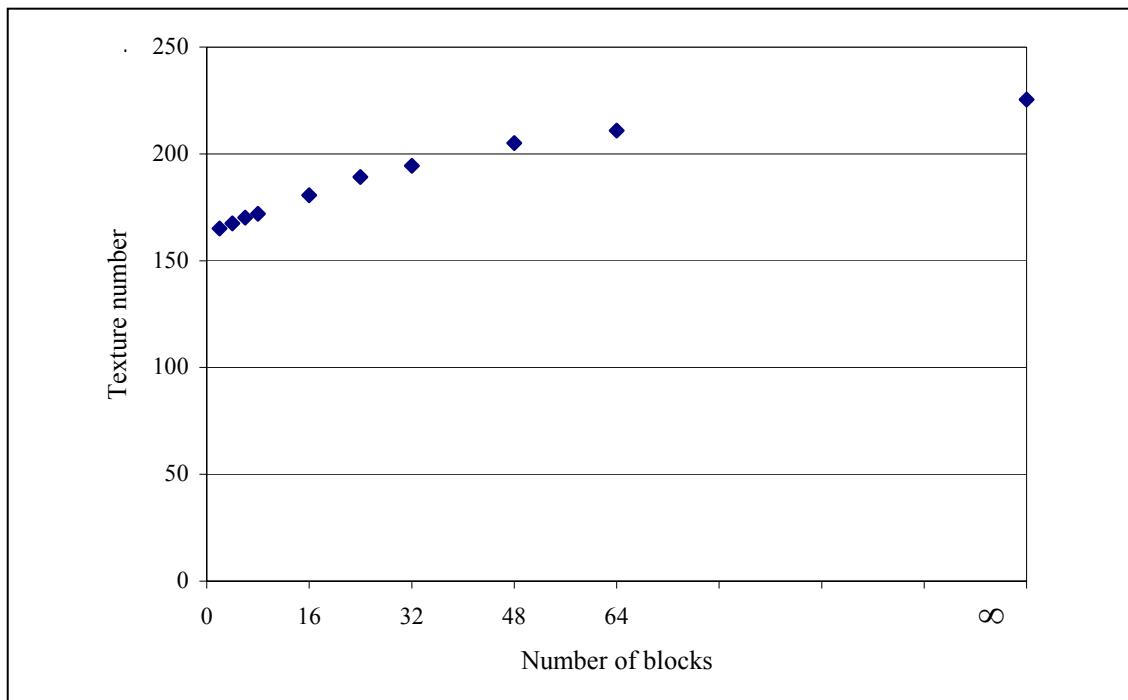


Fig. 60. Texture variation with number of blocks for Case 3

Further observation on the effect the fiber configuration and numbers of border lengths can be shown using the images shown at Fig. 61. In this Figure, fiber density was kept constant at 5040. In these images, all have same number border but with

different position of block. For part (b), (c) whose half of length border of part (a), the differences were unnoticeable. The border length at these two levels had a minimal effect to dispersion level. The difference in configuration of fibers seemed also to play minimum role to determine the dispersion level as can be seen from part (b) and (c).

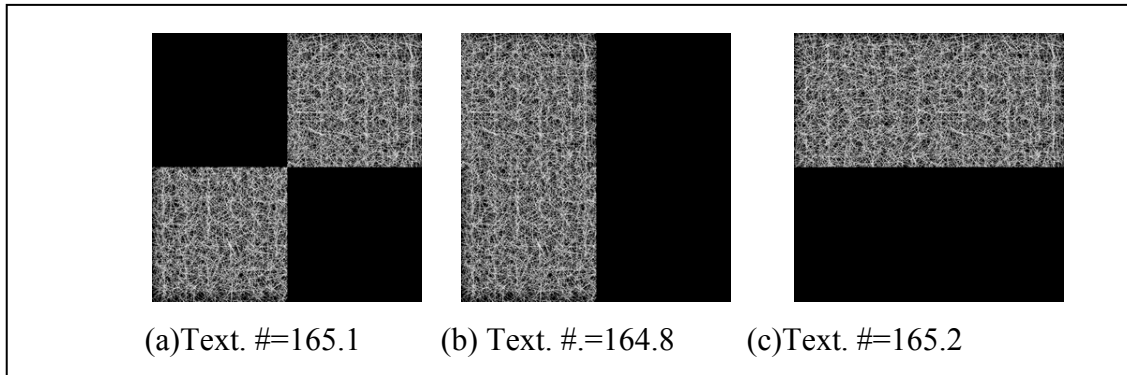


Fig. 61. Image used to test the border length differences and the corresponding texture number.

d. Case 4

On Case 4, the 8x8 block of size 360x360 pixels was used. The density was kept to be constant at 10080 fibers by changing the fibers amount both at higher and lower density blocks as shown in Fig. 62. Again initially (Figure 62a), the higher density blocks can be perceived as the flocs inside water flow that undergo the dynamic equilibrium process, while lower density blocks is water void with no fiber. Slowly, the ratio between the lower and higher density block was increased from 0 to 1. As the ratio of density increases (Figs. 62b-d), the process can be imagined as fibers moves from higher density blocks to lower density blocks as described in Fig. 58. The process finally stops when all the fibers have equally dispersed through lower and higher density blocks (Fig. 62e).

The results in Fig. 63 show that as the ratio is increased, the texture number is also increased. At lower ratio, the increase of lower density blocks apparently has higher effect to texture number than the decrease of the higher density blocks. No initial fiber existing inside lower density blocks also contributes much less dispersion. The less

effect of higher density blocks was because that at the higher fiber density, the fibers overlapped each other more and caused the rate of change of grayscale variation became less as explained in Case 1 discussion. The effect of dispersion rate from both lower and higher density block became approximately equals when they reached the ratio of 0.4, as shown in Fig. 63 as the slope become less steeper.

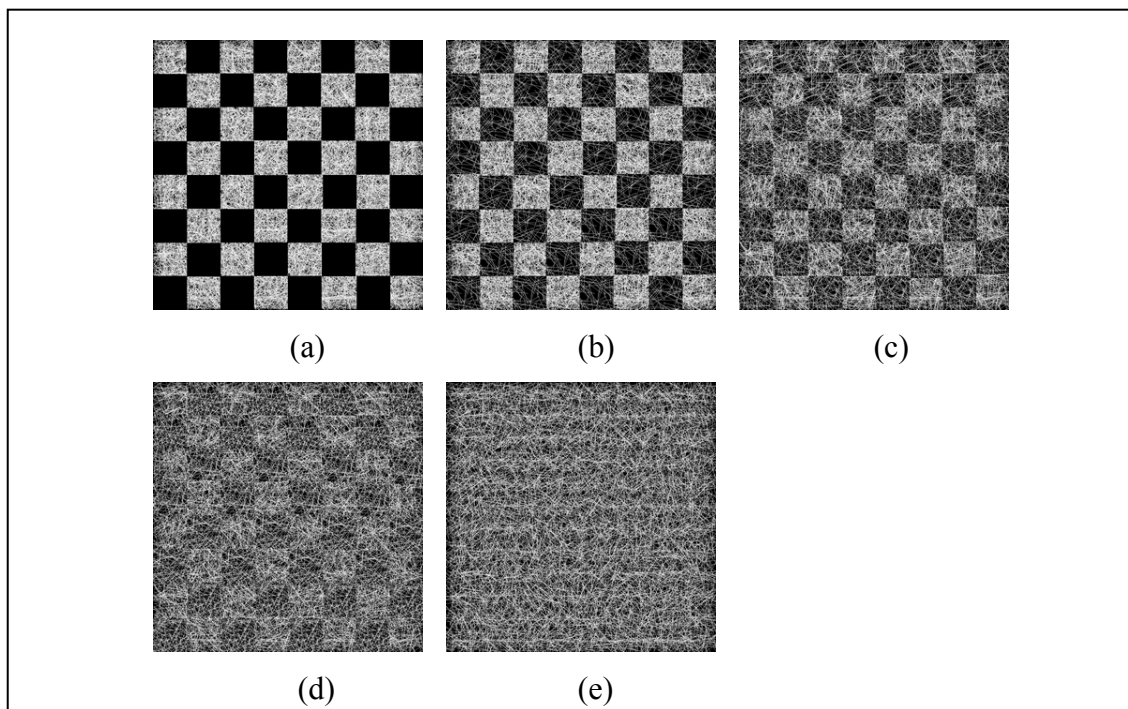


Fig. 62. Sample images used in case 4 with varied ratio between lower and higher density blocks. (a)0:10080; (b) 1440:8640; (c)2880:7200; (d)4320:5760 and (e) 5040:5040 fibers

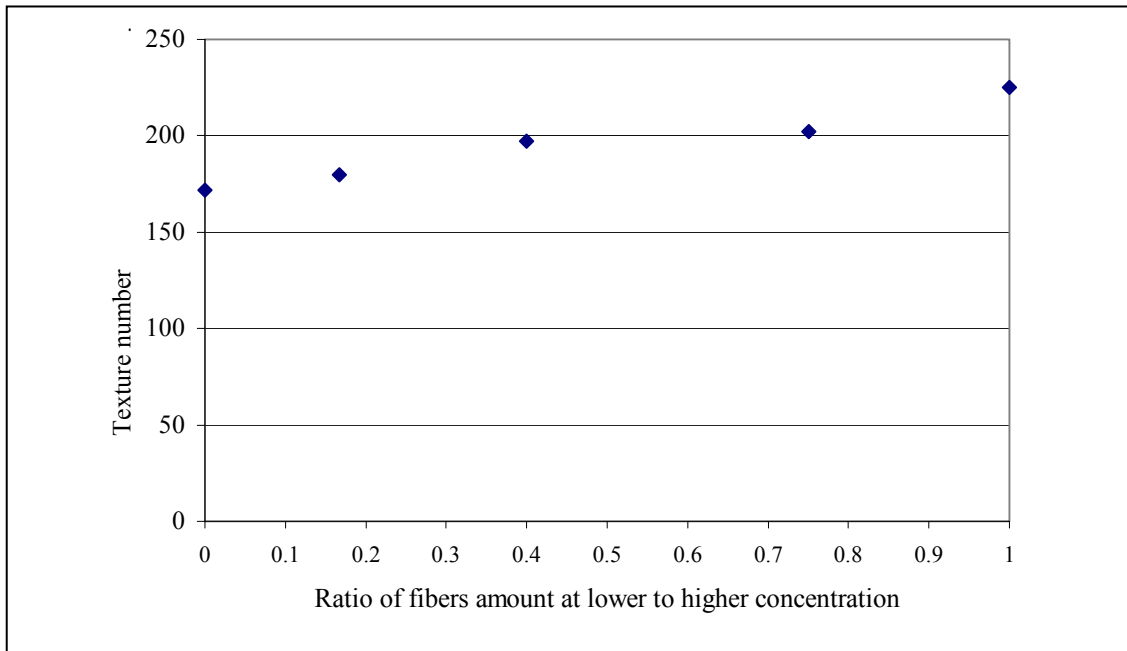


Fig. 63. Texture number variation as function of the ratio of fiber densities of lower to higher blocks.

5.5. Summary

The use of the computer-synthesized image is effective to simulate situations and conditions that is almost difficult to achieve experimentally. In this study, fiber aggregation location and density can be chosen. The location of concentrated fibers can be perceived as flocs in real fiber dispersion experiments. The results show that computer-synthesized image analysis was very helpful to understand and analyze not only the fiber dispersion level but also some other theories in pulp and paper research, for instance, static and dynamic equilibrium concept of fiber flocs. This study has showed that the computer-synthesized image is capable to simulate the dispersion situations that are difficult to obtain during real experiment.

CHAPTER VI

DRY PAPER EXPERIMENT

6.1. Introduction

During the papermaking process, the arrangement of fibers is critical inside the wet end stage (Fig. 10). After the wet end stage, the fibers position and orientation are almost unchanged until the final form of paper. The fibers arrangement at the final/dry form will then be expected to be about similar to the arrangement inside wet end. It is important, however, to understand that each type of paper will have different fiber arrangements and properties. These properties of paper depend on:

- type of pulp used,
- amount of bleaching,
- thickness of pulp mat created,
- pressure applied during paper manufacture,
- chemical additives,
- beating,
- coating.
- Additives include alum, starches, clays and sizing agents, all of which are intended to increase the density of the paper, and provide a good printing surface.

Other chemicals may be added to enhance the effectiveness of dyes.

The purpose of this study was to investigate the dispersion level of fibers inside these final/dry forms of papers. The study related the study conducted on Chapter V and the treatment during papermaking for each paper type

6.2. Physics behind paper translucency

Some properties of paper can be observed easily through the appearance of the paper. Although paper looks fairly opaque from the outside, it is transparent on the inside. Paper is made up of tiny, transparent cellulose fibers that have been matted together. Air lurks in-between the fibers. When light tries to go through the fibers, it refracts at every fiber-air interface, and cannot find a straight path to get through the

paper. Any additional substances or variation in concentration will make the appearance of paper will be different. It is important to remember that the gray scale variation appeared during the imaging processing can be used as a measure of weight variation too.

6.3 Description of paper samples

Five different paper samples have been obtained and analyzed: handmade paper, crepe paper, brownbag, regular printing paper, and gift wrap. In daily life, clearly, five paper samples taken are made for different purposes that the fiber types, size and shape are different from each other.

Handmade papers can be found in fine art stores. These papers are easily distinguished from the papers with their long acid- and lignin-free fibers and nubby textures. The fibers used are vary, but unlike fibers of regular paper, they are extremely tough, making it possible to produce a delicate-appearing sheet, which actually has a great deal of tensile strength [56].

Regular printing fibers vary significantly in quality, but generally contain significant proportions of bleached sulphite pulp and a rosin/starch size. High brightness is also a common factor. Highest quality bond papers may include components of cotton/linen stock and alpha pulp and a starch or rosin size.

Brown Bag papers made from unbleached kraft pulps because the first requirement is strength. This is achieved by using pulp with long, well formed fibers evenly laid and well-crossed [57]. These papers must flexible and have as little grain as possible (i.e. not tear across the grain more readily than with it),

Crepe papers are usually made of well-bleached sulphate or sulphite pulp with special treatment to enhance softness, absorbency and strength. Some forms are also have wet strength properties. These papers with high elasticity produced by creping. Crinkling of paper during drying to produce a soft, elastic sheet. Quality ranges from about 40% of stretch to double-sided crepe paper of about 140% of stretch [57].

Gift-wrap papers like brown bag paper are made from unbleached kraft pulps. However some chemical additives are added to improve the smoothness to the surface.

6.4 Experimental apparatus

Figure 64 describes the schematic of the apparatus. Fluorescence light was to provide the illumination to paper sample. The reflective surface was put around the paper sample to provide lighting uniformity. In this problem, a digital camera was used at shutter speed of 1/60 sec. and F-stop of 5.6. Surrounding area was also set to be dark to ensure uniform light of images. Unlike fiber-inside-water-flow study, no flash was employed. The images produced were set to have gray color mode. All images were then tested to determine their fiber dispersion level using texture procedure that introduced earlier in Chapter II.

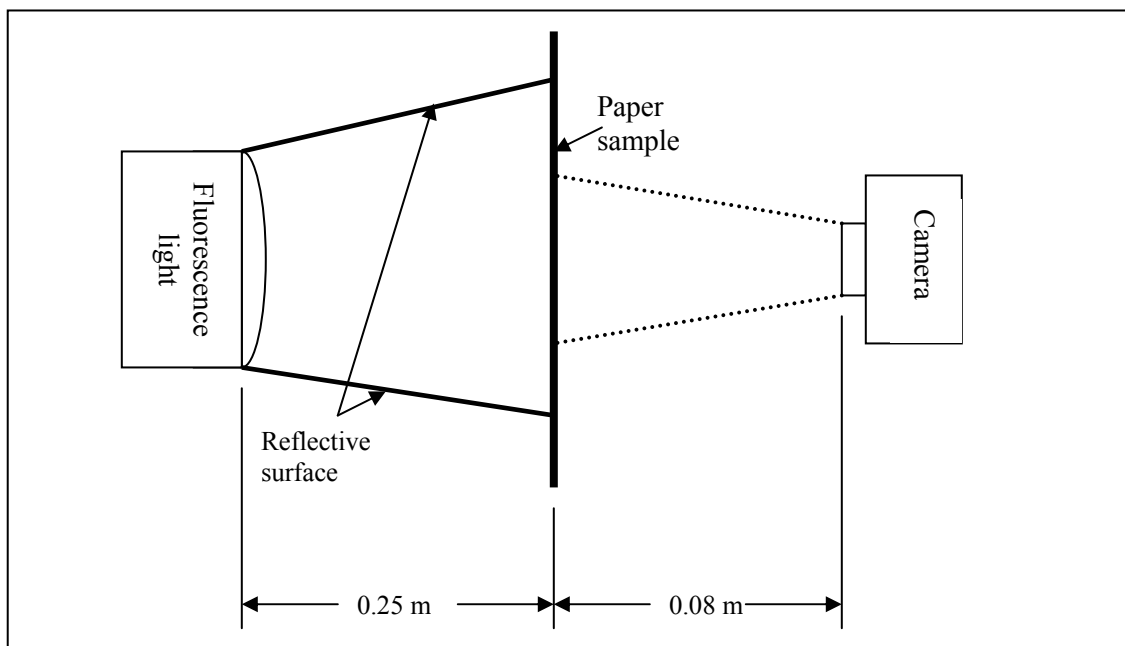


Fig. 64. Apparatus schematic of the dry paper analysis.

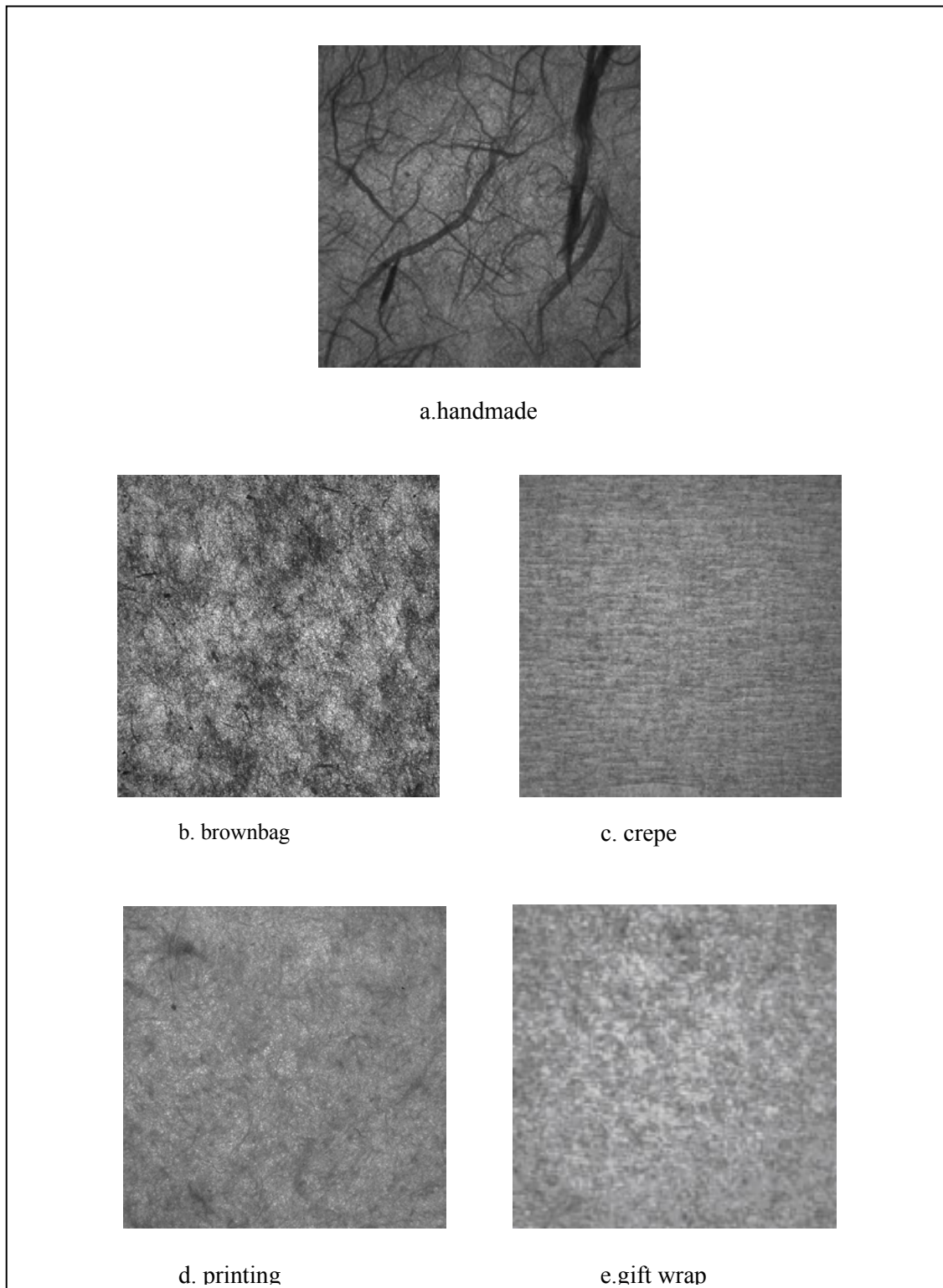


Fig. 65. Sample images of different dry papers.

6.5 Results and discussion

Figure 65 shows the sample image taken during the experiment. Table 11 shows the texture number as its procedure presented in Chapter II. Both Table 11 and Fig. 65 have already sorted results. The results show that handmade paper has the smallest dispersion while the gift-wrap paper has the highest dispersion. From the observation, the handmade has the most random fiber configuration and the most irregularity in fiber shape and size. All of these make the texture number become decreasing since those randomness and irregularity make the more pixel area in the image have similar gray value. This problem can be related to Case 3 problem from computer-synthesized image analysis (Chapter V), where the variation of the void area becomes important to determine the fiber dispersion. More void area due to the absence of fiber tends to decrease the fiber dispersion. Handmade paper definitely is not manufactured by standard paper machine. Since the handmade paper was made mainly as a learning tool to understand the fundamental of papermaking, there is no need to obtain paper with high fiber dispersion. Irregularity in size and shape of fibers becomes unimportant for this type of paper. Unfortunately the exact making process of this particular handmade paper is unknown.

On the brown bag paper, some irregular black notches are spotted and might contribute to smaller texture value. In this type of paper, the irregularity of fiber distribution probably will be tolerable. The use of Kraft pulp indicates the main purpose of this paper is to have good strength to withstand certain amount of forces. Appearance and surface roughness become a secondary factor in producing this type of paper.

Crepe papers have more regular pattern due to the straight crinkling that allows the paper to stretch uniformly. This regular pattern also may be necessary to improve appearance since often crepe papers are used for home decoration purpose.

On the regular printing paper and giftwrap paper, they have about uniform gray value variation. Regular printing paper regular requires better uniformity in dispersion that leads to better surface smoothness and appearance. Ink is expected to behave similarly regardless its placement in paper. With no good fiber dispersion, the ink may

not mix with high degree of accuracy inside paper surface. Additional materials like cotton fibers can be added to improve the ink absorbance quality and paper appearance. However on gift-wrap paper, apparently more light is able to go through the paper, and color variation among pixel are more. These variations tend to make the gift wrap paper to have highest texture number. The gift-wrap paper needs a good appearance and at the same time it should have sufficient strength to withstand some forces. While brownbag and gift-wrap papers are made by kraft pulp, from visual observation, the gift-wrap fibers are shorter than the brownbag fibers. As discussed previously, shorter fibers will produce more uniform paper. Beyond the fiber physical properties, additional chemical substance may be added to improve not only the appearance but also the dispersion level of fibers.

Table 11. Dry paper types and their corresponding texture numbers.

Paper type	Texture number
Handmade-fine	160.11
Brownbag	160.44
Crepe	166.12
Regular printing	168.01
Giftwrap	171.25

6.6. Summary

The study revealed that different types of paper would have different fiber properties, configurations and distribution. Those factors affect the level of fiber dispersion in the final form of paper. Although the optical procedure was not capable to zoom the fibers in such detail, the gray intensity variation on each sample was easily detected. The visual observation also used to detect some properties of fibers, such as length, diameter, and how they are concentrated. The texture method has successfully

detected the dispersion level of each sample. The purpose of the paper produced ultimately determined if a certain level of fiber dispersion is necessary. Depending on paper application, papermaker can adjust the dispersion level of paper, and at the same time emphasize the other commercial factors, such as appearance, strength, and ink absorption of paper

CHAPTER VII

CONCLUSIONS

The purpose of this dissertation was to investigate the use of texture analysis as a tool for micro fiber dispersion measurement. Micro fiber dispersion can be found in many applications such as in papermaking. The quality of final paper product depends heavily on the arrangement of fiber dispersion. The texture analysis used in current study was based on the theory built by Bhattacharyya and his colleagues [8-12]. They have shown that the method was successful to test the dispersion level of carbon black in carbon [11].

A critical review of fiber dispersion was carried out. Several different factors affecting to fiber dispersion and flocculation were discussed. These factors can be divided into two main factors: chemical and mechanical factors. The mechanical part involves the geometrical shape of the fibers while the chemical part involves the surface condition of the fibers. Many researchers have made various investigations to these factors. For some factors, such as aspect ratio and consistency, their result conclusions had good agreement among each other. However, how and at what degree of these factors affecting the fiber dispersion were relatively unknown. This disagreement between researchers also appeared as they brought variety of new methods and techniques to measure fiber dispersion level. It was found that lacks of physical mechanism and theory of fiber flocculation led to some unanswered questions. This critical review discussed also some of these unanswered questions: the concept on how fiber flocs are formed, the simulation of fiber formation, and the mathematical models.

Three problems related to micro fiber dispersion have been investigated. The first case was the experimental study on the fiber dispersion in turbulent flow inside an open water channel. Sets of synthetic fibers were put into water channel to simulate the process than can be found in papermaking. Using appropriate imaging process, the pictures were taken and digitally processed. The dispersion calculation by Bhattacharyya and his colleagues [8-12] was then employed to measure the dispersion level. The current research investigated the effect to fiber dispersion of three operating

parameters: fluid velocity, fiber consistency, and fiber aspect ratio. The results showed a satisfying result in identifying the level of dispersion using the method by Bhattacharyya and his colleagues [8-12]. In general, the current study found that the increase in fluid velocity, aspect ratio and consistency would decrease the fiber dispersion. The decrease in dispersion level or the increase in flocculation was mainly caused by the increase of the chance of collision and entanglement among fibers.

Investigation to aspect ratio and fluid consistency effect showed that the current study had good agreement with the literature. On fluid velocity factor, the current results agreed partially with conclusion shown by Hourani [33,34] but had disagreement with results shown by Jokinen and Ebeling [29] and Takeuchi et al. [31]. This disagreement can be caused by various factors notably the size and shape of water channel. Fiber properties may also contribute to the difference. Hourani furthermore explained the discrepancy of results by stating that the velocity effect may be more complex due to different mechanisms. Vortices generated within fibers may favor flocculation while shear force, contrarily may break flocs. He suggested that these two mechanisms are dependent on consistency and fiber properties [33, 34].

Two-factorial design was used to determine the critical parameters in fiber dispersion. Using two-factorial experimental design concept, the main and interaction effects of these parameters were then evaluated. Two-factorial design also minimized the number of data taken and the time consumed to process them. The analysis using crowding factor concept introduced by Kerekes and Schell [24] and two-factorial design analysis yielded that aspect ratio had the largest contribution compared to the other two parameters. Two-factorial design analysis also indicated that the main effect of individual factors had significant effect to fiber dispersion level. The interactive effect also had significant effect but not as large as the main effect of individual factors.

The current research also investigated the effect of Reynolds number to fiber dispersion using water channel experimental results. The current results showed that the Reynolds number had minimal effect to fiber dispersion. The results also showed that use of Reynolds number could be expanded to investigate not only the effect of the fluid velocity but also the effect of consistency to fluid viscosity, and the effect of water

channel shape and size to fiber dispersion and flocculation. Non-Newtonian fluid behavior of solution influenced heavily to the Reynolds number calculation by taking the effect of solution consistency to fluid viscosity into account. The current study found that fluid velocity and fiber aspect ratio effects to the fluid viscosity were small and negligible. The study also found that in order to achieve more reliable value of fluid viscosity, it became a necessity to assume the fluid velocity profile more accurately. Better approximation of velocity profile would lead to better approximation of shear rate, viscosity, and finally, Reynolds number. The current velocity profile was used due to its simplicity and was believed to be adequate to represent the actual velocity profile. The actual fluid velocity profile was difficult to achieve due to the presence of turbulence and fibers inside flow. The minimal effect of Reynolds number indicates that Reynolds number effect as a combined factor can have a more complicated effect than when it is broken down into individual factors.

While crowding factor and Reynolds number are two dimensionless numbers that are very useful to describe the physics of fiber dispersion, they cannot be used as an effective tool to indicate the degree of flocculation of each factor. The current study showed that two different experimental parameters could have a one crowding factor value, but with significant dispersion level difference in their results. Reynolds number, on the other hand, had minimal effect due to contradiction of effects of some results found during the study.

To accommodate the degree of effect of each factor to fiber dispersion level properly, a dimensionless variable was proposed. This dimensionless variable consists not only of the three main factors studied, but also of the other supporting parameters such as fluid viscosity and channel size and shape. In the dimensionless number of $[(L/D)^6(C)^4(N_{Re})]$, clearly the aspect ratio has the most dominant role, followed by fluid consistency, while fluid velocity has the lowest effect due to the conflicting results achieved by the current study. Attempts to apply this dimensionless number to other previous researches were made. Unfortunately, proper comparison cannot be made because their results did not provide enough information on their experimental

parameters, such as relation between consistency and viscosity of fiber solution, and the shear rate used or assumed.

The second case was the analysis to computer-synthesized images consisting of different arrangements of fibers. These images represented the idealized situations that are almost impossible to achieve during the experiments. Four sub-cases have been picked based on the fiber-concentrated location and fiber consistency. However, the location and orientation of a single fiber in the image were set to be random. These arrangements allowed building models that could predict the dispersion level on the real experimental data. The first two sub-cases had varying fiber consistency while the other two had constant fiber concentration. It was found that both fiber-concentrated location and fiber consistency play important factor to determine the dispersion level.

The third case investigated the fiber distribution inside the dry paper. Different sets of papers had been evaluated to see the dispersion level of each type of paper. The results were then compared with the conclusions found in study of fiber-in-water channel and computer-synthesized image dispersion. The results show that the size, shape, and distribution of fibers play an important role in determining the fiber dispersion. The purposes and application of each paper type also play important role to determine if a certain level of dispersion is needed.

While the three cases indicate that the texture analysis can be used to investigate the fiber dispersion, the texture analysis used here is not a perfect method that might not suitable to other application of dispersion. The human vision will be and always be essential to determine if the texture analysis is applicable to any other problem. The study of fiber dispersion itself is a wide-open topic. Many unanswered question are still need to be solved. The use of digital image processing will increase due to fact that it is cheap, reliable, and effective to solve many problems in fluid mechanics. The advance of computer definitely helps the popularity of the technique.

REFERENCES

1. GONZALEZ, R.C. and WINTZ, P., "Digital Image Processing", Addison-Wesley, Reading, Massachusetts (1987).
2. JAHNE, B., Practical Handbook on Image Processing for Scientific Applications, CRC Press, Boca Raton, Florida (1997).
3. GANESAN, L. and BHATTACHARYYA, P., "A Statistical Design of Experiments Approach for Texture Description", *Pattern Recognition* 28 (1):99-105 (1995).
4. TOMITA, F. and TSUJI, S., "Computer Analysis of Visual Textures", Kluwer Academic, Norwell, Massachusetts (1990).
5. HARALICK, R.M., "A Statistical and Structural Approaches to Texture", *Proc. IEEE* 67(5):786-804 (1979).
6. HARALICK, R.M., SHANMUGAM, K., AND DINSTEIN, I, "On Some Quickly Computable Features for Texture", *IEEE Trans. on Systems, Man and Cybernetics*, SMC3:610-621 (1973).
7. BRODATZ, P. "Textures: A Photographic Album for Artists and Designers", Dover Publications, New York (1968).
8. BHATTACHARYYA, P. and GANESAN, L., "A Orthogonal Polynomials Based Framework for Edge Detection in 2-D Monochrome Images", *Pattern Recognition Lett.* 18:319-333 (1997).
9. GANESAN, L. and BHATTACHARYYA, P., "Edge Detection in Untextured and Textured Images—A Common Computational Framework", *IEEE Trans. Systems, Man and Cybernetics- Part B: Cybernetics*, 27(5):823-834 (1997).
10. GANESAN, L. and BHATTACHARYYA, P., "A New Statistical Approach for Micro Texture Description", *Pattern Recognition Lett.* 16(5):471-478 (1995).
11. GANESAN, L. and BHATTACHARYYA, P., Quantitative Measurement of Dispersion of Carbon Black in Rubber by an Image Processing Technique", *J. Appl. Polymer Sci.*, Vol 56, 17-39 (1995).

12. GANESAN, L., BHATTACHARYYA, P., and BHOWMICK, A.K., "Quantitative Analysis of Domain Size of Polymer Blend by an Image Processing Technique", *Polymer Networks Blends*, 5(3):151-158 (1995).
13. GANESAN, L., BHATTACHARYYA, P., and BHOWMICK, A.K., "Quantitative Fractography of Rubber by an Image Processing Technique", *J. Rubber Chem. Tech. A.C.S.* 68(1):1-14 (1995).
14. SZEGO, G., "American Mathematical Society Colloquium Publications: Orthogonal Polynomials", American Mathematical Soc., Providence, Rhode Island (1939).
15. BISHOP, D.J. and NAIR, U.S., "A Note on Certain Methods of Testing for the Homogeneity of a Set of Estimated Variances", *Supp. to J. of Royal Statistical Soc.* 6:89-99 (1939).
16. FISHER, R.A. and YATES, F., "Statistical Tables for Biological, Agricultural and Medical Research", Oliver and Boyd, London (1947).
17. Hunter, D. "Papermaking: The History and Technique of an Ancient Craft", AA Knopf, New York (1947).
18. MASON, S.G., "Some Factors Involved in the Flocculation of Pulp Suspensions", *Pulp Paper Mag. Can.* 51(5):94-98 (1950).
19. ROBERTSON, A.A. and MASON, S.G., "Flocculation in Flowing Pulp Suspensions", *Pulp Paper Mag. Can.* 55(3):263-269 (1954).
20. HUBLEY, C.E., ROBERTSON, A.A. and MASON, G., "Flocculation in Suspensions of Large Particle", *Canadian Journal of Research.* 28 Sect. B:770-787 (1950).
21. KEREKES, R.J., "Perspectives on Fibre Flocculation in Papermaking", Int'l Paper Physics Conf, Lake Ontario, Canada (Sept. 11-14, 1995).
22. KEREKES, R.J., SOSZYNSKI, R.M. and TAM DOO, P.A., "The Flocculation of Pulp Fibres", *Fund. Res. Symp.*, Oxford, UK 1:265-310 (1985).
23. KEREKES, R.J. and SCHELL, C.J., "Characterization of Fibre Flocculation Regimes by a Crowding Factor", *J. Pulp and Paper Sci.* 18(1):J32-J38 (1992).
24. KEREKES, R.J. and SCHELL, C., "Effect of Fiber and Coarseness on Pulp Flocculation", *Tappi J.* 78(2):133-139 (1995).

25. BEGHELLO, L. and EKLUND, D., "Some Mechanisms That Govern Fiber Flocculation", *Nordic Pulp Paper Research J.* 12 (2):119-123 (1997).
26. BEGHELLO, L., "Some Factors That Influence Fiber Flocculation", *Nordic Pulp Paper Research J.* 13 (4):274-279 (1998).
27. BEGHELLO, L. and EKLUND, D., "Influence of the Crowding Factor and the Chemical Environment of Floc Size", *J. Pulp and Paper Sci.* 25(7):246-250 (1999).
28. BEGHELLO, L. TOIVAKKA, M., EKLUND, D. and LINDSTROM, T., "A Device for Measuring Fiber Floc Sizes in Highly Turbulent Fiber Suspension", *Nordic Pulp Paper Research J.* 11(4):249-253 (1996).
29. JOKINEN, O. and EBELING, K., "Flocculation Tendency of Papermaking Fibres", *Paperi ja Puu.* 67(5):317-325 (1985).
30. TICHY, J. and KARNIS, A., "Flocculation and Retention of Fibres and Filler Particles in Flowing Pulp Suspensions", *CPPA Transactions of the Tech. Sect.* 4 (1):19-25 (1978).
31. TAKEUCHI, N., SENDA, S., NAMBA, K. and KUWAHARA, G., "Formation and Destruction of Fibre Flocs in a Flowing Pulp Suspension", 2nd Pacific Meeting of ESPRA. Rotorua, New Zealand. (1981).
32. DOTSON, C.T.J., "Fiber Crowding, Fiber Contacts and Fiber Flocculation", *Tappi J.* 79 (9):542-545 (1996).
33. HOURANI, M.J., "Fiber Flocculation in Pulp Suspensions Flow: Part 1: Theoretical Model", *Tappi J.* 71(5):115-118 (1988).
34. HOURANI, M.J., "Fiber Flocculation in Pulp Suspensions Flow: Part 2: Experimental Study", *Tappi J.* 71(6):186-189 (1988).
35. ZHAO, R.H. and KEREKES, R.J., "The Effect Suspending Liquid Viscosity of Fiber Flocculation", *Tappi J.* 76(2):183-188 (1993).
36. KEREKES, R.J. and SCHELL, C.J., "Pulp Flocculation in Decaying Turbulence: A Literature Review", *J. Pulp and Paper Sci.* 9(3):TR86-91 (1983).
37. ERSPAMER, A., "The Flocculation and Dispersion of Papermaking Fibers", Proc. Ann. Meeting of Tappi, New York 23(1):132-138 (Feb 19-22, 1940).

38. JAGANNADH, S.V.S., JORDAN, H. and BRODKEY, R.S., Formation and Characterization of Paper Pulp Floccs. *Chemical Eng. Science*, 46(12):87-100 (1991).
39. STRAZDINS, E. "Factor Affecting the Electrokinetic Properties of Cellulose Fibers", *Tappi J.* 55(12):1691- 1695 (1972).
40. WASSER, R.B., "Formation Aids for Paper: An Evaluation of Chemical Additives for Dispersing Long-Fibered Pulps", *Tappi J.* 61(11):115-118 (1978).
41. LINDSTROM, T., "Chemical Factor Affecting the Behaviour of Fibres during Papermaking", *Nordic Pulp Paper Research J.* 7(4):342-351 (1992).
42. SOSZYNSKI, R.M. and KEREEKES, R.J., "Elastic Interlocking of Nylon Fibres Suspended in a Liquid: Part I", *Nordic Pulp Paper Research J.* 3(4):172-179 (1988).
43. SOSZYNSKI, R.M. and KEREEKES, R.J., "Elastic Interlocking of Nylon Fibres Suspended in a Liquid: Part II", *Nordic Pulp Paper Research J.* 3 (4):189-184 (1988).
44. WOOLLWAGE, J.C., "The Flocculation of Papermaking Fibers", *Paper Trade J.* 12(108):41-48 (1939).
45. DUFFY, G.G. and NORMAN, B.G., "Fibre Flocculation in Conical Contractions Simulating the Papermachine Flowbox Slice", Proc. Of the Int'l Symp. On Papermachine Headboxes, Montreal:43-53 (June 3-5, 1979).
46. HOURANI, M.J., "A Molecular Thermodynamic Model for Surfactant Aggregate Formation", Ph.D. dissertation, Univ. of Florida, 1984.
47. OLSON, J.A. and KEREEKES R.J., "The Motion of Fibres in Turbulent Flow", *J. Fluid Mechanics* 37(7):47-64 (1998).
48. JACQUELIN, G., "Consolidation of the Paper Web", Transactions of the 3rd fundamental research symposium, Bolam F. (ed.)Cambridge, England (1965) T.S.B.P. & B.M.A., London:299-235 (1966).
49. RAMIN, R.F., LOEWEN, S.R. and DODSON, C.T.J., "Estimation Inter-floc Forces", *Appita J.* 47(5):391-396 (1994).

50. PRESS, W.H., FLANNERY, B.P., TEUKOLSKY, S. and VETTERLING, W.T., “Numerical Recipes: The Art of Scientific Computing”, Cambridge University Press, Cambridge (1989).
51. NORMAN, B.G. and WAHREN, D., “A Comprehensive Method for the Description of Mass Distribution in Sheets and Flocculation and Turbulence in Suspensions”, *Svensk Papperstidn.*, 75 (20):807-814, (1972).
52. EATON, J.K. and FESSLER, J.R., “Preferential Concentration of Particles by Turbulence”, *Int. J. Multiphase Flow* 20: 169-209 Suppl. S (1994).
53. FOX, R.W. and MCDONALD, A.T., “Introduction to Fluid Mechanics”, John Wiley and Sons, New York (1992).
54. WHITE, F.M., “Fluid Mechanics”, McGraw-Hill, New York (1986).
55. HAYS, W.L., Statistics (3rd ed.), CBS College Publishing, New York (1981).
56. “Timber characteristics - Products and Processes”, Online(http://www.insights.co.nz/products_processes_ppr.asp) (Accessed January 1, 2003).
57. “Papers By Catherine – your source for fine handmade and decorative paper”, Online (<http://www.papersbycatherine.com/paperworldjournal4.shtml>) (Accessed January 1, 2003).

APPENDIX A: NAIR'S TEST

Let $v_{a1}, v_{a2}, \dots, v_{ak}$ be the set of variances with $\Omega_1, \Omega_2, \dots, \Omega_k$ degree of freedom, respectively.

The average variances:

$$v_{av} = \frac{1}{\Omega} \sum_{i=1}^k v_{ai} \Omega_i$$

where Ω is the total degree of freedom given as $\Omega = \sum_{i=1}^k \Omega_i$

The criterion for computing the divergence among variances is

$$D = \Omega \ln v_{av} - \sum_{i=1}^k \Omega_i \ln v_{ai}$$

Compare the D with Nair's table as sample table presented below.

Confidence level/ DOF	2	3	4	5
5%	5.1	7.7	10.0	12.0
1%	8.3	11.5	14.0	16.5

If value of D falls below the tabulated value, variances were said to have homogenous variances (convergence), otherwise, they were divergence.

APPENDIX B: F-RATIO TEST TABLE

DOF/Confidence level	5%	10%	20%	25%
2	18.51	8.53	3.56	0.667
3	10.13	5.54	2.68	2.02
4	7.71	4.54	2.35	1.8

APPENDIX C: COMPUTER CODE

```

clear
%usdreamgirls
%hcautographs-com
% creator: j hendrarsakti
% based on Bhattacharyya
% Last update: 09/28/2001

clear
%READING THE IMAGE
tic
%imshow M:\RESEARCH2002\kertas\12x12\001\2160_2block_720x720.tif;
%K=getimage; % GET THE MATRIX INTENSITY
K=imread('M:\RESEARCH2002\microfiber\harvard\harvard\001A\001A-1.tif');
%I = [98 101 101 104 104 99;102 107 105 109 103;100 106
105 105 102;104 108 107 108 104;102 106 106 106
101]

I=double(K)/1; % CONVERTING INTO 0-1 IF WE STAY WITH 256 THEN
I=K
%I=[.3 .2 .41 .42;.3 .3 .21 .12;.3 .62 .5 .23;.3 .52 .5 .5]
pixel=length(I(1:end,1)); % WIDTH OF IMAGE
pixel2=length(I(1,1:end)); % Length of image
flimit=.15 % FOR THE F-RATIO TEST LIMIT OF CONFIDENCE LEVEL

%DEFINING THE MATRIX

for row=2:(pixel-1),
    if mod(row,150)==0
        row
    end
    %prinum(row,pixel)=0
    for col=2:(pixel2-1),
        %col=9

%f=[220,12,150;10,202,120;50,130,132]
f=[I(row-1,col-1) I(row-1,col) I(row-1,col+1);I(row,col-1) I(row,col)
I(row,col+1);I(row+1,col) I(row+1,col) I(row+1,col+1)];
m=[1 -1 1;1 0 -2;1 1 1] ;

% DEFINING THE TEXTURE MATRIX

%CHECKING THE TEXTURE
=====

%NAIRS TEST
%FOR THIS TEST, WE WILL ASSUME THAT THE NUMBER OF SAMPLE IS 512X512=
AROUND 100,000
%ASSUME DOF=5 FOR EACH VARIANCE (see p 477), 40 comes from 5x8
%m=[1,-1,1;1,0,-2;1,-2,1];
b=inv(m)*f*inv(transpose(m));

```

```

s=inv(transpose(m)*m);

mfm=transpose(m)*f*m;
mfm_sq=mfm.^2;

b2=s*mfm*s;

z_sqr0=s*mfm_sq*s;
z=z_sqr0;

z_sqr1=inv(m).^2*f.^2*inv(transpose(m)).^2;

%%%%%%%%%%%%%%%%%%%%%%%%%%%%%%%%%%%%%%%%%%%%%%%%%%%%%%%%%%%%%%%%%%%%%%%%
%%%%%%%%%%%%%%%%%%%%%%%%%%%%%%%%%%%%%%%%%%%%%%%%%%%%%%%%%%%%%%%%%%%%%%%%
dof=1;

% TO MAKE COMPUTATION FASTER ++ PROCESS 19 ++ ADDED ON MARCH 20, 2002

if z(1,1)==0;z(1,1)=0.00000001;end
if z(1,2)==0;z(1,2)=0.00000001;end
if z(1,3)==0;z(1,3)=0.00000001;end
if z(2,1)==0;z(2,1)=0.00000001;end
if z(2,2)==0;z(2,2)=0.00000001;end
if z(2,3)==0;z(2,3)=0.00000001;end
if z(3,1)==0;z(3,1)=0.00000001;end
if z(3,2)==0;z(3,2)=0.00000001;end
if z(3,3)==0;z(3,3)=0.00000001;end

% END OF PROCESS 19

%TEST OF MAIN EFFECT
main_effect=[z(1,2) z(1,3) z(2,1) z(3,1)];
n=length(main_effect);
chi=n*dof;

dof=1;

%TEST OF MAIN EFFECT
%TEST OF MAIN EFFECT
%TEST OF MAIN EFFECT
%TEST OF MAIN EFFECT
%TEST OF MAIN EFFECT

main_effect=[z(1,2) z(1,3) z(2,1) z(3,1)];
n=length(main_effect);
chi=n*dof;

```

```

%with
var=4=====
=====

totalvar_main=(dof*z(1,2)+dof*z(1,3)+dof*z(2,1)+dof*z(3,1))/(n-
0)*dof);
subtotal_main=(n-0)*dof*log(totalvar_main);
temp_main=dof*log(z(1,2))+dof*log(z(1,3))+dof*log(z(2,1))+dof*log(z(3,1
));
H_main=subtotal_main-temp_main;

if H_main>=25.0 % TRY WITH var=3
    totalvar_main=(dof*z(1,2)+dof*z(1,3)+dof*z(2,1)+dof*z(3,1)-
dof*max(main_effect))/(n-1)*dof);
    subtotal_main=(n-1)*dof*log(totalvar_main);

temp_main=dof*log(z(1,2))+dof*log(z(1,3))+dof*log(z(2,1))+dof*log(z(3,1
))-dof*log(max(main_effect));
    H_main=subtotal_main-temp_main;

    if H_main>=2.0 ;
        totalvar_main=(dof*z(1,2)+dof*z(1,3)+dof*z(2,1)+dof*z(3,1)-
dof*min(main_effect))/(n-1)*dof);
        subtotal_main=(n-1)*dof*log(totalvar_main);

        temp_main=dof*log(z(1,2))+dof*log(z(1,3))+dof*log(z(2,1))+dof*log(z(
3,1))-dof*log(min(main_effect));
        H_main=subtotal_main-temp_main ;

        if H_main>=2.0 %TRY WITH var=2
            totalvar_main=(dof*z(1,2)+dof*z(1,3)+dof*z(2,1)+dof*z(3,1)-
max(main_effect)-min(main_effect))/(n-2)*dof);
            subtotal_main=(n-2)*dof*log(totalvar_main);

            temp_main=dof*log(z(1,2))+dof*log(z(1,3))+dof*log(z(2,1))+dof*log(z(
3,1))-dof*log(max(main_effect))-dof*log(min(main_effect));
            H_main=subtotal_main-temp_main;
            if H_main>=2.0;
                prnum(row,col)=0;
            else
                msv=(z(1,2)+z(1,3)+z(2,1)+z(3,1)-max(main_effect)-
min(main_effect))/(n-2);
                le=2;
            end
        else
            msv=(z(1,2)+z(1,3)+z(2,1)+z(3,1)-min(main_effect))/(n-1);
            le=3;
        end
    else
        msv=(z(1,2)+z(1,3)+z(2,1)+z(3,1)-max(main_effect))/(n-1);
        le=3;
    end
else
msv=(z(1,2)+z(1,3)+z(2,1)+z(3,1))/(n);

```

```

le=n ;
end

%END OF TEST OF MAIN EFFECT
%END OF TEST OF MAIN EFFECT
%END OF TEST OF MAIN EFFECT
%END OF TEST OF MAIN EFFECT
%END OF TEST OF MAIN EFFECT

%TEST OF INTER EFFECT
%TEST OF INTER EFFECT
%TEST OF INTER EFFECT
%TEST OF INTER EFFECT
%TEST OF INTER EFFECT

inter_effect=sort([z(2,2) z(2,3) z(3,2) z(3,3)]);
%inter_effect=sort([1 1 1 30]);
ie=inter_effect;
n=length(main_effect);
chi=n*dof;

%with
var=4=====
=====

totalvar_main=(dof*ie(1,1)+dof*ie(1,2)+dof*ie(1,3)+dof*ie(1,4))/((n-0)*dof);
subtotal_main=(n-0)*dof*log(totalvar_main);
temp_main=dof*log(ie(1,1))+dof*log(ie(1,2))+dof*log(ie(1,3))+dof*log(ie(1,4));
H_inter=subtotal_main-temp_main;

if H_inter<0.50 % TRY WITH var=3;
totalvar_main=(dof*ie(1,1)+dof*ie(1,3)+dof*ie(1,4))/((n-1)*dof);
subtotal_main=(n-1)*dof*log(totalvar_main);
temp_main=dof*log(ie(1,1))+dof*log(ie(1,3))+dof*log(ie(1,4));
H_inter=subtotal_main-temp_main;

if H_inter<0.5
totalvar_main=(dof*ie(1,1)+dof*ie(1,2)+dof*ie(1,4))/((n-1)*dof);
subtotal_main=(n-1)*dof*log(totalvar_main);
temp_main=dof*log(ie(1,1))+dof*log(ie(1,2))+dof*log(ie(1,4));
H_inter=subtotal_main-temp_main ;

if H_inter<0.5 %TRY WITH var=2
totalvar_main=(dof*ie(1,1)+dof*ie(1,4))/((n-2)*dof);
subtotal_main=(n-2)*dof*log(totalvar_main);
temp_main=dof*log(ie(1,1))+dof*log(ie(1,4));
H_inter=subtotal_main-temp_main;
if H_inter<0.5;
pronom(row,col)=0;
else

```

```

        msvi=(ie(1,1)+ie(1,4))/(n-2);
        le=2;
    end
else
    msvi=(ie(1,2)+ie(1,1)+ie(1,4))/(n-1);
    le=3;
end
else
    msvi=(ie(1,1)+ie(1,3)+ie(1,4))/(n-1);
    le=3;
end
else
msvi=(z(2,2)+z(2,3)+z(3,2)+z(3,3))/(n);
le=n ;
end

%END OF TEST OF INTER EFFECT
%END OF TEST OF INTER EFFECT
%END OF TEST OF INTER EFFECT
%END OF TEST OF INTER EFFECT
%END OF TEST OF INTER EFFECT

% CALCULATING THE MSV VALUE BASED ON MAIN
z;
msv;
le;
if msv==0 ;
    msv=0.00000000000001;
end
for i=1:3;
for j=1:3;
    if (z(i,j)/msv)>=flimit;    % CHECKING THE F-RATIO
        prounumber(i,j)=1;
    else
        prounumber(i,j)=0;
    end
end
end
row;
col;
prounumber;

prounum(row,col)=prounumber(1,2)*(2^0)+prounumber(1,3)*(2^1)+prounumber(2,1)
)*(2^2)+prounumber(2,2)*(2^3)+prounumber(2,3)*(2^4)+prounumber(3,1)*(2^5)+
prounumber(3,2)*(2^6)+prounumber(3,3)*(2^7) ;

end    %for row=2:pixel
end    %for col=2:pixel

for row=59:(pixel-3),

```

```

for col=3:(pixel2-3),
    if I(row,col)==255
        if I(row,col+1)==255
            if I(row+1,col)==22
                if (row+1,col+1)==255
                    pronom(row-1,col-1)=0;
                    pronom(row-1,col)=0;
                    pronom(row-1,col+1)=0;
                    pronom(row-1,col+2)=0;
                    pronom(row,col-1)=0;
                    pronom(row,col)=0;
                    pronom(row,col+1)=0;
                    pronom(row,col+2)=0;
                    pronom(row+1,col-1)=0;
                    pronom(row+1,col)=0;
                    pronom(row+1,col+1)=0;
                    pronom(row+1,col+2)=0;
                    pronom(row+2,col)=0;
                    pronom(row+2,col+1)=0;
                    pronom(row+2,col-1)=0;
                    pronom(row+2,col+2)=0;
                end
            end
        end
    end
end
end
end
end

pronom(pixel,pixel2)=255

% TO PRODUCE HISTOGRAM
ns=hist(pronom,256); % TO PRODUCE A MATRIX NS WITH 256 DIVISION FOR
EACH COLUMN OF PRONOM

rows=length(ns(1:end,1)); % NUMBER OF ROWS IN NS
cols=length(ns(1,1:end)); % NUMBER OF COLS IN NS

totalsum1=zeros(256,1); % INITIAL 256x1 VECTOR MATRIX WITH 0 VALUE
for i=1:cols; % START SUM EACH COLUMN (WITH 256 DIVISION)
    totalsum1=ns(:,i)+totalsum1;
end
totalsum1; % DISTRIBUTION OF 0-255 POINT OF PRONOM
mss=[0:255] ; % PRODUCING A VECTOR MATRIX WITH
[0,1,2,...,255), USED TO PRODUCE GRAPH

figure
bar(mss,totalsum1)
saveas(gcf,'M:\RESEARCH2002\microfiber\harvard\harvard\001A\001A-
1.fig');

% CALCULATING THE MEAN

totalmeansum=0;

```

```

msstrans=transpose(mss);
for ik=1:rows;
    meansum=msstrans(ik)*totalsum1(ik);
    totalmeansum=totalmeansum+meansum ;
end
totalmeansum
fff=sum(pronum)

%SUBTRACT WITH 255 (DUMMY VARIABLE TO MAKE SURE IT RANGES FROM 0-255)

totalmeansum=totalmeansum-255
jenna=sum(fff)
chasey=sum(jenna)-255

%END

diary M:\RESEARCH2002\microfiber\harvard\harvard\001A\001A-1.m
means=totalmeansum/((row-1)*(col-1))      %row and col here is the last
number

% CALCULATING THE VARIANCE

totalvarsum=0;
for ik=2:rows;
    varsum=((msstrans(ik)-means)^2)*totalsum1(ik);
    totalvarsum=varsum+totalvarsum;
end

var=totalvarsum/((row-1)*(col-1))
toc
diary off

```

APPENDIX D: TWO-FACTORIAL DESIGN

Parameter	Low (-)	High (+)
Reynolds number (N_{Re})	15000	53000
Consistency (C)	0.1004 + 0.0125 %	0.4001 ± 0.0133 %
Aspect Ratio (L/D)	200.61 ± 2.35	400 ± 3.89

Calculation Matrix

Test		N_{Re}	C	L/D	N_{Re} & C	N_{Re} & L/D	L/D & C	N_{Re} C, & L/D	Ave
1	+1	-1	-1	-1	+1	+1	+1	-1	164.7
2	+1	+1	-1	-1	-1	-1	+1	+1	132.4
3	+1	-1	+1	-1	-1	+1	-1	+1	132.1
4	+1	+1	+1	-1	+1	-1	-1	-1	128.4
5	+1	-1	-1	+1	+1	-1	-1	+1	119.4
6	+1	+1	-1	+1	-1	+1	-1	-1	108.2
7	+1	-1	+1	+1	-1	-1	+1	-1	114.4
8	+1	+1	+1	+1	+1	+1	+1	+1	106.6

$$\text{Mean} = (164.7+132.4+132.1+128.4+119.4+108.2+114.4+106.6)/(8) = 125.76$$

$$\text{For } N_{Re}, E_1 = (-164.7+132.4-132.1+128.4-119.4+108.2-114.4+106.6)/4 = -13.8$$

$$\text{For } C, E_2 = (-164.7-132.4+132.1+128.4-119.4-108.2+114.4+106.6)/4 = 10.75$$

$$\text{For } L/D, E_3 = (-164.7-132.4-132.1-128.4+119.4+108.2+114.4+106.6)/4 = 27.30$$

$$\text{For } N_{Re} \& C, E_{12} = (164.7-132.4-132.1+128.4+119.4-108.2-114.4+106.6)/4 = 7.95$$

$$\text{For } N_{Re} \& L/d, E_{13} = (164.7-132.4+132.1-128.4-119.4+108.2-114.4+106.6)/4 = 4.30$$

$$\text{For } C \& L/d, E_{23} = (164.7+132.4-132.1-128.4-119.4-108.2+114.4+106.6)/4 = 7.55$$

$$\text{For } N_{Re}, C, \& L/D,$$

$$E_{123} = (-164.7+132.4+132.1-128.4+119.4-108.2-114.4+106.6)/4 = 6.35$$

APPENDIX E: EXPERIMENTAL PARAMETERS AND CONDITION OF PREVIOUS STUDIES

TABLE E1. Experimental parameters and condition of various researchers

Investigator	Fiber Type (density)	Length (mm)	Diameter (μm)	Aspect ratio	Fluid velocity (m/s)	Channel cross sectional	Channel type	Consistency (%)
Beghello et al.[3.8-3.12]	Fir softwood (unknown)	0.4-2.64	25	25-100	1-10	150x10 mm	closed	0.3-0.9
Kerekes et al.[3.7,3.8]	NYLON, fir, cedar(unknown)	3, 2.69, 2.47 mm	46, 40, 35	65, 67.3, 70.6	1.3	243x457x 23 mm	closed	0.3
Takeuchi et al.[3.15]	softwood and hardwood(unknown)	unknown	unknown	unknown	0.83 – 20.16	circular (d=25 mm),and	Closed	0.7 for hardwood d 0.14-
Jokinen & Ebeling {3.13}	pine kraft and birch kraft(unknown)	pine=2.33, 1.3 mm	unknown	unknown	.15,0.3 and 0.6 m/s	d=8 mm	closed	0.5
Hourani [3.18]	softwood and hardwood(unknown)	softwood=4mm, hardwood=1	unknown	unknown	1.5-15 m/s	d= 7.62 cm	closed	0.2

APPENDIX F: FLUID DENSITY CALCULATION

Density of mixture (ρ_{mix}):

$$\begin{aligned}\rho_{\text{mix}} &= \frac{m_{\text{mix}}}{V_{\text{mix}}} \\ \rho_{\text{mix}} &= \frac{m_w + m_f}{V_w + V_f} \\ \rho_{\text{mix}} &= \frac{m_w + m_f}{m_w/\rho_w + m_f/\rho_f}\end{aligned}\tag{F.1}$$

Consistency (C):

$$\begin{aligned}C &= \frac{m_f}{m_f + m_w} \\ m_w &= \left(\frac{1-C}{C}\right)m_f\end{aligned}\tag{F.2}$$

Substitute (F.2) into (F.1):

$$\rho_{\text{mix}} = \frac{\left(\frac{1-C}{C}\right)m_f + m_f}{\frac{\left(\frac{1-C}{C}\right)m_f}{\rho_w} + \frac{m_f}{\rho_f}}$$

Simplify,

$$\rho_{\text{mix}} = \frac{\rho_w \rho_f}{\rho_f(1-C) + \rho_w C}$$

APPENDIX G: SUMMARY OF ERROR ANALYSIS

Table G.1. Initial Parameters

Parameter	Low	High
Fluid velocity	0.20 ± 0.0074 m/s	0.40 ± 0.0072 m/s
Consistency/concentration	$0.10\% + 0.0125\%$	$0.40\% \pm 0.0133\%$
Fiber Aspect Ratio	200 ± 2.35	400 ± 3.89

Table G.2. Results

Set A: $l/d = 200$ & $C = 0.1\%$

U in m/s	Result from Fig. 36	Results from additional study
0.2010 ± 0.0074	164.7 ± 3.3	168.5 ± 3.5
0.2502 ± 0.0054	n/a	153.4 ± 3.1
0.3001 ± 0.0067	n/a	142.6 ± 2.8
0.3504 ± 0.0071	n/a	139.4 ± 2.5
0.4005 ± 0.0072	132.4 ± 2.8	133.2 ± 3.2

Set B: $l/d = 200$ & $C = 0.4\%$

U in m/s	Result from Fig. 36	Results from additional study
0.2010 ± 0.0074	132.1 ± 1.2	132.5 ± 2.5
0.2502 ± 0.0054	n/a	130.4 ± 1.6
0.3001 ± 0.0067	n/a	130.1 ± 4.4
0.3504 ± 0.0071	n/a	130.0 ± 2.4
0.4005 ± 0.0072	128.4 ± 1.4	128.0 ± 3.5

Set C: $l/d = 400$ & $C = 0.4\%$

U in m/s	Result from Fig. 36	Results from additional study
0.2010 \pm 0.0074	114.4 \pm 3.7	113.5 \pm 2.6
0.2502 \pm 0.0054	n/a	112.1 \pm 1.6
0.3001 \pm 0.0067	n/a	108.4 \pm 3.7
0.3504 \pm 0.0071	n/a	106.1 \pm 2.5
0.4005 \pm 0.0072	106.6 \pm 2.1	103.4 \pm 5.1

Set D: $l/d = 400$ $C = 0.1\%$

U in m/s	Result from Fig. 36	Results from additional study
0.2010 \pm 0.0074	119.4 \pm 8.0	121.1 \pm 1.9
0.2502 \pm 0.0054	n/a	120.3 \pm 3.4
0.3001 \pm 0.0067	n/a	120.1 \pm 2.2
0.3504 \pm 0.0071	n/a	117.5 \pm 4.1
0.4005 \pm 0.0072	108.6 \pm 0.9	107.2 \pm 1.7

VITA

Jooned Hendrarsakti was born in Jakarta, Indonesia on April 23, 1974. He received the Bachelor of Science and Master of Science in Mechanical Engineering from Texas A&M University. His current research interests include fluid mechanics, particle science, pulp and paper, and digital image processing. He can be reached through his parent's address: Jl. Pangkalan Jati I No. 9 RT/RW 05/13, Jakarta, INDONESIA 13620 or through email: jooned@ganja.com or jooned2001@yahoo.com.